OUKA
The University of Osaka
Institutional Knowledge Archive

| | |
|---|---|
| Title | Molecular phylogenetic analysis of cuttlefishes (Sepiidae, Cephalopoda, Mollusca) based on mitochondrial genes |
| Author(s) | Yoshida, Masa-aki |
| Citation | 大阪大学, 2009, 博士論文 |
| Version Type | VoR |
| URL | https://hdl.handle.net/11094/23463 |
| rights | |
| Note | |

*The University of Osaka Institutional Knowledge Archive : OUKA*

https://ir.library.osaka-u.ac.jp/

The University of Osaka

理学 13181

# Molecular phylogenetic analysis of cuttlefishes (Sepiidae, Cephalopoda, Mollusca) based on mitochondrial genes

# (ミトコンドリア遺伝子を用いたコウイカ類の分子系統解析)

2008.

Masa-aki Yoshida

Laboratory of Evolutionary Biology, Department of Biological Sciences,
Graduate School of Science, Osaka University

理学 13181

# Molecular phylogenetic analysis of cuttlefishes (Sepiidae, Cephalopoda, Mollusca) based on mitochondrial genes

# (ミトコンドリア遺伝子を用いたコウイカ類の分子系統解析)

2008.

Masa-aki Yoshida

Laboratory of Evolutionary Biology, Department of Biological Sciences,
Graduate School of Science, Osaka University

## Table of contents

## Introduction

Cuttlefishes (the family Sepiidae) are the large taxonomic group of extant cephalopod molluscs. The family Sepiidae is well-established group and characterized by the presence of a cuttlebone. The cuttlebone, which is made of aragonitic calcium carbonate, distinguishes the cuttlefishes from the other coleoid cephalopods. The shell shares common characters between extant and extinct lineages of cephalopods and it is a useful structure available for systematics and evolutionary study of decapodiformes. The cuttlebones provide traditionally very good materials for cuttlefish systematic study. The cuttlebone serves as buoyancy device and limits the habitat depth, so their morphology is related to the niche of the cuttlefishes. In the present study, twenty-five species of cuttlefishes were collected from the world and their phylogenetic relationships were investigated using molecular phylogenetic methods. Four well-supported clades were found in the phylogenetic trees based on maximum likelihood, maximum parsimony, and Bayesian methods. The results did not support phylogenetic reliability of prior classifications mainly based on the cuttlebone shape. A new taxonomic character, membranous structures, was found in a section of their cuttlebones. A loss of these structures was consistently observed in *Doratosepion* species and distinguishes them from the other cuttlefishes.

Cuttlefishes belong to the Sepioidea together with sepiolids (bobtail squids), sepidariids, and idiosepiids (pygmy squids). The family Idiosepiidae has both sepiolid- and teuthoid-like characters and this situation causing systematic confusions in decapodiformes. There are divergent views on the position of idiosepiids (Voss, 1977;

Fioroni, 1981; Clarke and Trueman, 1988; Boletzky, 2003). Recent molecular phylogenetic analyses have revealed some relationships among several cephalopod groups (see Nishiguchi and Mapes, 2008). Systematics and phylogenetic relationships of the major cephalopod groups, however, remain controversial. Idiosepiids have been argued as related either Teuthoidea or Sepioidea (Boletzky, 2005). Using comprehensive molecular data sets for decapodiformes (2,871 bp+1,016 aa), the phylogenetic position of idiosepiid was studied. The result suggested the basal position of idiosepiid among teuthoids, not in sepiolids.

The cephalopod is one of major groups of the phylum Mollusca, although they exhibit many functional innovations, e.g. intelligence with large sized brain, active locomotion with high metabolic rates and closed circulatory system. The cephalopod vascular wall is also different from the other molluscs in the presence of endothelial cells and bears resemblance to the vertebrate vascular wall. These innovations occurred in the cephalopod lineage after their branching. Recent molecular analyses have discovered conserved developmental genes across a large phylognetic scale, such as Hox gene clusters. The evolutionary developmental biology (evo-devo) has brought a new focus on the developmental mechanisms, which generate new variations, and the discovery of the widespread evolutionary conservation of the genes with prominent roles in development. A pygmy-squid, *Idiosepius paradoxus* lays transparent eggs that are suitable for developmental studies. Thus, *I. paradoxus* provide a useful model system. I have cloned a receptor of vascular endothelial growth factor (VEGFR), which is known to be critical inducer of vascular development and regulator of permeability of

blood vessels in vertebrates. The *Idiosepius* VEGFR gene was expressed in developing blood vessels of the embryos. This suggests that both vertebrates and cephalopods possess similar mechanisms in development of vascular systems.

**References**

Boletzky, S. v. (2003) Biology of early life stages in cephalopod molluscs. Advancs in Marine Biology, 44: 144-184.

Boletzky, S. v. (2005) *Idiosepius*: Ecology, biology and biogeography of a mini-maximalist. Phuket Marine Biological Research Bulletin, 66: 11-22.

Clarke, M. R. and Trueman, E. R. (1988) Introduction. In; Clarke, M. R., Trueman, E. R. (eds.) The Mollusca 12, Paleontology and Neontology of Cephalopods. Academic Press, London, 1-10.

Fioroni, P. (1981) The exceptional position of sepiolids, a comparison of the orders of cephalopods. Zoologische Jahrbücher, Systematik, Ökologie und Geographie der Tiere. Jena, 108: 178-228 (in German with English abstract).

Nishiguchi M. K. and Mapes, R. H. (2008) Cephalopoda. In; Ponder, W. F., Lindberg, D. R. (eds.) Phylogeny and Evolution of the Mollusca. University of California Press, California. pp. 163-199.

Voss, G. L. (1977) Present status and new trends in cephalopod systemtics. Symposium of Zoological Society of London, 38: 49-60.

# Chapter 1

Molecular phylogeny among the Sepiidae (Cephalopoda, Mollusca) inferred from mitochondrial COI, Cytb and ND5 genes

**ABSTRUCT**

Cuttlefish is a major group of recent cephalopods and characterized by presence of a cuttlebone. The traditional taxonomy of the cuttlefishes was mainly based on the cuttlebone morphology. Phylogenetic relationships among 25 species of cuttlefishes from the world were studied using partial sequences of three mitochondrial genes, Cytochrome *c* oxidase subunit I, Cytochrome *b*, and NADH dehydrogenase subunit 5. The nucleotide sequences of these three genes were analyzed using maximum likelihood, maximum parsimony, and Bayesian methods. Four well-supported clades were found in the phylogenetic trees. The first clade includes *Sepia esculenta, S. aculeata, S. lycidas, S. recurvirostra, S.* cf. *singaporensis, S. pharaonis, S. prashadi, S. elegans, and S. gibba.* The second clade consists of *Metasepia tullbergi* and *S. latimanus*. The third clade includes *S. officinalis, S. bertheloti* and *Sepiella japonica.* The fourth clade includes the *Doratosepion* species complex, *S. kobiensis, S. peterseni, S. tokioensis, S. andreana, S. pardex, S. lorigera, S.* sp. SI0604, *S. aureomaculata, S. tenuipes, S. subtenuipes,* and *S. madokai*. Saturation plots suggested that substitution saturation occurred at the third codon positions. Separation of four clades was also supported by the analyses using the first and second codon positions, and amino acid sequences. The molecular phylogenetic trees showed the polyphyly of the genus *Sepia*. This analysis did not support taxonomic reliability of prior classifications based on the cuttlebone shapes and the suckers on tentacular clubs. The fourth "*Doratosepion*" clade forms a monophyletic group characterized by the loss of membranous structure in cuttlebones.

## INTRODUCTION

Cuttlefishes (Sepiidae, Cephalopoda) are a major group of extant cephalopods, which are specified by a chambered cuttlebone (Fig. 1). The cuttlebone, which is made of aragonitic calcium carbonate, distinguishes the cuttlefishes from the other coleoid cephalopods. Several authors reported morphological diversity of cuttlebones and discussed function and evolution of these cuttlebones (Bandel & Boletzky, 1979; Khromov, 1998; Ward & Boletzky, 1984). The cuttlebone serves as buoyancy device and limits the habitat depth (Sherrard, 2000). In fact, the cuttlefishes segregate their niche in the habitat depth (Okutani *et al.*, 1987), suggesting that function and morphology of cuttlebones are associated with speciation in the cuttlefishes.

On the basis of morphological characters, the cuttlefishes are divided into three genera *Sepia*, *Sepiella*, and *Metasepia* (Voss, 1977; Khromov *et al.*, 1998; Lu, 1998). The genus *Sepiella* is characterized by a posterior gland and pore (Khromov *et al.*, 1998). Gray (1849) classified the genus *Sepia* into several sections and named one of the sections as *Sepiella*. Steenstrup (1875) redescribed the Gray's section as a separate genus and mentioned the posterior gland and locking apparatus, which differ from the other cuttlefishes. The genus *Metasepia* has a rhomboidal diamond-shaped cuttlebone (Khromov *et al.*, 1998). Hoyle (1885) has created a sub-genus *Metasepia* for *Sepia pfefferi*. The valid status of this genus was supported by the peculiar color pattern and locomotory behavior (Roper & Hochberg, 1988).

In the early classification of the Sepiidae, Orbigny (1845-1847) classified twenty-one species of cuttlefishes into three sections according to the arrangement and

the relative size of the suckers of the arm and the tentacular club. Gray (1849) classified the genus *Sepia* into sub-division based on the number of series of arm-suckers and of tentacular suckers as well as on the characters of the shell. Rochebrune (1884) separated the Sepiidae into ten genera, *Hemisepion, Diphtherosepion, Rhombosepion, Sepiella, Lophosepion, Spathidosepion, Doratosepion, Ascarosepion, Acanthosepion*, and *Sepia*, based on the cuttlebone shapes. Naef (1921-23) divided them into three genera, *Sepiella, Hemisepius*, and *Sepia*. The genus *Sepia* was divided into seven subgenera, *Eusepia, Parasepia , Acanthosepia, Doratosepia, Platysepia, Lophosepia* and *Metasepia* based on the morphological characters of the animal and the shell. Iredale (1926) created three families with thirteen genera based only on the shell of the Australian species. Adam & Rees (1966) reviewed the history of classification of the Sepiidae and recognized only two genera, *Sepia* and *Sepiella*. Khromov *et al.* (1998) recently divided the genus *Sepia* into six species complexes, *Sepia* sensu stricto, *Acanthosepion*, *Rhombosepion*, *Anomalosepia*, *Doratosepion* and *Hemisepius* based on the morphological characters of the shell and the animal, but mentioned that other kind of data would be important for further resolving taxonomic issues.

Recent molecular phylogenetic analyses have been utilized for several cephalopod groups (Carlini & Graves, 1999; Anderson, 2000; Strugnell *et al.*, 2005). Our previous molecular analysis using 12S and 16S rRNAs as well as COI genes suggested *Sepiella japonica* has a closer relationship with *Sepia officinalis* rather than the other *Sepia* species, so the genus *Sepia* was not a monophyletic group (Yoshida *et al.* 2006). Surprisingly *Metasepia tullbergi* was closely related to *Sepia latimanus*. These two

species differ in the body color, morphology such as the cuttlebone shape, and the mature size (Khromov *et al.*, 1998; Bonnaud *et al.*, 2006). Bonnaud *et al.* (2006) also recognized <*Metasepia*> and <*Sepiella*> groups from the analysis using mitochondrial 12S and 16S rRNAs as well as COII genes. These molecular analyses suggested the genus *Sepia* is not monophyletic and the cuttlebone is not a robust phylogenetic marker. A more comprehensive phylogenetic analysis is required for reconstruction of a true phylogenetic system of the Sepiidae with well-defined monophyletic groups (Khromov *et al.*, 1998; Reid, 2000).

Here we studied phylogenetic relationships of extant sepiid species using additional ten species from the various regions of the world and additional two markers in the mitochondrial genome. We used 2,200 bp of 31 species of cephalopods in this study. We had an unambiguous alignment according to the sequences without deletion. Base composition heterogeneity and partition heterogeneity in the data set have no influence on the relationships among the cuttlefishes. However, choices of outgroup species influenced the basal relationships among the sepiids. The analyses exhibited substantially higher support values among the cuttlefishes and revealed a monophyletic group, the *Doratosepion*, with a reliable taxonomic character; the loss of membranous structure in their cuttlebone.

## MATERIAL AND METHODS

We collected twenty-five species of cuttlefishes from the world (Table 1), and sequenced three mitochondrial genes, COI, Cytb and ND5. Tissue samples for DNA

extractions were obtained from the tips of arms. The samples were fixed in 70% ethanol and were stored at -20°C until the DNA extraction. The genomic DNA was extracted from the tissue using a DNeasy® Tissue kit (QIAGEN). Most of the specimens used in this study were fixed in 10% formaldehyde and deposited in the Museum of Osaka University (MOU).

*PCR amplifications and sequencings*

The polymerase chain reaction (PCR) was performed in 20μl reaction volumes containing 200-300μg extracted genomic DNA, 2μl 10×PCR buffer, 1.6μl 10mM dNTPs, 1μl 10μM primer each, and 0.5U Takara Ex Taq polymerase. A partial sequence of the mitochondrial cytochrome *c* oxidase subunit I (COI) gene was amplified with primers HCO2198 (5'-TAAACTTCAGGGTGACCAAAAAATCA-3') and LCO1490 (5'-GGTCAACAAATCATAAAGATATTGG-3') (Folmer *et al.*, 1994). Primers for amplifications of partial gene sequences of Cytochrome *b* and NADH dehydrogenase subunit 5 were designed in this study. The primers were as follows: Cytochrome *b* (Cytb-F1, GTTCATTRCGWAAAAVWCATCCTG / Cytb-R1, GGRCTDCYHCCAATYCAWGTTA), and NADH dehydrogenase subunit 5 (ND5-F1, TTRGGDTGRGAYGGDTTAGG / ND5-R1, SWRTGRTAATATTWCCHCCACA). The temperature regimen of PCR was 1 min at 94°C, 2 min at 45-55°C, 1-1.5 min at 72°C for 30 cycles.

The amplified fragment was cloned into a pGEM-T Vector (Promega). Plasmid DNA from transformant colonies was purified with a QIAprep® Miniprep kit

(QIAGEN). Both strands of the plasmid DNA were fully sequenced using T7 primer upstream and SP6 primer downstream of an insert site by the dideoxy chain-termination method using Applied Biosystems BigDye® Terminators v. 3.1 (Sanger *et al.*, 1997). Fluorescence-labeled DNA was analyzed using an ABI Prism 3100 sequencer (Applied Biosystems, USA). The accession numbers of sequences used in this study are shown in Table 1.

*Phylogenetic analysis of COI, Cytb, and ND5 data set*

Determined sequences were concatenated into one data set. There was no in-del among the determined sequences. We obtained sequences of mitochondrial genome of the other cephalopod species from the database as outgroups. Sequences were aligned using ClustalX (Thompson et al., 1997). There was no in-del between Octopodiformes and Decapodiformes. One amino acid deletion in Cytochrome *b* was observed between *Nautilus* and the other cephalopods. The base frequency of each gene was calculated by the program PAUP* ver. 4.0b10 (Swofford, 1993; Table 2). Numbers of constant characters and parsimony informative characters of the data set were also calculated using the PAUP* (Table 3). Homogeneity of three gene loci was tested by the partition-homogeneity test option implemented in PAUP*. The data set was partitioned into three genes and then analyzed using heuristic search with 1,000 repetitions. Homogeneity between COI and Cytb sequences were tested in a pair-wise fashion. Homogeneity between COI and ND5 and between Cytb and ND5 sequences was also tested in the same way. Homogeneity among three codon positions was also analyzed.

To test substitution saturation of the sequences, numbers of transversion was plotted against pairwise ML distances in accordance with Sullivan & Joyce (2005) (Fig. 2). ML distances were calculated under GTR+I+G model with the same parameters of maximum likelihood searches.

The nucleotide data set was analyzed by the maximum likelihood (ML) analysis using a heuristic search with PAUP*. The best-fit substitution model for the ML analysis was found using the program Modeltest 3.7 (Posada & Crandall, 1998). GTR+I+G model was selected by Akaike information criterion (AIC). Model parameters were estimated by the Modeltest and fixed prior to each analysis. The ML tree was searched using three independent searches, not to be trapped into the local optima. Analyses were done starting from Neighbor-joining (NJ) tree by Tree-bisection-and-reconnection (TBR) swapping, and starting from maximum parsimony (MP) tree by TBR swapping. Another search was done starting from a random tree and TBR swapping. Bootstrap support values for the ML trees were tested using bootstrap search option by Nearest-neighbor-interchange (NNI) with 1,000 repetitions. MP analysis was done using Branch-and-Bound search using PAUP*. Bootstrap support values for the MP trees were tested using PAUP* by heuristic searches with 1,000 repetition. Bayesian analysis was done using the program MrBayes ver. 3.1.2 (Huelsenbeck & Ronquist, 2001; Ronquist & Huelsenbeck, 2003). Metropolis-coupled Markov chain Monte Carlo (MCMCMC) from a random tree was run with sampled each 100 cycles. Four chains were run simultaneously; three were heated and one was cold. MCMC chains were run 1 to 500,000 generations. Two

independent run were conducted until the average standard deviation of split frequencies dropped below 0.1. Analyses were run repeatedly to check the consistency of results. The 1,250 trees were discarded by "burnin" option that corresponds to 25% of the samples (as recommended in the MrBayes 3.1 manual). The best-fit substitution model for the Bayesian analysis was found using the program Modelgenerator (Keane *et al.*, 2006). GTR+I+G model was selected by Akaike information criterion (AIC). The model parameters were estimated during the analysis.

To check an influence of noise due to the data heterogeneity the Bayesian analysis was performed with data partition. The data set was partitioned into three individual genes and analyzed in the same way to the Bayesian search with no partition. The best-fit substitution model for the Bayesian analysis was found using the program Modelgenerator. GTR+I+G model was selected by AIC value. The model parameters were estimated during the analysis. MCMCMC from a random tree was run with sampled each 100 cycles. Four chains were run simultaneously; three were heated and one was cold. MCMC chains were run 1 to 500,000 generations. Two independent runs were conducted until the average standard deviation of split frequencies dropped below 0.1. The 1,250 trees were discarded by "burnin" option that corresponds to 25% of the samples. The data set was also analyzed with a character partition by three codon positions.

To assess the influence of noise due to substitution saturation of the third codon position, the ML and MP analyses were applied to a data set including the first and second codon sites. The data set did not include *Octopus* and *Nautilus* due to their

severe saturation. The best-fit substitution model was found using the Modeltest. TvM+I+G model was estimated by AIC value. The ML and MP searches were carried out in a similar way to that used in the all codon site analysis. The best-fit substitution models for each data set were found using the Modeltest.

Stability of the basal relationships among the sepiids was investigated by replacing outgroup taxa. Five data sets with 24 taxon-ingroup including one teuthoid as a outgroup were generated: *Loligo, Sepiotethis, Watasenia, Todarodes* and *Rossia* were used as a outgroup. The ML searches were carried by heuristic searches using the five data sets. Analyses were done starting from NJ trees by TBR swapping. Model parameters of each data set were estimated by the Modeltest and fixed prior to each analysis. Base composition homogeneities about each data set were tested using PAUP*. Analyses with the data sets excluding the third codon position were also performed similarly. To assess the basal relationships among the cuttlefishes, the likelihood difference between the ML tree (the sister relationships between clade III and IV) and the tree clustering clade I with clade II was tested statistically. The ML and the constraint trees were analysed using the all codon data set including four teuthoid outgroups. The constraint tree forming clade I+II was analyzed using constraint option implemented in PAUP*. Site-wise likelihood scores of the trees were calculated using PAUP*. The approximately unbiased (AU) test (Shimodaira, 2002) in the CONSEL program (Shimodaira and Hasegawa, 2001) was employed to test between the ML topology and the constraint tree topology. Alternative tree topologies among the basal nodes, such as trees forming a clade I+III, clade I+IV, clade II+III and clade II+IV,

were also tested simultaneously. The *P*-values of each hypothesis were listed in Table 4.

*Phylogenetic analysis using amino acid sequences of COI, Cytb, and ND5 data set*

For amino acid sequence data set of three mitochondrial genes, ML analysis was performed using Treefinder (Jobb *et al.*, 2004). Best-fit model for ML analysis was tested using the program Modelgenerator. The best-fit was the program indicating mtART+F+I+G model. However, the likelihood score of the best tree under the mtART+F+I+G model (L=-5,465.9) was lower than under the mtREV+F+I+G model (L=-5,448.7). Model proportion using Treefinder also supported mtREV+F+I+G model as the best-fit. For the ML analysis, we used the mtREV+I+G model (Adachi & Hasegawa, 1996) for the substitution model and we used the search depth 2. Bootstrap support values for the ML trees were tested using bootstrap search option by search depth 1 with 1,000 repetitions. MP analysis was performed by Branch-and-Bound search using PAUP*. Bootstrap support values for MP trees were tested using PAUP* by heuristic searches with 1,000 repetition. Bayesian analysis was performed by MrBayes ver. 3.12. Metropolis-coupled Markov chain Monte Carlo (MCMCMC) from a random tree was run with sampled each 100 cycles. Four chains were run simultaneously, three were heated and one was cold. MCMC chains were run 1 to 500,000 generations and 1,250 trees were discarded by "burnin" option.

Phylogenetic analysis using sequences of COI gene

Four COI sequences of cuttlefish were obtained from the database. ML and MP

analyses were performed using totally thirty-three species of cephalopods. The ML analysis was performed using PAUP*. The best-fit model for ML analysis was found using the Modeltest. Bootstrap support values for the ML trees were tested using bootstrap search option by NNI with 1,000 repetitions. The MP analysis was performed using PAUP* by Branch and Bound search. Bootstrap support values for the MP trees were tested using bootstrap search option by Nearest-neighbor-interchange (NNI) with 1,000 repetitions.

## RESULTS

*General features of sequences*

Relationships between ML distance and the number of transversion are shown in Fig. 2. Saturation plots were obtained for the transversion numbers (Tv) of all codon positions, the first and second codon positions, and only the third codon position in the three mitochondrial genes. The plateau appeared in curves of the first + second codon positions and the third codon position only, suggesting substitution is saturated between *Nautilus* and the other cephalopods (ML distance>3). The plot of Tv at first and second positions between the Sepiidae and the other teuthoid outgroups exhibited a linear relation.

*Phylogenetic searches using nucleotide data set*

In each data set, three independent heuristic searches resulted in the same ML topology. In the phylogenetic tree using the nucleotide data set, four well-supported

clades were found (Fig. 3, L=23,579.2). The first clade (clade I) includes *Sepia esculenta, S. aculeata, S. lycidas, S. recurvirostra, S.* cf. *singaporensis, S. pharaonis, S. prashadi, S. elegans, and S. gibba.* The second clade (clade II) consists of *Metasepia tullbergi* and *S. latimanus*. The third clade (clade III) includes *S. officinalis, S. bertheloti* and *Sepiella japonica*. The fourth clade (clade IV) includes the *Doratosepion* species complex, *S. kobiensis, S. peterseni, S. tokioensis, S. andreana, S. pardex, S. lorigera, S.* sp.SI0604, *S. aureomaculata, S. tenuipes, S. subtenuipes,* and *S. madokai*. In the clade IV, two subgroups were found. The subgroup A includes *S. kobiensis, S. peterseni, S. tokioensis*, and *S. andreana*. The subgroup B include *S. pardex, S. aureomaculata, S. lorigera*, and *S.* sp.SI0614. Subgroup A was supported with high values. The clade III and the clade IV are closely related, although the support values were not so high (78% by ML and 67% by MP, but 1.0 by Bayesian PP).

*Relationships among the basal clades and effects of partition heterogeneity, base composition, and substitution saturation*

The partition homogeneity test (P=0.001) suggested partition heterogeneity among three genes, COI, Cytb, and ND5. Partition heterogeneities were also observed among between two genes (P<0.01). To assess influence of the data incongruence we analyzed the data set partitioned into three genes by the Bayesian analysis. The similar topology was obtained in the Bayesian analysis with or without the partition of the genes. Relationships among the four clades were conserved in the all trees, although different topologies occurred within the fourth *Doratosepion* clade. Thus the data incongruence

did not affect resulting phylogenetic relationships. No heterogeneity was found among the three-codon positions (p=0.811). The analysis with partition of three codon sites resulted in the same topology as the analysis with no partition.

The third codon data were discarded in the PAUP* analysis for twenty-nine species, because of the substitution saturation at the third codon position. When the data set including the first and second codon was used in the analysis, a single topology was obtained in the ML and MP searches (Fig. 4). Four well-supported clades were obtained in this tree as in the analysis using data set including three codon sites. However, the basal relationships differed from the tree using three codon data sets. The clade I is sister to the clade II, and this group is sister to the clade IV. The clade III was basal to the whole clades. This relationship was described as (III, (IV, (I, II))) in a Newick format. The clade IV was supported with high support value, although the position of *S. tenuipes, S. subtenuipes, and S. kobinesis* were differed from the tree using three codon data set.

The basal relationships differed, depending on the outgroup used in the analysis (Table 4). The analyses using all codon data set showed the basal clade relationships, (I, (II, (III, IV))) and ((I, II), (III, IV)). The analysis using the first and second codon data showed two relationships, (III, (IV, (I, II))) and ((I, II), (III, IV)). Chi-squared homogeneity test showed that base composition heterogeneities were observed in the nucleotide data sets including *Nautilus* and *Octopus*, but not in the nucleotide data sets excluding these cephalopods.

The ML tree using the nucleotide data set with four teuthid outgroups suggested a

sister relationship between the clade III and clade IV. A tree constraining clade I+III showed a lower likelihood value than the ML tree (Table 5). Statistical test for the ML analysis severely rejected the hypothesis of sister relationship between the clade I and III (P=0.005). Trees constraining clade I+IV and clade II+IV were also rejected by the AU test (P<0.05). The hypotheses constraining clade I+ II and clade II+III were not rejected in this analysis.

*Phylogenetic searches using amino acid data set*

The phylogenetic tree using the amino acid data set yielded four well-supported clades, I, II, III, and IV (Fig. 5). The analyses showed two clusters, the clade I +II and the clade III + IV. These basal relationships were not supported with high values (BP<67, PP<0.95).

*Phylogenetic searches using COI gene only*

In the phylogenetic tree using COI sequences well-supported four clades were identified (Fig. 6). The tree using the COI sequences showed rather low support values at the basal branches. The topology varied depending on the choice of outgroups. *S. opipara* is a sister to *M. tullbergi*. *S. furcata* and *S. hirunda* living around Taiwan were deposited within the clade IV.

**DISCUSSION**

Our previous analysis using 16S, 12S rRNA and COI genes showed four clades in

the cuttlefish relationships, but different topologies were obtained in analyses of NJ, MP, and ML. This was possibly caused by a large number of gaps in 16S and 12S rRNA sequences among the sepiids. Strugnell & Nishiguchi (2007) showed that an alignment method influenced the result of phylogenetic analysis, using three mitochondrial and six nuclear genes, among the cephalopods. In the present study, four clades were identical and well supported by the ML, MP, and Bayesian analyses. Addition of two genes (Cytb and ND5) and the data sets of unambiguous alignment of the sequences without gaps apparently improved the analysis.

The present analysis included six major lineages of extant cuttlefishes, i.e., the genus *Sepiella*, the genus *Metasepia*, and the *Sepia* species complexes containing *Sepia* sensu stricto, *Acanthosepion*, *Doratosepion*, and *Rhombosepion*. The species within the *Sepia* s. s. and *Rhombosepion* species complex were obviously paraphyletic in the present analysis. The molecular phylogeny suggests the necessity of revision of key morphological characters of the extant cuttlefish classifications.

The present study revealed that nine sepiid species are clustered in a single clade (the clade I) that includes *Sepia esculenta*, *S. aculeata*, *S. lycidas*, *S. recurvirostra*, *S.* cf. *singaporensis*, *S. pharaonis*, *S. prashadi*, *S. elegans*, and *S. gibba*. This clade contains five species (*Sepia esculenta*, *S. aculeata*, *S. lycidas*, *S. recurvirostra*, and *S. prashadi*) that Khromov *et al.* (1998) treated as the *Acanthosepion* species complex. Khromov *et al.* (1998) included both *S. pharaonis* and *S. gibba* in the *Sepia* species complex, and *S. elegans* in the *Rhombosepion* species complex. In *S. pharaonis* and *S. elegans*, we

found incongruity between the present study and our previous study (Yoshida *et al.* 2006). In the previous study, sequence data of these two species were taken from the database. The reason of incongruity is unknown at present.

Khromov *et al.* (1998) included *S. pharaonis* in the *Sepia* species complex. However, Lu (1998) considered that *S. pharaonis* has an affinity for a group including *S. aculeata, S. lycidas,* and *S. prashadi*, which have a well-developed ventral inner cone in common. The present study supports Lu's classification. The cuttlebone of *S. pharaonis* differs from that of *S. aculeata*, *S. lycidas*, and *S. prashadi* in the presence of broadly U-shaped deposit on the inner cone (also called the secondary inner cone). Adam & Rees (1966) considered the peculiar form of the inner cone has a limited value in phylogenetic anaysis. The molecular phylogeny supported the treatment that *S. pharaonis* is deposited within the *Acanthosepion* complex. *S. gibba* lives in high salinity waters (the northern part of the Red Sea), and so a distinct high phragmocone might be formed under these ionic conditions (Adam & Rees, 1966). This characteristic may be species-specific adaptive modification to the habitat.

The clade II consists of *Metasepia tullbergi* and *S. latimanus*. Some distinct morphological gaps, such as the body size and cuttlebone morphology, are found between these two species. The phylogenetic analysis using only COI suggested these two species are related to a small cuttlefish *S. opipara* living in tropical waters. Bonnaud *et al.* (2006) showed the <*Metasepia*> group consists of small-sized tropical species by phylogenetic analyses using the COII, 16S, and 12S rRNA. In their analyses, *S. latimanus*, *S. filibrachia*, *S. opipara*, *S. papuensis*, and *S. plangon* were clustered with

*Metasepia*. Males of *S. latimanus* and *S. papuensis* lack hectocotylized arms (Adam and Rees, 1966). Bonnaud *et al.* (2006) proposed the lack of hectocotyliztion is a characteristic of the <*Metasepia*> group. In fact, *M. tullbergi* belongs to the tropical species. The morphological specialization likely increased after the branching of these species.

The clade III includes *S. officinalis, S. bertheloti,* and *Sepiella japonica.* The analysis using only COI showed a monophyly of two *Sepiella* species and the sister relationship between *Sepiella* and *S. officinalis*. This leads to an apparent polyphyly of the *Sepia.* Bonnaud *et al.* (2006) proposed that *S. officinalis* and *Sepiella japonica* form the <*Sepiella*> group characterized by the presence of a single pair of spermathecae. Another common feature between *S. officinalis* and *Sepiella japonica* is the spawned egg capsule that is stained with ink. *S. officinalis* is the type species of the *Sepia* and Sepiidae (Linnaeus, 1758). However, *S. officinalis* has an affinity with *Sepiella* rather than with the other *Sepia* species in the molecular analysis. Further studies are apparently needed to revise the systematics of the Sepiidae.

The clade IV includes the *Doratosepion* species complex, *S. kobiensis, S. peterseni, S. tokioensis, S. andreana, S. pardex, S. lorigera, S.* sp. SI0604, *S. aureomaculata, S. tenuipes, S. subtenuipes, S. furcata, S. hirunda* and *S. madokai*. Our previous report indicated that *S. madokai* was included in the *Acanthosepion* complex (Yoshida *et al.* 2006). We erroneously identified *S.* sp.SI0604 as *S. madokai*. The *Doratosepion* was made based on distinct cuttlebone characters, such as a lanceolate shape and cup-like outer cone (Rochebrune, 1884). *S. madokai* have neither narrow cuttlebone nor peculiar

cup-like outer cone, suggesting the ancestral state of *Doratosepion*. In fact, phylogenetic trees show that *S. madokai* is separated early in the *Doratosepion* lineage. We found a new taxonomic character of *Doratosepion*, that is a loss of membranous structure in their cuttlebones (Yoshida *et al*, 2006). This character was found also in the specimens of *S. madokai*, *S. tokioensis*, *S. andreana*, *S. aureomaculata*, *S. tenuipes*, and *S. subtenuipes* (personal observations). Membranous structure is commonly observed in the other sepiids. Thus the loss of membranous structure is considered as a synapomorphy for the *Doratosepion* clade. In the cuttlebones, deep-water species have some devices to reduce the size of chamber cross-section, making the septa thinner and spaces between pillars smaller. These devices may provide resistance to hydrostatic pressure in the deep water (Sherrard, 2000). These features cause the decrease in cuttlebone density, and are apparently efficient for the diurnal vertical migration.

The phylogenetic tree of *Doratosepion* clade shows small interspecies distances. An explosive, recent radiation possively occurred in the *Doratosepion.* Khromov (1998) suggested that diversity of the *Doratosepion* species was caused by recent radiation along the periphery of the distributional range, such as South Africa, South Australia, and Japan. The low water temperatures around Japan in the Pleistocene are likely to form a thermal barrier against the sepiids. Our phylogeny supports the assumption that the recent explosive colonization and speciation occurred in Japanese *Doratosepion* species. In fact, more than half of the Japanese cuttlefishes are *Doratosepion* species. The *Doratosepion* species exhibit the sexual dimorphism in arms that is probably associated with the reproductive behavior. It is well knouwn that sexual selection

caused the rapid evolutionary radiation in African cichlid fishes (Turner, 1999). The sexual dimorphism is likely to drive speciation in *Doratosepion.*

An outgroup choice likely yields different basal relationships. The group most closely related to the Sepiidae is in an argument (Strugnell *et al.*, 2005), so that it was hard to choose a suitable outgroup. Different basal topologies occurred in the analyses using closely related loliginids, *L. bleekeri* and *S. lessoniana,* respectively. The present data sets have no base composition heterogeneities and no partition heterogeneities. Thus, the discrepancy of the basal relationships is still due to unknown reasons including outgroup problem. To improve the accuracy of basal relationships among the Sepiidae, we also have to increase the taxon sampling of the cuttlefishes.

We analysed three possible rooting positions ((I, II), (III, IV)), (I, (II, (III, IV))), and (III, (IV, (I, II))). The analysis using the amino acid data set supports that the rooting position ((I, II), (III, IV)) is most plausible. The sister relationship between clade III and clade IV was strongly supported by the several analyses and the AU test, but not by the morphological characters. In the analyses using 16S, 12S rRNAs and COII, *Doratosepion* sp. had a close relationship to <*Sepiella*> group together with *S. rex*, *S. elegans* and *S. orbigniana* (Bonnaud *et al.*, 2006). The position of *S. elegans* differs from our analyses, but their consensus tree indicated the basal relationship, (<*Metasepia*>, (Asian <*Sepia*>, (*Doratosepion*, <*Sepiella*>))).

The possibility of the sister relationship between the clade II and III was not rejected by the AU test. However, *S. latimanus* in the clade II differs from *S. officinalis* in the clade III in its stronger posterior spine, the fused protective membrane, and the

sucker-bearing surface detached from the stem of the tentacular club (Adam & Rees, 1966). The problem of rooting position still remains to be clarified.

The molecular and morphological analyses also still remain to be reconciled, but only the "*Doratosepion*" clade, among the Sepiidae, forms a monophyletic group both in molecular and morphological analyses. Therefore, we propose the *Doratosepion* clade, excluding *S. madokai*, as a distinct genus, *Doratosepion* Rochebrune, 1884.


## ACKNOWLEDGEMENTS

We thank Prof. Lu, C. C. and Ms. Ho C. W. of National Chung-Hsing University of Taiwan, Ms. Seow A. and Prof. Chou L. M. of National University of Singapore, Dr. Darmailacq A. of Interuniversity Institute for Marine Sciences of Israel, and Mr. Fernández M. E. of ANFACO-CECOPESCA of Spain for their kind help in collecting cuttlefish specimens.

This study was supported by the grants from the Research Institute of Marine Invertebrate Foundation and the Japan Society for the Promotion of Science (Research grant 18570087).


## References


Adachi, J. & Hasegawa, M. 1996. Model of amino acid substitution in protein encoded by mitochondrial DNA. *Journal of Molecular Evolution*, **42**: 459-468.

Adam, W. & Rees, W.J. 1966. A review of the cephalopod family Sepiidae. *Scientic*

*Reports of the John Murray Expedition 1933-34*, **11**: 1-165, pls. 1-46.

Anderson, F.E. 2000. Phylogeny and historical biogeography of the loliginid Squids (Mollusca: Cephalopoda) based on mitochondrial DNA sequence data. *Molecular Phylogenetics and Evolution*, **15**: 191-214.

Bandel, K. & Boletzky S.v. 1979. A comparative study of the structure, development and morphological relationships of chambered cephalopod shells. *The Veliger*, **21**: 313-354.

Bellardi, L. 1872. *I Molluschi dei terreni Terziari Piemonte e della Liguria, I: Cephalopoda, Pteropoda, Heteropoda, Gasteropoda (Muricide et Tritonidae).* Stamperia Reale, Trino.

Bonnaud, L., Lu, C.C. & Boucher-Rodoni, R. 2006. Morphological character evolution and molecular tree in sepiids (Mollusca: Cephalopoda): is the cuttlebone a robust phylogenetic marker? *Biological Journal of the Linnean Society*, **89**: 139-150.

Büllow-Trummer, E.v. 1920. *Fossilium Catalogus, I: Animaria, Pars 11: Cephalopoda Dibranchiata.* W. Junk, Berlin.

Carlini, D.B. & Graves, J.E. 1999. Phylogenetic analysis of cytochrome c oxidase I sequences to determine higher-level relationships within the coleoid cephalopods. *Bulletin of Marine Science*, **64**: 57-76.

Folmer, O., Black, M., Hoeh, W., Lutz, R. & Vrijenhoek, R. 1994. DNA primers for amplification of mitochondrial cytochrome *c* oxidase subunit I from diverse metazoan invertebrates. *Molecular Marine Biology and Biotechnology*, **3:**

294-299.

Gray, J.E. 1849. *Catalogue of the Mollusca in the British Museum. Part I Cephalopoda, Antepodia*. London.

Hoyle, W.E. 1885. Diagnosis new species of Cephalopoda collected during the cruise of H. M. S. "Challenger"-II: The Decepoda. *Annals and Magazine of Natural History (Series 5)*, **16**: 181-203.

Huelsenbeck, J. P. & Ronquist, F. 2001. MRBAYES: Bayesian inference of phylogeny. *Bioinformatics*, **17**: 754-755.

Iredale, T. 1954. Cuttlefish "Bones" again. *Australian Zoologist*, **12**: 63-82.

Jobb, G., von Haeseler, A. & Strimmer, K. 2004. TREEFINDER: A powerful graphical analysis environment for molecular phylogenetics. *BMC Evolutionary Biology*, **4**: 18.

Keane, T.M., Creevey, C.J., Pentony, M.M., Naughton, T.J. & McInerney, J.O. 2006. Assessment of methods for amino acid matrix selection and their use on empirical data shows that ad hoc assumptions for choice of matrix are not justified. *BMC Evolutionary Biology*, **6**: 29.

Khromov, D.N. 1998. Distribution pattern of Sepiidae. In: *Systematics and Biogeography of Cephalopods, Vol. 1* (N. A. Voss, M. Vecchione, R. B. Toll & M. Sweeny eds), 191-206. Smithsonian Institution Press, Washington D.C..

Khromov, D.N., Lu, C.C., Guerra, A., Dong, Z. & Boletzky, S.v. 1998. A synopsis of Sepiidae outside Australian waters (Cephalopoda: Sepiolidae). In: *Systematics and Biogeography of Cephalopods, Vol. 1* (N. A. Voss, M. Vecchione, R. B. Toll & M.

Sweeny eds), 77-157. Smithsonian Institution Press, Washington D.C..

Linnaeus, C. 1758. *Systema naturae per regna tria naturae, secundum classes, ordines, genera, species cum characteribus, differentiis, synonymis, locis.* Laur. Salvius., Stockholm.

Lu, C.C. 1998. A synopsis of Sepiidae in Australian waters (Cephalopoda: Sepiolidae). In: *Systematics and Biogeography of Cephalopods, Vol. 1* (N. A. Voss, M. Vecchione, R. B. Toll & M. Sweeny eds), 159-190. Smithsonian Institution Press, Washington D.C..

Naef, A. 1921-1923. *Cephalopoda. Fauna e Flora del Golfo di Napoli, Monograph 35.* (translated from German by the Israel Program for Scientific Translations, Jerusalem 1972)

Neige, P. 2003. Spatial patterns of disparity and diversity of the Recent cuttlefishes (Cephalopoda) across the Old World. *Journal of Biogeography*, **30**: 1125-1137.

Okutani, T., Tagawa, M. & Horikawa, H. 1987. *Cephalopods from continental shelf and slope around Japan.* Japan Fisheries Resource Conservation Association, Tokyo.

Orbigny A. 1845-1847. *Mollusque vivants et fossiles ou description de toutes les espèces de conquilles et de mollusques.* Adolphe Delahays, Paris.

Posada, D. & Crandall, K.A. 1998. Modeltest: testing the model of DNA substitution. *Bioinfomatics*, **14**: 817-818.

Reid, A.L. 2000. Australian cuttlefishes (Cephalopoda: Sepiidae): the 'doratosepion' species complex. *Invertebrate Taxonomy*, **14**: 1-76.

Rochebrune, A.T. 1884. Étude monographique de la famile des Sepiidae. *Bulletin des*

*Sciences par la Société Philomathique de Paris*, **7**: 74-122.

Ronquist, F. & Huelsenbeck, J.P. 2003. MRBAYES 3: Bayesian phylogenetic inference under mixed models. *Bioinformatics*, **19**: 1572-1574.

Roper, C.F.E. & Hochberg, F.G. 1988. Behavior and systematics of cephalopods from Lizard Island, Australia, based on color and body patterns. *Malacologia*, **29**: 153-193.

Sanger, F., Nicklen, S. & Coulson, A. R. 1977. DNA sequencing with chain-terminating inhibitors. *Proceedings of National Academy of Sciences*, **74**: 5436-5467.

Sherrard, K.M. 2000. Cuttlebone morphology limits habitat depth in eleven species of *Sepia* (Cephalopoda: Sepiidae). *Biological Bulletin*, **198**: 404-410.

Shimodaira H. 2002. An approximate unbiased test of phylogenetic tree selection. *Systematic Biology*, **51**: 492-508.

Shimodaira, H. & Hasegawa, M. 2001. CONSEL: for assessing the confidence of phylogenetic tree selection. *Bioinformatics*, **17**: 1246-1247.

Steenstrup, J. 1875. Hemisepius, en ny Slaegt af Sepia- Blaeksprutternes Familie, med Bemaekninger om Sepia-Formerne i Almindelighed. *Kongelige Danske Videnskabernes Selskabs Skrifter, Series5*, **10**: 465–482.

Strugnell, J.M., & Nishiguchi, M.K. 2007. Molecular phylogeny of coleoid cephalopods (Mollusca: Cephalopoda) inferred from three mitochondrial and six nuclear loci: A comparison of alignment, implied alignment and analysis methods. *Journal of Molluscan studies*, **73**: 399-410.

Strugnell, J.M., Norman, M., Jackson, J., Drummond, A.J. & Cooper, A. 2005.

Molecular phylogeny of coleoid cephalopods (Mollusca: Cephalopoda) using a multigene approach; the effect of data partitioning on resolving phylogenies in a Bayesian framework. *Molecular Phylogenetics and Evolution*, **37**: 426-441.

Sullivan, J. & Joyce P. 2005. Model selection in phylogenetics. *Annual Review of Ecology, Evolution, and Systematics*, **36**: 445-466

Swofford, D.L. 1993. PAUP - *Phylogenetic Analysis Using Parsimony. Ver. 3. 1.* [Computer software and manual]. Champaign, Illinois: Illinois Natural History Survey.

Thompson, J.D., Gibson, T.J., Plewniak, F., Jeanmougin F. & Higgins, D.G. 1997. The CLUSTAL_X windows interface: flexible strategies for multiple sequence alignment aided by quality analysis tools. *Nucleic Acids Research*, **25**: 4876-4882.

Turner, G.F. 1999. Explosive speciation of African cichlid fishes. In: *Evolution of Biological Diversity* (A. E. Magurran & R. M. May eds), 113–129. Oxford University Press, Oxford.

Voss, G.L. 1977. Classification of recent cephalopods. *Symposia of the Zoological Society of London*, **38**: 575-579.

Yoshida, M., Tsuneki, K. & Furuya, H. 2006. Phylogeny of Selected Sepiidae (Mollusca, Cephalopoda) based on 12S, 16S, and COI sequences, with comments on the taxonomic reliability of several morphological characters. *Zoological Science*, **23**: 341-351.

Ward, P. & Boletzky, S.v. 1984. Shell implosion depth and implosion morphologies in

three species of *Sepia* (Cephalopoda) from the Mediterranean Sea. *Journal of Marine Biological Association UK.*, **64** 955-966.

## Figure legends

**Figure 1. A,** The cuttlebone of *Sepia esculenta*, ventral view, **B,** The cuttlebone of *S. gibba*, ventral view, **C,** The cuttlebone of *S. gibba*, lateral view. IC, inner cone; OC, outer cone; P, phragmocone; S, spine.

**Figure 2.** Saturation plot. Saturation plots were generated for the transversion numbers (Tv) of all codon positions of the three mitochondrial genes, the first and second codon positions, and the third codon position only.

**Figure 3.** Phylogenetic relationships among the cuttlefishes using the nucleotide sequences of COI, Cytb and ND5 genes. Maximum likelihood tree derived from the analysis of the all codon position of the genes. The best-fit model for the mitochondrial protein gene (all codon) data set under AIC framework was defined as GTR+I+G model: Base=(0.3126, 0.0778, 0.1393), Rmat=(1.3678, 15.0057, 1.4590, 5.5165, 19.8956), Rates=gamma, Shape=0.4772, Pinvar=0.3815. Numbers at node indicate the support values: bootstrap values of the maximum likelihood analysis/bootstrap values of the maximum parsimony analysis/posterior probabilities of the Bayesian analysis. Bootstrap values were estimated with 1,000 replications. Support values under 50% or 0.50 are not shown. Asterisks indicate the support values were 100/100/1.0 respectively. Bar length is indicative of the number of substitution per site.

**Figure 4.** Maximum likelihood tree derived from the analysis of the first and second codon position of the genes. The best-fit model for the mitochondrial protein gene (all codon) data set under AIC framework was defined as TVM+I+G model:

Base=(0.2310, 0.1529, 0.1951), Nst=6, Rmat=(0.0000, 10.3987, 1.7523, 2.6218, 10.3987), Rates=gamma, Shape=0.5529, Pinvar=0.6115. Numbers at node indicate the support values: bootstrap values of the maximum likelihood analysis/bootstrap values of the maximum parsimony analysis/posterior probabilities of the Bayesian analysis. Bootstrap values were estimated with 1,000 replications. Support values under 50% or 0.50 are not shown. Asterisks indicate the support values were 100/100/1.0 respectively. Bar length is indicative of the number of substitution per site. In the representative species, the cuttlebones are shown on the right.

**Figure 5.** Maximum likelihood tree derived from the analyses of amino acid sequences of COI, Cytb, and ND5 genes. The best-fit model for the mitochondrial protein gene data set under AIC framework was defined as MtRev+F+I+G model. Numbers at node indicate the support values: bootstrap values of the maximum likelihood analysis/bootstrap values of the maximum parsimony analysis/posterior probabilities of the Bayesian analysis. Bootstrap values were estimated with 1,000 replications. Asterisks indicate the support values were 100/100/1.0 respectively.Support values under 50% or 0.50 are not shown. Bar length is indicative of the number of substitution per site.

**Figure 6.** Maximum likelihood tree derived from the analyses of nucleotide sequences of COI gene. The best-fit model for the mitochondrial protein gene (all codon) data set under AIC framework was defined as TVM+I+G model: Base=(0.3703, 0.1629, 0.0565), Rmat=(0.0795, 8.1900, 0.5437, 2.3607, 8.1900), Rates=gamma, Shape=0.3910, Pinvar=0.4168. Numbers at node indicate the support values:

bootstrap values of the maximum likelihood analysis/bootstrap values of the maximum parsimony analysis. Bootstrap values were estimated with 1,000 replications. Support values under 50% or 0.50 are not shown. Bar length is indicative of the number of substitution per site.

**Table 1.** Specimens used in this study

| Species | ML [a] (cm) | Sex | Locality | Collection date | Accession No.(COI/Cytb/ND5) | Sepecimen No. |
|---|---|---|---|---|---|---|
| *Sepia aculeata* | 13.6 | female | Taichun, Taiwan | Dec. 11. 2006 | AB430400 [b] /AB430415 [b] /AB430487 [b] | OUM-MO-00060 |
| *Sepia andreana* | 9.1 | male | Izumisano, Osaka, Japan | Apr. 26. 2007 | AB430401 [b] /AB430416 [b] /AB430488 [b] | OUM-MO-00089 |
| *Sepia aureomaculata* | 10 | male | Heta, Sizuoka, Japan | Dec. 13. 2007 | AB430402 [b] /AB430417 [b] /AB430489 [b] | OUM-MO-00103 |
| *Sepia bertheloti* | 9.8 | - | Spain | - | AB430403 [b] /AB430416 [b] /AB430490 [b] | - |
| *Sepia esculenta* | 15.3 | male | Minabe, Wakayama, Japan | Oct. 23. 2003 | AB192335/ AB430419 [b] /AB430491 [b] | - |
| *Sepia elegans* | 7.8 | - | Spain | - | AB430404 [b] /AB430420/AB430492 | - |
| *Sepia furcata* | - | - | - | - | AY530207 | - |
| *Sepia gibba* | - | - | The Red Sea, Israel | Jul. 5. 2007 | AB430405 [b] /AB430421 [b] /AB430493 [b] | OUM-MO-00101 |
| *Sepia hirunda* | - | - | - | - | AY530206 | - |
| *Sepia kobiensis* | 3.5 | - | Irino, Kochi, Japan | Feb. 14. 2002 | AB193813/ AB430422 [b] /AB430494 [b] | OUM-MO-00051 |
| *Sepia latimanus* | 21 | male | Okinawa, Japan | Nov. 17. 2003 | AB192338/AB430423 [b] /AB430495 [b] | - |
| *Sepia lorigera* | 20.5 | male | Owase, Mie, Japan | Jun. 14. 2004 | AB193810/AB430425 [b] /AB430497 [b] | OUM-MO-00031 |
| *Sepia lycidas* | 24.9 | male | Minabe, Wakayama, Japan | Jan. 30. 2002 | AB192337/AB430426 [b] /AB430498 [b] | - |
| *Sepia madokai* | 7.1 | female | Karo, Tottori, Japan | Jan. 19. 2007 | AB430407 [b] /AB430427 [b] /AB430499 [b] | OUM-MO-00077 |

| | | | | | | |
|---|---|---|---|---|---|---|
| *Sepia officinalis* | - | - | - | - | NC_007895 [c] | - |
| *Sepia opipara* | - | - | - | - | AF000063 | - |
| *Sepia pardex* | 19.5 | male | Sakaiminato, Tottori, Japan | Nov. 12. 2004 | AB193809/AB430428 [b] /AB430500 [b] | OUM-MO-00025 |
| *Sepia peterseni* | 9.5 | male | Irino, Kochi, Japan | Feb. 14. 2002 | AB192339/AB430429 [b] /AB430501 [b] | OUM-MO-00049 |
| *Sepia pharaonis* | 27.2 | male | Taichun, Taiwan | Dec. 11. 2006 | AB430408 [b] /AB430430 [b] /AB430502 [b] | OUM-MO-00059 |
| *Sepia prashardi* | - | - | Thailand | Oct. 29. 2007 | AB430409 [b] /AB430431 [b] /AB430503 [b] | OUM-MO-00102 |
| *Sepia recurvirostra* | 9 | female | Taichun, Taiwan | Dec. 11. 2006 | AB430410 [b] /AB430432 [b] /AB430504 [b] | OUM-MO-00073 |
| *Sepia tenuipes* | 9.2 | male | Heta, Sizuoka, Japan | Dec. 13. 2007 | AB430411 [b] /AB430433 [b] /AB430505 [b] | OUM-MO-00106 |
| *Sepia tokioensis* | 8.1 | male | Karo, Tottori, Japan | Jan. 19. 2007 | AB430412 [b] /AB430434 [b] /AB430506 [b] | OUM-MO-00082 |
| *Sepia* cf. *singaporensis* [d] | 7.3 | male | Semakau island, Singapore | Dec. 28. 2006 | AB430413 [b] /AB430435 [b] /AB430507 [b] | OUM-MO-00075 |
| *Sepia* sp.SI0604 | 12.3 | female | Irino, Kochi, Japan | Jun. 29. 2004 | AB193811/AB430436 [b] /AB430508 [b] | OUM-MO-00050 |
| *Sepia subtenuipes* | 8.2 | male | Heta, Sizuoka, Japan | Dec. 13. 2007 | AB430414 [b] /AB430437 [b] /AB430509 [b] | OUM-MO-00105 |
| *Sepiella inermis* | - | - | - | - | AY557522 | - |
| *Sepiella japonica* | 5.7 | male | Izumisano, Osaka, Japan | Feb. 20. 2003 | AB192341/AB430438 [b] /AB430510 [b] | - |
| *Metasepia tullbergi* | 4.7 | male | Irino, Kochi, Japan | Feb. 14. 2003 | AB192340/AB430440 [b] /AB430512 [b] | - |
| *Loligo bleekeri* | - | - | - | - | AB029616 [c] | - |

| | | | | | | |
|---|---|---|---|---|---|---|
| *Sepioteuthis lessoniana* | - | - | - | - | AB240154[c] | - |
| *Todarodes pacificus* | - | - | - | - | AB158364[c] | - |
| *Watasenia scintillans* | - | - | - | - | AB240152[c] | - |
| *Rossia pacifica* | 7.1 | female | Uozu, Toyama, Japan | May. 5. 2003 | AB191289/AB470277[b]/ AB470278[b] | |
| *Octopus ocellutus* | - | - | - | - | AB240156[c] | - |
| *Nautilus macromphalus* | - | - | - | - | DQ472026[c] | - |

[a], Dorsal mantle length; [b], Sequences determined in this study; [c], Whole mitochondrial genome was deposited in Database; [d], *Sepia singaporensis* was a synonym of *Sepia recurvirostra*. However, this specimen is distinguished from *S. recurvirostra* with the 10% sequence difference.

**Table 2.** Amplified length and base frequecies of the genes

| | | | Base frequencies | | | |
|---|---|---|---|---|---|---|
| | Length (bp) | Length (AA) | A | C | G | T |
| COI | 657 | 196 | 0.2874 | 0.1805 | 0.1528 | 0.3793 |
| Cytb | 975 | 324 | 0.2454 | 0.0994 | 0.1825 | 0.4727 |
| ND5 | 568 | 189 | 0.2872 | 0.1086 | 0.1592 | 0.445 |

**Table 3.** Numbers of characters of the aligned data sets

| | Total numbers of characters | Numbers of constant characters | Variable characters | Parsimony informative characters |
|---|---|---|---|---|
| All codon | 2,200 | 1,053 | 1,147 | 885 |
| 1st. and 2nd. codon | 1,466 | 1,011 | 455 | 271 |

**Table 4.** Sister relationships using different outgroups

| | all outgroups *(Nau., Oct., Lol., Sep., Wata., Toda.)* | teuthoids (*Lol., Sep., Wata., Toda.)* | *Loligo* | *Sepioteuthis* | *Watasenia* | *Todarodes* | *Rossia* |
|---|---|---|---|---|---|---|---|
| all codon data | (I,(II,(III,IV)) | (I,(II,(III,IV))) | ((I,II),(III,IV)) | (I,(II,(III,IV))) | (I,(II,(III,IV))) | ((I,II),(III,IV)) | (I,(II,(III,IV))) |
| first and second codon data | (III,(IV,(I,II))) | (III,(IV,(I,II))) | (I,(II,(III,IV))) | (III, (IV,(I,II))) | (I,(II,(III,IV))) | (III,(IV,(I,II))) | (I,(II,(III,IV))) |

**Table 5.** Test of hypothesis about the basal clades of cuttlefishes

| Hypothesis | clade I+II | clade I+III | clade I+IV | clade II+III | clade II+IV | clade III+IV |
|---|---|---|---|---|---|---|
| Likelihood score | 20,644 | 20,661 | 20,656 | 20,647 | 20,651 | ML (L=20,639) |
| AU test (p-value) | 0.31 | 0.005 | 0.024 | 0.276 | 0.011 | 0.822 |

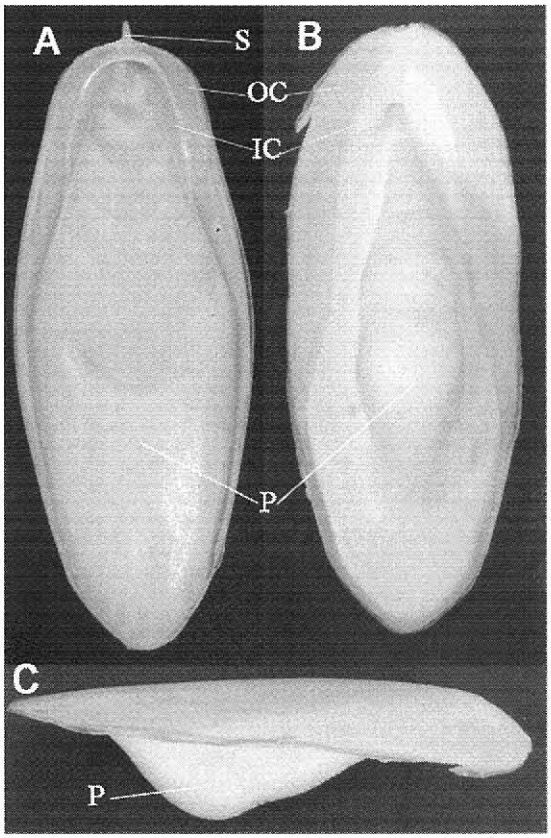


**Figure 1**

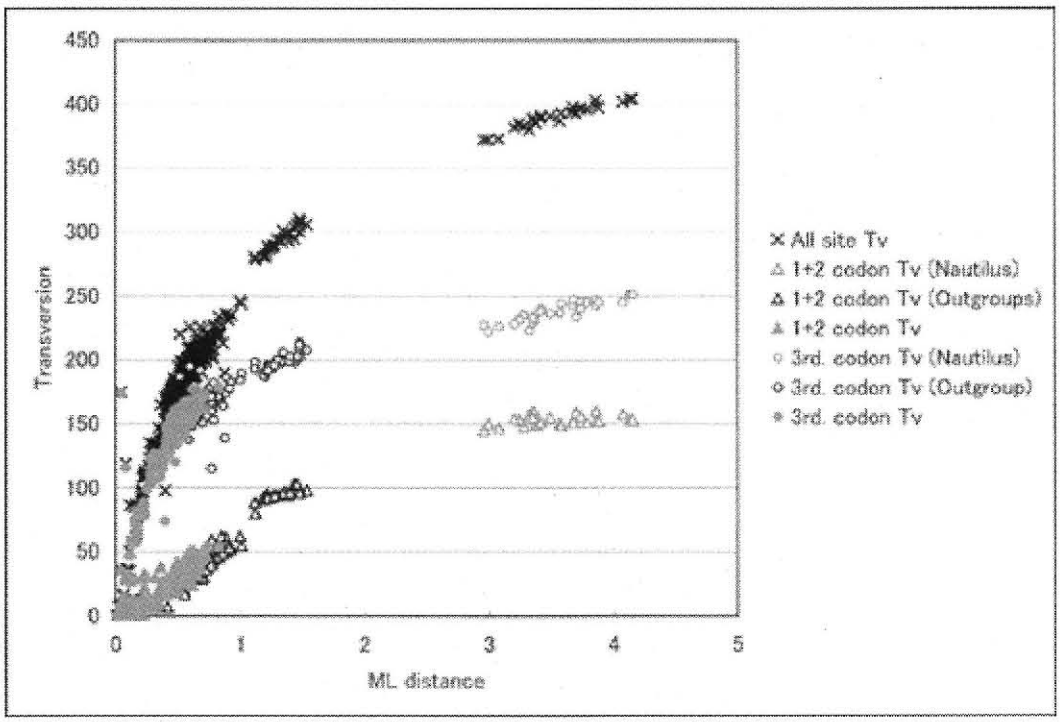
450
400
350
300
250
200
150
100
50
0
Transversion
0
1
2
3
4
5
ML distance
All site Tv
1+2 codon Tv (Nautilus)
1+2 codon Tv (Outgroups)
1+2 codon Tv
3rd. codon Tv (Nautilus)
3rd. codon Tv (Outgroup)
3rd. codon Tv

**Figure 2**

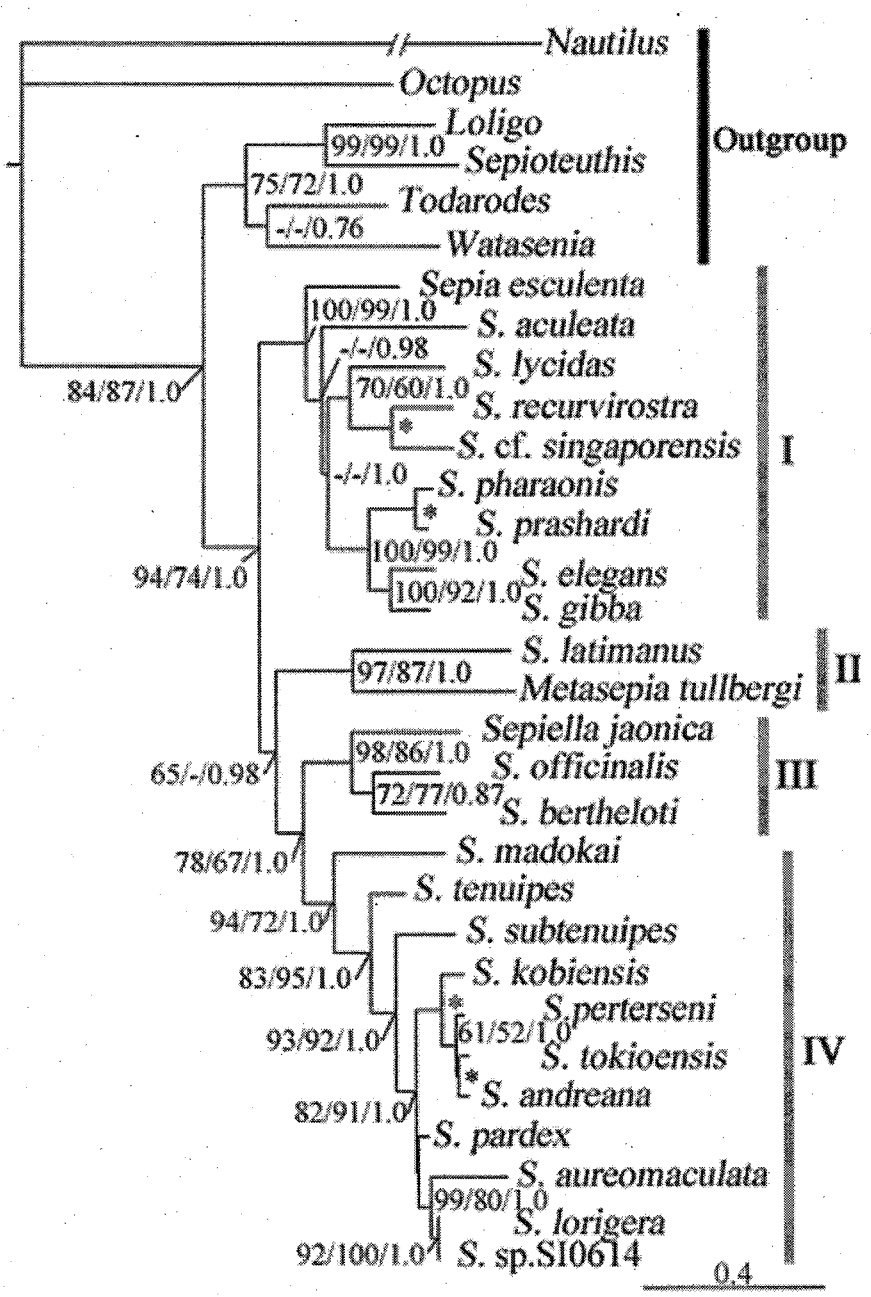
Nautilus
Octopus
Loligo
99/99/1.0
Sepioteuthis
75/72/1.0
Todarodes
-/-/0.76
Watasenia
Outgroup
Sepia esculenta
100/99/1.0
S. aculeata
-/-/0.98
S. lycidas
84/87/1.0
70/60/1.0
S. recurvirostra
S. cf. singaporensis
-/-/1.0
S. pharaonis
S. prashardi
100/99/1.0
94/74/1.0
S. elegans
100/92/1.0
S. gibba
I
S. latimanus
97/87/1.0
Metasepia tullbergi
II
Sepiella jaonica
98/86/1.0
S. officinalis
65/-/0.98
72/77/0.87
S. bertheloti
III
78/67/1.0
S. madokai
S. tenuipes
94/72/1.0
S. subtenuipes
83/95/1.0
S. kobiensis
S. perterseni
93/92/1.0
61/52/1.0
S. tokioensis
S. andreana
IV
82/91/1.0
S. pardex
S. aureomaculata
99/80/1.0
S. lorigera
92/100/1.0
S. sp.SI0614
0.4

**Figure 3**

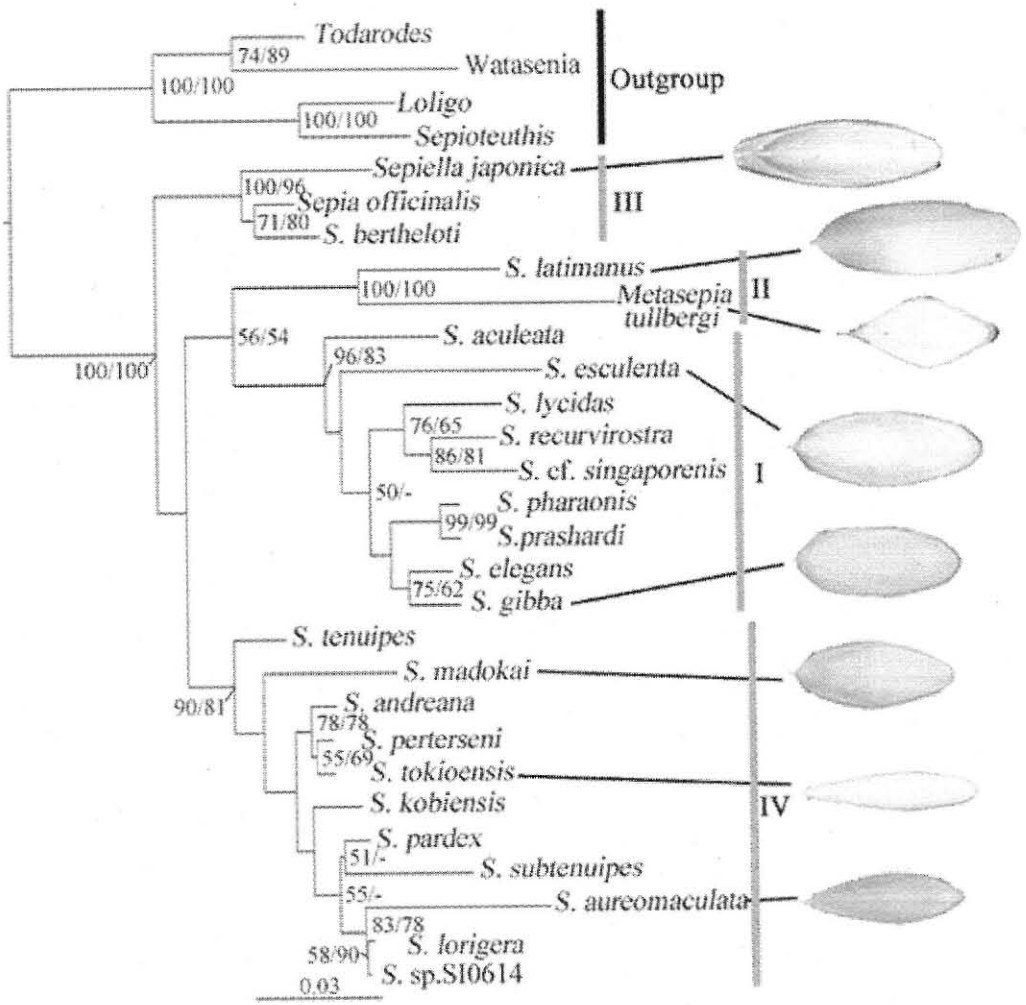
Todarodes
74/89
Watasenia
100/100
Loligo
100/100
Sepioteuthis
Outgroup
Sepiella japonica
100/96
Sepia officinalis
71/80
S. bertheloti
III
S. latimanus
100/100
Metasepia tullbergi
II
56/54
S. aculeata
96/83
S. esculenta
100/100
S. lycidas
76/65
S. recurvirostra
86/81
S. cf. singaporenis
I
50/-
S. pharaonis
99/99
S.prashardi
S. elegans
75/62
S. gibba
S. tenuipes
S. madokai
90/81
S. andreana
78/78
S. perterseni
55/69
S. tokioensis
IV
S. kobiensis
S. pardex
51/-
S. subtenuipes
55/-
S. aureomaculata
83/78
58/90
S. lorigera
S. sp.SI0614
0.03

**Figure 4**

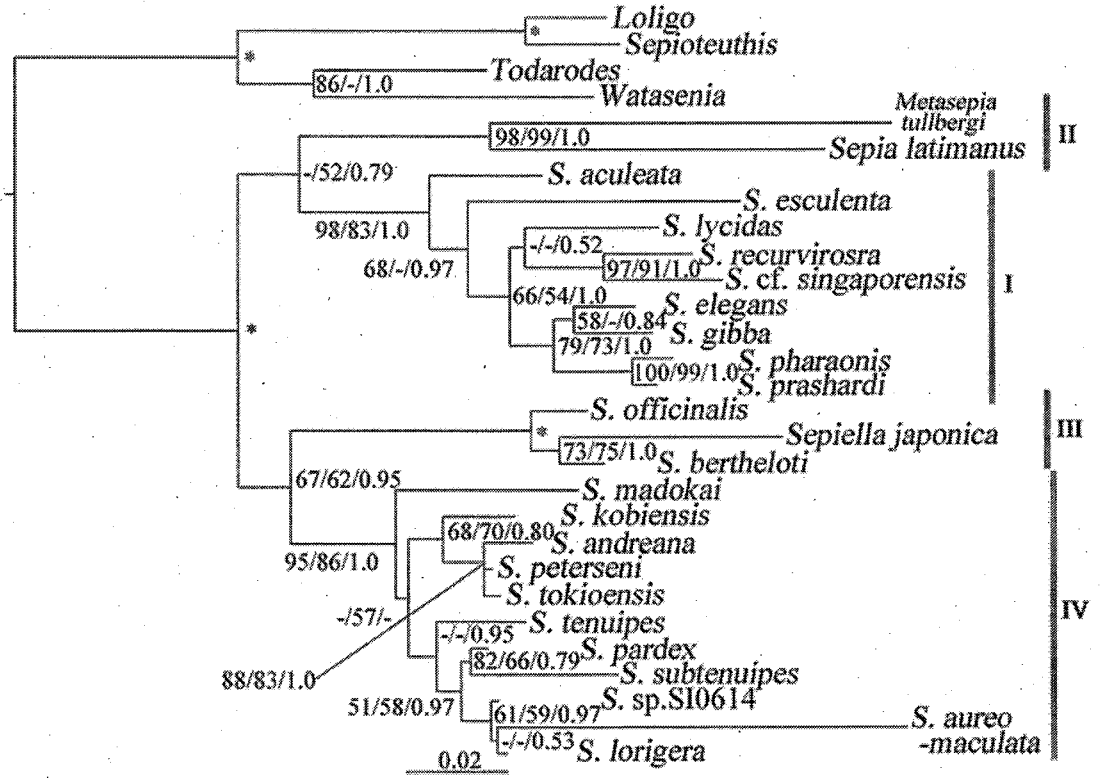
Loligo
Sepioteuthis
Todarodes
Watasenia
Metasepia tullbergi
Sepia latimanus
S. aculeata
S. esculenta
S. lycidas
S. recurvirosra
S. cf. singaporensis
S. elegans
S. gibba
S. pharaonis
S. prashardi
S. officinalis
Sepiella japonica
S. bertheloti
S. madokai
S. kobiensis
S. andreana
S. peterseni
S. tokioensis
S. tenuipes
S. pardex
S. subtenuipes
S. sp.SI0614
S. aureo
-maculata
S. lorigera
86/-/1.0
98/99/1.0
-/52/0.79
98/83/1.0
68/-/0.97
-/-/0.52
97/91/1.0
66/54/1.0
58/-/0.84
79/73/1.0
100/99/1.0
73/75/1.0
67/62/0.95
68/70/0.80
95/86/1.0
-/57/-
-/-/0.95
82/66/0.79
88/83/1.0
51/58/0.97
61/59/0.97
-/-/0.53
0.02
II
I
III
IV

**Figure 5**

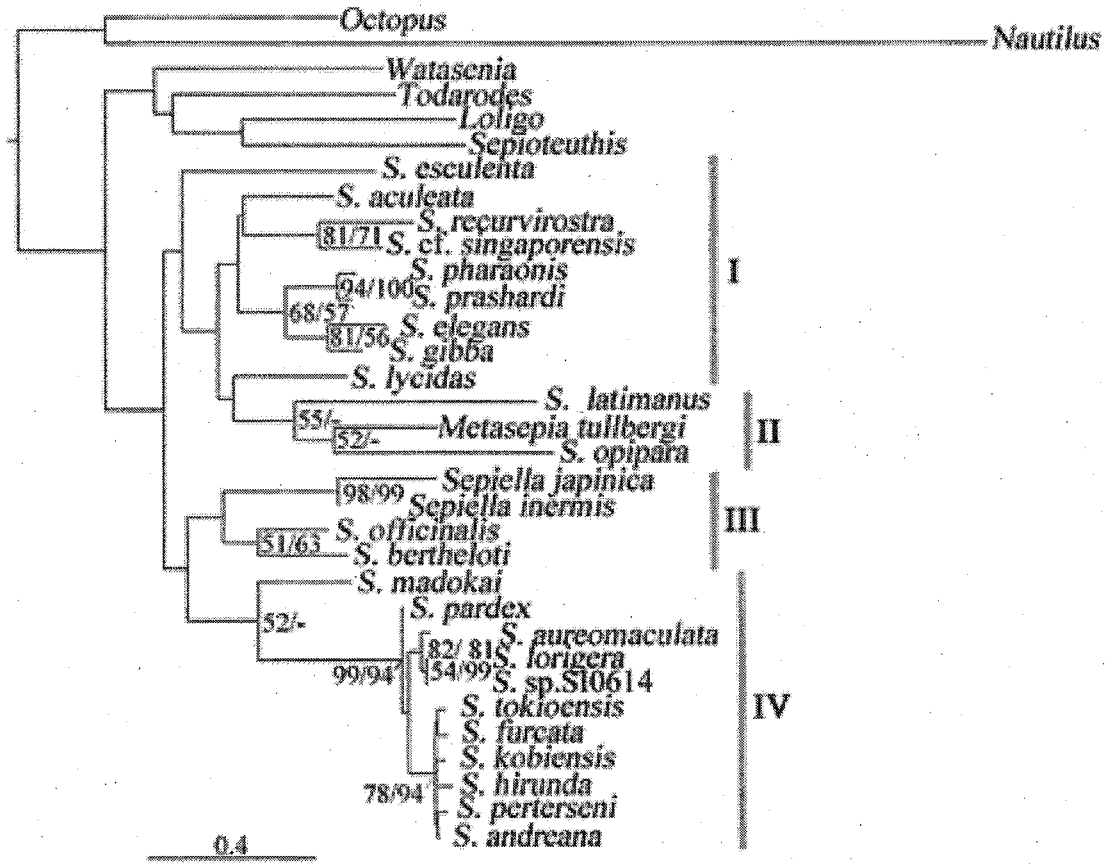
Octopus
Nautilus
Watasenia
Todarodes
Loligo
Sepioteuthis
S. esculenta
S. aculeata
S. recurvirostra
81/71
S. cf. singaporensis
S. pharaonis
94/100
S. prashardi
68/57
81/56
S. elegans
S. gibba
S. lycidas
S. latimanus
55/-
52/-
Metasepia tullbergi
S. opipara
98/99
Sepiella japinica
Sepiella inermis
51/63
S. officinalis
S. bertheloti
S. madokai
52/-
S. pardex
S. aureomaculata
82/ 81
S. lorigera
90/94
54/99
S. sp.S10614
S. tokioensis
S. furcata
S. kobiensis
78/94
S. hirunda
S. perterseni
S. andreana
0.4
I
II
III
IV

**Figure 6**

## Chapter 2

*Idiosepius* is a member of teuthoids: molecular phylogeny using nine genes of nuclear and mitochondrial genes

**Abstract**

We studied the phylogenetic position of *Idiosepius* among five higher taxonomic groups, sepiids, sepiolids containing myopsids, oegopsids and Sepiadariidae. Twenty three species of cephalopods were analyzed using four data sets, nuclear rRNA data set (18S+28S), nuclear and mitochondrial rRNA data set (18S+28S+16S+12S), nuclear protein gene data set (Pax-6+Rhodopsin), and mitochondrial protein gene data set (COI+Cytb+ND5). Sister taxon of idiosepiids was analyzed in each data set using the maximum likelihood, maximum parsimony, and Bayesian methods. Analyses using nucleotide sequences of the rRNAs and the mitochondrial protein suggested that idiosepiids were related to oegopsids among teuthoids. However, the analysis using the nuclear protein data sets did not support this relationship. The likelihood-based tests suggested that the idiosepiid is not related to sepiolid.

Phylogenetic relationships were analyzed using the amino acid sequences of the mitochondrial data set and total evidence analysis via concatenation of the likelihood. The analysis using the mitochondrial protein data set showed that sepiids and sepiolids were basal to teuthoids including idiosepiids. The total analysis evaluated by the likelihood values some controversial topologies. The tree for the second highest likelihood scores showed the same relationship as the analysis using the nucleotide sequences of rRNAs and the amino acid sequences of the mitochondrial protein data set, although the first tree indicated that the teuthoid clade including idiosepiids were basal to the clade of sepiids+sepiolids. All analyses did not support sister relationships between the idiosepiid and the sepiolid.

## Introduction

*Idiosepius* is one of the smallest cephalopods, exhibits both sepiolid and teuthoid like characters causing systematic confusions in Decapodiformes. Steenstrup (1881) placed *Idiosepius* in the *Sepia-Loligo* family that is the large group of the myopsid including Sepioloidea, *Sepiadarium*, and *Spirula*. Appellöf (1898) elevated *Idiosepius* to the family, Idiosepiidae. Voss (1977) proposed that the order Sepioidea included Idiosepiidae, Sepiolidae, Sepiidae, and Spirulidae. However, Fioroni (1981) included Idiosepiidae in the order Sepiolioidea with Sepiolidae and Sepiadariidae. Clarke and Trueman (1988) proposed the order Sepiolida containing Sepiolidae and Idiosepiidae, Sepiadariidae was deposited in the order Sepiida with Sepiidae. Subsequently, Boletzky (2003) elevated Idiosepiidae to the order and proposed five orders in Decabrachia (=decapodiformes), namely Spirulida, Sepiida, Sepiolida, Idiosepiida and Teuthoida.

Bonnaud *et al.* (1997) suggested that *Idiosepius* was related to the oegopsids by molecular phylogeny using the mitochondrial COIII genes. Carlini and Graves (1999) suggested a close relationship between *Idiosepius* and Sepioloidea using the COI genes. Carlini *et al.* (2000) exhibited a close relationship between *Idiosepius* and sepiolids using Actin I genes, although they showed a close relationship between *Idiosepius* and oegopsids using Actin II. Bonnaud *et al.* (2005) and Takumiya *et al.* (2005) suggested *Idiosepius* was related to the oegopsids, not to the sepiolids using some mitochondrial genes. Nishiguchi *et al.* (2004) suggested separation of the idiosepiids from sepiolids based on the analysis using mitochondrial 12S, 16S, COI, and nuclear 28S sequences. We showed previous relationships based on the morphological and molecular studies in

Fig. 1. The phylogenetic position of *Idiosepius* remained to be determined as Boletzky (2005) noted.

The analysis of a small number of loci suffers from a large sampling error and lack of the high statistical support. It has caused the different results as the previous molecular studies (Rokas *et al.*, 2003). Genes or regions with different evolutionary history have to be analyzed independently or using the appropriate evolutionary model. Strugnell *et al.* (2004) suggested a close relationship between *Idiosepius* and Sepiolids using three nuclear and three mitochondrial genes with data partitionings. *Sepiadarium* was not studied in their analysis, so the relationships among these groups have not been cleared. There is some confusion in the phylogenetic relationships among higher taxonomic groups within cephalopods.

We analyzed comprehensive molecular data sets for decapodiformes (2,871 bp+1,016 aa) to study the position of Idiosepiidae among higher taxonomic groups, sepiid, myopsid, oegopsid, and sepiolid. We used a total evidence approach by analyses to resolve the difficult and controversial phylogeny, evaluated the controversial tree topologies among decapodiformes using the maximum likelihood method.

## Materials and Methods

*PCR amplifications and sequencings*

We collected thirteen species of coleoid cephalopods in Japanese waters (Table 1), and sequenced four nuclear genes and five mitochondrial genes. Additionally, we obtained sequences of ten cephalopod species from the database. These sequences of nine genes of 23 coleoid cephalopods species were shown in Appendix 1.

Tissue samples for DNA extractions were obtained from the arm or the mantle. The samples were fixed in 70% ethanol and were stored at -20°C until the DNA extractions. The genomic DNA was extracted from the tissue using DNeasy® Tissue kit (QIAGEN).

The polymerase chain reaction (PCR) was performed in 20μl containing 200-300μg extracted genomic DNA, 2μl 10×PCR buffer, 1.6μl 10mM dNTPs, 1μl 10μM primer each, and 0.5U Takara Ex Taq polymerase. The primers were used to amplify of each gene (Table 2). The complete 18S rRNA was amplified and sequenced in three overlapping fragments using these primer sets, 18S1F/4R, 18S3bf/bi, and 18Sa2.0/9R. The partial gene sequences (of which primers for amplification) are as follows: 28S rRNA (28Sa/b), Pax-6 (PaxF1/R1), Rhodopsin (RhodF1/R1N or RhodF2/R3), Cytochrome *b* (CytbF1/R1), and NADH dehydrogenase subunit 5 (ND5F1/R1). The temperature regimen of PCR was 1min at 94°C, 2min at 45-55°C, 1-1.5min at 72°C for 30 cycles.

The amplified fragment was cloned into pGEM-T Vector (Promega). Plasmid DNA from transformant colonies was purified with QIAprep® Miniprep kit (QIAGEN). Both strands of the plasmid DNA were fully sequenced using T7 primer upstream and SP6

primer downstream of an insert site by the dideoxy chain-termination method using Applied Biosystems BigDye® Terminators v. 3.1 (Sanger *et al.*, 1997). Additional primer 5'-GCATTCCCGGCCCTTTCGGCC-3' was used to sequence 18S rRNA of *Sepiadarium kochii* (modified from 18S5bf by Lindgren *et al.*, 2004). The fluorescent-labeled DNA was analyzed using ABI Prism 3100 sequencer. The sequences were deposited in the DNA Database of Japan (DDBJ) database. The accession numbers of sequences used in this study are shown in Appendix 1.

*Phylogenetic analysis using nucleotide sequences*

Sequences were aligned using ClustalX ver. 1.83 (Thompson *et al.*, 1997) and adjusted manually. Indels and non-homologous regions were excluded from the analysis. The length of sequence used in the analyses was shown in Table 2.

We analyzed four gene sets for nucleotide sequences, nuclear rRNA (18S+28S rRNA), all rRNA (18S+28S+16S+12S rRNA), nuclear protein genes (Pax-6+Rhodopsin), and mitochondrial protein genes (COI+Cytb+ND5). The nuclear protein gene data set and the mitochondrial protein gene data set were analyzed using all codon positions, or the first and the second codon positions. The analyzed lengths of sequences in each data set were shown in Table 3.

The base frequency of each gene was calculated by the program PAUP* ver. 4.0b10 (Swofford, 2003). Homogeneity of the data set was tested by the partition-homogeneity test option implemented in PAUP* with 1,000 random repetitions. The nucleotide data set was analyzed by the maximum likelihood (ML) analysis using heuristic search with

PAUP*. The best-fit substitution model for the ML analysis was found using the program Modeltest 3.7 (Posada and Crandall, 1998). The substitution models were selected by Akaike information criterion (AIC) or hierarchical likelihood ratio test (hLRT) in Modeltest. Identical topology was found using the substitution model selected by AIC and by hLRT excepting the nuclear protein data set. The base frequencies of the model were estimated in each data set. The ML tree was searched using three independent searches, not to be trapped into the local optima. Analyses were done starting from Neighbor-joining (NJ) tree by Tree-bisection-and-reconnection (TBR) swapping, and starting from maximum parsimony (MP) tree by TBR swapping. Another search was done starting from a random tree and TBR swapping with 1,000 times repetition. In each data set, these three searches resulted in the same ML topology. Bootstrap support values for ML trees were tested using bootstrap search option by Nearest-neighbor-interchange (NNI) with 1000 repetition. Maximum parsimony (MP) analysis was done using Branch-and-Bound search using PAUP*. Bootstrap support values for MP trees were tested using PAUP* by NNI searches with 1,000 repetition. Bayesian analysis was done using the program MrBayes ver. 3.1.2 (Huelsenbeck and Ronquist, 2001; Ronquist and Huelsenbeck, 2003). Metropolis-coupled Markov chain Monte Carlo from a random tree was run with sampled each 100 cycles. Four chains were run simultaneously, three were heated and one was cold. The best-fit substitution models for Bayesian analyses were found using the program Mrmodeltest v2. (Nylander, 2004). Model parameter values were estimated in each analysis. The sister taxon of idiosepiids using the maximum parsimony and the Bayesian methods was listed in

Table 4.

To assess idiosepiid+sepiolid clade, the likelihood difference between the ML tree and tree forming idiosepiid+sepiolid clade were tested on statistically. Constraint trees making *Idiosepius* form a cluster with sepiolids were analyzed using constraint option implemented in PAUP*. The likelihood scores of the constraint tree were compared with those of the ML trees by Kishino-Hasegawa test (KH test, Kishino and Hasegawa, 1989) and Shimodaira-Hasegawa test (SH test, Shimodaira and Hasegawa, 1999) implemented in PAUP*.

*Phylogenetic analysis using amino acid sequences*

For amino acid sequence data set of three mitochondrial genes, ML analysis was performed using protml in the program molphy 2.3b3 (Adachi *et al.*, 1996a). For the ML analysis, we used the mtREV-f model (Adachi and Hasegawa, 1996b) for their substitution model. Bootstrap support values for ML tree were tested by RELL (resumpling of the estimated log-likelihood) method with 10,000 replications. MP analysis was performed by Branch-and-Bound search using PAUP*. Bayesian analysis was done by MrBayes ver. 3.12. Best-fit model for Bayesian analysis was found using the program modelgenerator (Keane, 2006).

*Total evidence analysis on likelihood analysis*

We analyzed the three data set of the nuclear rRNA sequences, the nuclear protein sequences, and the mitochondrial protein sequences using molphy. We obtained the ML

trees from each data set. The likelihood scores were concatenated using totalml in molphy. Analyses were performed on 9 OTUs. The sequences of *I. paradoxus*, *Loligo bleekeri*, *Ommastrephes bartramii*, *Sepia officinalis*, *Sepiadarium kochii*, and *Sepioteuthis lessoniana* were analyzed on an OTU. The rRNA sequences of *Graneledone recosa* and the protein sequences of *Octopus vulgaris* were concatenated to be used as an outgroup. Similarly, the rRNA sequences of *Sthenoteuthis oaulaniensis* and the protein sequences of *Todarodes pacificus*, the sequences of rRNAs of *Sepiola affinis* and the protein sequences of *Euprymna morsei* were concatenated.

Total evidence analyses of the nuclear rRNA sequence data set (18S+28S rRNA) and the mitochondrial rRNA data set (16S+12S) were performed with HKY 85 model (Hasegawa *et al.* 1985) using nucml (p-option, default setting). Amino acid sequences of the nuclear protein data set were analyzed with JTT-f model (Jones *et al.*, 1992) using protml. The mitochondrial data set was analyzed with mtREV-f model using protml. The NJ tree was analyzed using nucml (or protml, d-option) and njdist. The ML analysis was performed by staring from a NJ tree using nucml (or protml, R-option). The topologies of the NJ and ML tree were obtained for each data set. Eight topologies of the NJ and ML trees were obtained by the four data sets. The log-likelihoods of eight topologies were calculated using nucml and protml (l-option, t-option). In the eight tree topologies log-likelihood values for each data set were calculated using nucml (or protml, l-option, and u-option). The resulting log-likelihood values were concatenated using totalml in molphy. RELL bootstrap values for each topology were estimated using nucml (or protml) and totalml with 10,000 replications (Table 6).

## Results

*Alignment and data partition of nucleotide sequences*

Sequences of 18S rRNA consisted of highly variable and conserved regions. The 18S rRNAs of cephalopods with secondary structure of *Calicophoron calicophorum* (Accession number: L06566, Platyhelminthes) and these of *Daphnia pulex* (AF014011, Arthropoda) deposited in the European Ribosomal RNA database (http://rrna.uia.ac.be), It is doust that their variable regions are consistent with stems E10_1, E23_1-7, 43, and 49. These highly variable regions appeared not to be aligned, hence they were excluded in the analyses. There were differences between octopods and decapodiformes at the stem 6-9, E23_12, E23_14, 24, 28 and 44. These variable regions contained apparently indels, but the in-del patterns were not correlated to the taxonomic groups.

Nucleotide frequencies of genes were equal among cephalopod species examined. $X^2$ tests of each genes using PAUP* showed coincidence among species ($P>0.9$, data not shown). However, base frequencies were quite different between the nuclear and the mitochondrial genes (Table 1). Sequences of 18S and 28S rRNA were G-rich (0.31 or 0.35). Sequences of 16S and 12S rRNA were A-rich. Sequences of COI and Cytb and ND5 were T-rich. Regions with different evolutionary history have to be analyzed independently or using the appropriate evolutionary model. Therefore, we analyzed nucleotide sequences with four data sets, nuclear rRNA (18S+28S rRNA), all rRNA (18S+28S+16S+12S rRNA), nuclear protein genes (Pax-6+Rhodopsin), and mitochondrial protein genes (COI+Cytb+ND5). Substitution saturations were evident

within the mitochondrial genes among cephalopods (Guzik *et al.*, 2005; Strugnell *et al.*, 2005). Strugnell *et al.*, 2005 found saturations within Rhodopsin and Pax-6 genes. Substitution saturations affected phylogenetic analyses via multiple changes per site, so the nuclear and mitochondrial protein data sets were analyzed with the third codon position or without the third codon. Each data set was analyzed by maximum likelihood (ML), maximum parsimony (MP), and Bayesian analysis. Data partitioning among genes or codons in each data set was evaluated by partition homogeneity tests using PAUP*.

*Phylogeny based on nucleotide data*

Phylogenetic relationships were analyzed using the maximum likelihood method for the four data sets of nucleotide sequences. Sister taxon of idiosepiids was analyzed using the maximum parsimony and the Bayesian methods as listed in Table 4. The bootstrap support values using the MP and the posterior probabilities using the Bayesian method were also analyzed. Best-fit model for nuclear rRNA (18S+28S rRNA) data set was estimated as GTR+I+G model under AIC. The ML tree for the nuclear rRNA data set is shown in Fig. 2a (L=5,554.70). The Bayesian tree was analyzed with 500,000 generations, and with burnin=1,250 (L=5,560.57). Partition homogeneity test for the nuclear rRNA data set showed no significant heterogeneity between 18S and 28S rRNA genes ($P$=0.08). ML analysis was performed with the partition into two sites, 18S rRNA and 28S rRNA to assess an influence of the heterogeneity. The ML tree calculated with GTR+site-specific rate (SS) model for each partition (18S rRNA and 28S rRNA)

showed the same topology as the ML tree with TrN+I+G model (L=5,536.17). In these trees, *Sthenoteuthis oaulaniensis* and *Ommastrephes bartramii* form an oegopsids clade with high bootstrap (BP) support in ML and MP, and posterior probability (PP) in the Two *Idiosepius* species and two outgroup octopod species were also comprised the clades with strong supports. Oegopsids and myopsids exhibit monophyletic clade each. Idiosepiids was the sister taxa to the teuthoids (myopsid+oegopsid). Relationships among oegopsids, myopsids and idiosepiids were supported with high posterior probability (PP=0.98), but with low bootstrap values by ML and MP analyses (30-40%). *Sepiadarium kochii* formed a clade with *Sepia officinalis*. The other sepiolids were included in a monophyletic clade. Sepiolids and sepiids were single clade, apart from the teuthoid+idiosepiid clade.

The ML tree for nuclear rRNA data set is shown in Fig. 2b (L=8969.11). The Bayesian analysis (L=8975.97, 500,000 generations, and burnin=1250) showed a multifurcating tree, in which relationships among teuthoids, idiosepiids+sepiids, and sepiolids were not cleared. Partition homogeneity test for all rRNA data set indicated significant heterogeneity among the rRNA genes ($P$=0.001). ML tree with GTR+SS model to genes (18S, 28S, 16S, and 12S rRNA) was indicated to the topology with the tree by nuclear rRNA genes (Fig. 2a), with a lower score than ML tree (L=9099.03). Analysis using the nuclear rRNA data set supported myopsid clade, oegopsid clade and teuthoid clade. However, the other clades were supported by high PP, but not by BP. Sepiolids formed a monophyly clade in the ML analysis.

The nuclear protein gene data set was analyzed using all codon or except the third

codon. In this data set the different tree topologies were obtained from the ML and MP analyses, using the third codon or not. The ML tree using the first and second codon positions of the nuclear protein data set is shown in Fig. 3a (L=2209.27). Partition homogeneity test for the nuclear protein data set show no heterogeneity between the first and the second codon positions ($P$=0.649). The ML tree for nuclear protein data set (all codon included) is shown in Fig. 3b (L=5,299.85). The Bayesian tree was analyzed with 500,000 generations and burnin=1,250 (L=5,304.29). Partition homogeneity test for the nuclear protein data set showed significant heterogeneity between Pax-6 and Rhodopsin genes ($P$=0.014). In the ML tree with GTR+SS to genes (Pax-6 and Rhodopsin) model showed another topology (L=5,561.25), idiosepiids were positioned in the next to outgroup as well as the ML trees analysis using the first and the second codon data set. Partition homogeneity test indicated no significant incongruence among codon positions ($P$=0.062).

Mitochondrial protein gene data set was also analyzed using all codon or the first and the second codon. The ML tree of the mitochondrial protein gene data set is shown in Fig. 4a (L=5756.50). Partition homogeneity test for the mitochondrial protein gene data set exhibited no significant heterogeneity between the first and the second codon positions ($P$=0.71). In this tree *I. paradoxus* was included in oegopsids, and oegopsids were paraphyletic. *Ommastrephes* formed a clade with *Watasenia scintilluns*. The ML tree using all codon position of the mitochondrial protein gene data set is shown in Fig. 4b (L=14709.86). Analyses on the all codon position showed that *O. bartramii* form a clade with *T. pacificus*. *Idiosepius* was included in oegopsids, and sepiolids form a

clade with myopsids. The Bayesian analysis showed a multifurcating tree (L=14,724.52, 3,000,000 generations, and burnin=7500). Partition homogeneity test for the mitochondrial protein gene data set showed significant incongruence among genes ($P$=0.005). Mitochondrial gene data set with GTR+SS model to genes (COI, Cytb, and ND5) recovered the agreement with the topology of mitochondrial data set (first+second codon) with differences in the taxonomic groups. In the ML trees with GTR+SS model, the oegopsids form a clade, and *T. pacificus* appeared, followed by *O. bartramii*. Partition homogeneity test for the mitochondrial protein gene data set didn't show significant heterogeneity among codon positions ($P$=0.41).

*Likelihood ratio test among the topologies*

We compared the log-likelihood of topologies to test a hypothesis that idiosepiids is related to sepiolids. The constraint tree making idiosepiids form a clade with *Sepiadarium* conducted using PAUP*. The ML trees of the nuclear rRNA data set, the nuclear protein data set (first+second codon) and the mitochondrial protein data set (first+second codon) were analyzed under this constraint tree. Analyses were performed with another constraint in each of the data set; idiosepiids and *Sepiadarium*, and sepiolids form sister clade. The log-likelihood of each ML tree was calculated (Table 5). The difference of log-likelihood was tested by KH and SH tests using PAUP*. The ML trees with Idiosepiids+*Sepiadarium* clade by the three data sets were rejected by SH test ($P$<0.05), although the constraint trees of the nuclear rRNA data set and the mitochondrial protein data set were not rejected by KH test. The ML trees with

idiosepiid +sepiolids clade by the three data sets were rejected by all tests ($P<0.05$).

*Phylogeny based on amino acid data*

Aligned sequences of the mitochondrial protein genes were translated into amino acids and concatenated. The mitochondrial amino acid data set was analyzed using mtREV-f model. The ML tree (L=4287.30) was shown in Fig. 5. The analysis using JTT-f model showed the same topology as the ML tree using mtREV-f model. Result of the MP analysis showed multifucating tree, suggesting that several relationships among sepiolids, *Idiosepius*+oegopsids, myopsids, and sepiids colud not be resolved in the MP consensus tree. The Bayesian tree analyzed using JTT+I+G model differed from the ML tree in the topology (L=5159.73, 2,000,000 generations, and burnin=5,000). Oegopsids were basal to the other decapodiformes, and sepiolids formed a clade including myopsids, although the PP values were not high at basal nodes (PP<0.6).

*Concatenation of likelihood and topology evaluation*

Concatenated sequences were used for analuzes in *Sepiolla affinis*+*Euprymna morsei*, and two Ommastrephidae, *Sthenoteuthis oaulaniensis*+*Todarodes pacificus*. Takezaki *et al.* (2003) reported that interspecific differences were too small to influence the relationships among classes, i.e. amphioxus, hagfish, and lamprey lineages. These species in the same family can be concatenated and used for analysis among higher taxonomic groups.

Four data sets were analyzed independently and eight tree topologies were obtained

(Table 4). We calculated the log-likelihoods along the eight NJ and ML topologies using nucml and protml (l-option, t-option). The log-likelihood values were sum up using totalml (Table 6). Analyses of the nuclear protein data set showed this data set supported the various tree topologies and differences of the log-likelihoods of each topology was not significant. The ML topology of nuclear rRNA data set (-ln L=10802.0, see Fig. 6a) was supported with the highest log-likelihood and RELL BP. The second highest log-likelihood was achieved by the ML topology of the mitochondrial protein data set (-ln L=10818.7, Fig. 6b). The log-likelihood difference between the first and the second trees was under the standard error (±22.0). The second tree was supported by the RELL method with 25% of 10,000 replications. The other topologies were irreproducible by the RELL method (<0.028).

**Discussion**

We obtained a single topology from the analyses of the nuclear rRNA data set despite the models or the programs. Cephalopods contain some different 18S rRNA clones in their genomes, thus these sequences are not informative for phylogeny (Bonnaud *et al.*, 2002). Analyses of the nuclear rRNA data set showed similar results to those of the mitochondrial data. This relationship is also supported by the previous study on 28S rRNA (Bonnaud *et al.*, 2002).

The evolutionary model contained base frequencies estimated in the ML and the Bayesian analyses, hence incongruence in these frequencies among species may affect the analysis. Passamaneck *et al.* (2004) reported cephalopods have G-rich sequences of 18S rRNA genes, except *Nautilus* and *Histoteuthis*. The base frequency incongruence differs among these cephalopods, thus *Histoteuthis* (oegopsids) excluded from the other coleoids. In this analysis we did not find incongruence in 18S rRNA sequences. The number of taxon sampling also influenced the topology. We found different relationships between analysis using fourteen species and eight data sets by the nuclear rRNA dataset. The nuclear rRNA sequences of large numbers of taxon samplings and appropriate alignment will be required to study the higher relationships in the cephalopod phylogeny.

Our analyses showed an identical topology in the relationship based on analyses of the nucleotide sequences and the amino acid sequences of the mitochondrial protein data set. Analyses using the nuclear rRNA data set also indicated the identical

relationships. The second tree on the total evidence analysis also supported this relationship. This relationship was shown in other molecular phylogenetic analyses (Bonnaud *et al.*, 1997; Takumiya *et al.*, 2005). Phylogeny using amino acid sequences in mitochondrial genomes was consistent with the previous studies based on the rearrangement of mitochondrial genes and amino acid sequences of all mitochondrial genes (Yokobori *et al.*, 2004; Akasaki *et al.*, 2006). These analyses suggested that sepiid is basal to myopsids and oegopsids when the octopus was selected as an outgroup. It is supported by the analyses using the nuclear rRNA, all rRNA, and the mitochondrial protein genes data sets.

Mitochondrial genes are appropriate markers for relationships within the families in cephalopods (Anderson, 2000; Lindgren *et al.*, 2005; Yoshida *et al.*, 2006). Using several mitochondrial genes may cause more frequently the large sampling errors in analyses among higher taxonomic groups than in the family of cephalopods. Carlini and Graves (1999) suggested that the third codon positions were highly variable and informative for phylogenetic analyses on recently diverged taxa. In the mitochondrial protein data analyses, the phylogeny using the first and the second codon positions showed the same topology with analysis using amino acid sequences. The ML searches using GTR+SS models showed the same relationships as the analyses using the first and the second positions but not all codon positions. This result would suggest the third codon positions leaded to noises on the molecular analysis, and removal of the third codon may improve the resolution of phylogenetic analysis. Analyses using all codon positions supported another relationships among higher taxonomic groups. These results

suggest that careful study required for analyses using sequences of mitochondrial genes. Amino acid sequences of Rhodopsin may not be informative for analyses on the taxonomic groups due to an adaptation to environment.

In our analysis the relationships among oegopsids or among myopsids were supported with high statistical values. Some relationships among higher taxonomic groups were supported with high PP, although the bootstrap values were relatively low. Erixon *et al.* (2003) performed a simulation analysis, suggested that the Bayesian posterior probability (PP) values make erroneous conclusions more frequently than nonparametric bootstrapping. The relationships supported only with high PP may not be necessarily reliable. The total evidence analysis provided the two similar trees in topology. Trees among the higher taxonomic groups of cephalopods exhibited deep branches (Strugnell *et al.*, 2006), so it is required for more information and analyses.

This analysis did not show the close relationship between idiosepiids and sepiolids. The likelihood-based tests rejected the close relationships. Therefore, *Idiosepius* is not included in sepiolid as Bonnaud *et al.* (2005) studied. Steenstrup (1881) represented close relationship between *Idiosepius* and *Sepiadarium* based on the common feature, regression of gladius and medilateral rounded fins. Fioroni (1981) reported that the medilateral rounded fins were an apomorphy of the Sepiolidae and *Idiosepius.* Although, Berthold and Hamburg (1987) reported the rounded fins were also occurred in *Sepiadarium* and Loliginidae (*Pickfordiateuthis*). *Pickfordiateuthis* squids posses sepiolid-like fins, well-developed gladius, left functional oviduct, and hectocotylized

left ventral arm (Voss, 1953). They were characteristic of Loliginidae (myopsids), so the rounded fins were not apomorphy. *Idiosepius* had fully developed gladius (Boletzky, 1995; Hylleberg and Nateewathana, 1991a, b), but sepiolids indicate regression or lack of the gladius. This suggested that *Idiosepius* was not derived from sepiolids (Boletzky, 1995). Lack of cornea is an apomorphy of oegopsids, and presence of cornea suggests idiosepiids are not related to oegopsids. In our analysis idiosepiids were deposited within oegopsids or between oegopsids and myopsids. *Idiosepius* has no apomorphy in myopsid squids, such as bilobed digestive gland (Bonnaud *et al.*, 2005). Idiosepiid is possibly derived from myopsid-like ancestor. The first tree of the total evidence analysis suggested the most basal position of idiosepiids among decapodiformes. This position was supported the previous study using three nuclear protein genes (Strugnell et al., 2006). Anyway, the basal position of *Idiosepius* among teuthoids was suggested. To study the development and morphology of *Idiosepius* will give insight into the teuthoid evolution. Their fully described developmental stages (Yamamoto, 1988) and utility of eggs also make them suitable material for cephalopod developmental studies (Yamamoto *et al.*, 2003).

Also standing on the molecular phylogeny, we can conclude the exceptional position of sepiolids within decapodiformes, as Fioroni (1881) suggested by the morphological aspects. Our phylogeny showed sepiolids (containing Sepiadariidae) are basal to teuthoids with sepiids. Monophyly of sepiolids was not supported in any trees. The first total evidence tree didn't show monophyly between Sepiolidae and *Sepiadarium*. However the second tree and amino acid analysis supported monophyly

of sepiolids. The relationship between sepiolids and sepiids was not supported with high statistical values. Clarke (1988) proposed separation of sepiolids from the Sepioidea (sepiids) based on some common features in sepiids and sepiolids, such as fins, secondary eyelids, lateral funnel adductors and ventral septa, which may adapt for the benthic life. *Idiosepius* also has the ventral septum (Steenstrup, 1881) due to the bottom life. Thus it is not informative for their phylogenetic analyses. The change of life history (benthic or pelagic) and lack of fossil records caused confusion in phylogenetic relationships among cephalopods.

**Acknowledgment**

We thank to Dr. Shuichi Shigeno of the University of Chicago for his kind suggestion. We also thank to Prof. Tatsuya Sakamoto and Mr. Waichiro Godo of Ushimado Marine Laboratory of Okayama University for their kind help in collecting *Idiosepius* specimens.

M. Yoshida was supported by a grant from the Research Institute of Marine Invertebrates Foundation.

**References**

Adachi J, Hasegawa M (1996a) MOLPHY version 2.3: programs for molecular phylogenetics based on maximum likelihood. Computer Science Monographs of Institute of Statistical Mathematics 28: 1-150.

Adachi J, Hasegawa M (1996b) Model of amino acid substitution in protein encoded by mitochondrial DNA. J Mol Evo 42: 459-468

Akasaki T, Nikaido M, Tsuchiya K, Segawa S, Hasegawa M, Okada N (2006) Extensive mitochondrial gene arrangement in coleoid Cephalopoda and their phylogenetic implifications. Mol Phy Evo 38(3): 648-658

Alfaro ME, Zoller S, Lutzoni F (2003) Bayes or Bootstrap? A simulation study comparing the performance of Bayesian Markov Chain Monte Carlo sampling and bootstrapping in assessing phylogenetic confidence. Mol Biol Evo 20(2): 255-266

Anderson FE (2000) Phylogeny and historical biogeography of the loliginid Squids (Mollusca: Cephalopoda) based on mitochondrial DNA sequence data. Mol Phy Evo 15(2): 191-214.

Berry SS (1921) A review of the cephalopod genera Sepioloidea, Sepiadarium, and *Idiosepius*. Rec S Austr Mus 1: 347-364

Berthold T, Engeser T (1987) Phylogenetic analysis and systematization of the Cephalopoda (Mollusca). Ver naturwiss Ver Hamburg 29: 187-220

Boletzky Sv (1969) Zum vergleich der ontogenesen von *Octopus vulgaris*, *O. joubini* und *O. briareus*. Revue Suisse de Zoologie. 76: 716-726

Boletzky Sv (1977) Post-hatching behavior and mode of life in cephalopods. Symp Zool

Soc Lond 38: 557-567

Boletzky Sv (1995) The systematic position of the Sepiolidae (Mollusca: Cephalopoda). Bull l'Inst ocea, Monaco special 16: 99-104

Boletzky Sv (2003) Biology of early life stages in cephalopod molluscs. Adv Mar Biol 44: 144-184

Boletzky Sv ed. (2005) *Idiosepius*: Ecology, biology and biogeography of a mini-maximalist. Phuket mar biol Res Bull 66: 11-22

Bonnaud L, Boucher-Rodoni R, Monnerot M (1997) Phylogeny of cephalopods inferred from mitochondrial DNA sequences. Mol Phy Evo 7: 44-54

Bonnaud L, Saihi A, Boucher-Rodoni R (2002) Are 28S rDNA and 18S rDNA informative for cephalopod phylogeny? Bull Mar Sci 71(1): 197-208

Bonnaud L, Pichon D, Boucher-Rodoni R (2005) Molecular approach of decabrachia phylogeny: Is *Idiosepius* definitely not a sepiolid. Phulet mar biol Cent Res Bull 66: 203-212

Carlini DB, Graves JE (1999) Phylogenetic analysis of cytochrome c oxidase I sequences to determine higher-level relationships within the coleoid cephalopods. Bull Mar Sci 64: 57-76

Carlini DB, Reece KS, Graves JE (2000) Actin gene family evolution and the phylogeny of coleoid cephalopods (Mollusca, Cephalopoda). Mol Biol Evo 17(9): 1353-1370

Clarke MR (1988) Evolution of recent cephalopods – a brief review. In; Clarke MR, Trueman ER (ed.) The Mollusca 12, Paleontology and Neontology of

Cephalopods. Academic Press, London, 331-340

Clarke MR and Trueman ER (1988) Introduction In; Clarke MR, Trueman ER (ed.) The Mollusca 12, Paleontology and Neontology of Cephalopods. Academic Press, London, 1-10

Erixon P, Svennblad B, Britton T, Oxelman B (2003) Reliability of Bayesian Posterior Probabilities and Bootstrap Frequencies in Phylogenetics. Syst. Biol. 52(5): 665-673

Fioroni P (1981) The exceptional position of sepiolids, a comparison of the orders of cephalopods. Zool Jb Syst 108: 178-228 (in German with English abstract)

Folmer O, Black M, Hoeh W, Lutz R, Vrijenhoek R (1994) DNA primers for amplification of mitochondrial cytochrome *c* oxidase subunit I from diverse metazoan invertebrates. Mol Mar Biol Biotechnol. 3: 294-299

Furuya H, Ota M, Kimura R, Tsuneki K (2004) Renal organs of cephalopods: A habitat for dicyemids and chromidinids. J Mor 262: 629-643

Golodman N, Anderson JP, Rodrigo AG (2000) Likelihood-based tests of topologies in phylogenetics. Syst Biol 49: 652-670

Huelsenbeck JP, Ronquist F (2001) MRBAYES: Bayesian inference of phylogeny. Bioinformatics 17:754-755

Hylleberg J, Nateewathana A (1991a) Redescription of *Idiosepius pygmaeus* Steenstrup, 1881 (Cephalopoda: Idiosepiidae) with mention of additional morphological characters. Phuket mar biol Cent Res Bull 55: 33-42

Hylleberg J, Nateewathana A (1991b). Morphology, internal anatomy, and biometrics

of the cephalopod *Idiosepius* biserialis Voss, 1962. A new record for the Andaman Sea. Phuket mar biol Cent Res Bull 56: 1-9

Jones DT, Taylor WR, Thornton JM (1992) The rapid generation of mutation data matrices from protein sequences. Comput Appl Biosci 8:275-282

Keane TM, Creevey CJ, Pentony MM, Naughton TJ, McInerney JO (2006) Assessment of methods for amino acid matrix selection and their use on empirical data shows that ad hoc assumptions for choice of matrix are not justified. BMC Evolutionary Biology, 6:29

Kishino H, Hasegawa M (1989) Evaluation of the maximum likelihood estimate of the evolutionary tree topologies from DNA sequence data, and the branching order in Hominoidea. J Mol Evol 29: 170-179

Kuraku S, Hoshiyama D, Katoh K, Suga H, Miyata T (1999) Monophyly of lampreys and hagfishes supported by nuclear DNA-coded genes. J Mol Evol 49: 729-735

Lindgren AR, Giribet G, Nishiguchi MK (2004) A combined approach to the phylogeny of Cephalopoda (Mollusca). Cladistics 20: 454-486

Lindgren AR, Katugin ON, Amezquita E, Nishiguchi MK (2005) Evolutionary relationships among squids of the family Gonatidae (Mollusca: Cephalopoda) inferred from three mitochondrial loci. Mol Phy Evo 36: 101-111

Nishiguchi MK, Lopez JE, Boletzky Sv (2004) Enlightment of old idea from new investigations: more questions regarding the evolution of bacteriogenic light organs in squids Evo Dev 6(1): 41-49

Nishihara H, Hasegawa M, Okada N (2006) Pegasoferae, an unexpected mammalian

clade revealed by tracking ancient retroposon insertions. PNAS 103(26): 9929-9934

Nylander, JAA (2004) MrModeltest v2. Program distributed by the author. Evolutionary Biology Centre, Uppsala University.

Page RDM (1996) TREEVIEW: An application to display phylogenetic trees on personal computers. Computer Applications in the Biosciences 12: 357-358

Passamaneck YJ, Schander C, and Halanych KM (2004) Investigation of molluscan phylogeny using large-subunit and small-subunit nuclear rRNA sequences. Mol Phy Evo 32: 25-38

Posada D and Crandall KA (1998) Modeltest: testing the model of DNA substitution. Bioinformatics 14 (9): 817-818

Qiu YL, Li L, Wang B, Chen Z, Knoop V, Groth-Malonek M, Dombrovska O, Lee J, Kent L, Rest J, Estabrook GF, Hendry TA, Taylor DW, Testa CM, Ambros M, Crandall-Stotler B, Duff RJ, Stech M, Frey W, Quandt D, Davis CC (2006) The deepest divergences in land plants inferred from phylogenomic evidence. PNAS 103(42): 11511-11516

Rokas A, Williamas BL, King N, Carroll SB (2003) Genome-scale approaches to resolving incongruence in molecular phylogenies. Nature 425:798-805

Ronquist F, Huelsenbeck JP (2003) MRBAYES 3: Bayesian phylogenetic inference under mixed models. Bioinformatics 19:1572-1574

Sanger F, Nicklen S, Coulson AR (1977) DNA sequencing with chain-terminating inhibitors. Proc Nat Acad Sci USA 74: 5436-5467

Savard J, Tautz D, Richards S, Weinstock GM, Gibbs RA, Werren JH, Tettelin H, Lercher MJ (2006) Phylogenomic analysis reveals bees and wasps (Hymenoptera) at the base of tof Holometabolous insects. Genome Res 16: 1134-1138

Shimodaira H and Hasegawa M (1999) Multiple comparisons of log-likelihoods with applications to phylogenetic inference. Mol. Biol. Evo. 16:1114-1116

Steenstrup J (1881) Sepiadarium and *Idiosepius* two new genera of the family of Sepia. With remarks on the two related forms Sepioloidea d'Orb. and Spirula Lmk. (English translation, 1962)

Strugnell J, Jackson J, Drummond AJ, and Cooper A (2006) Divergence time for major cephalopod groups: evidence from multiple genes. Cladistics 22: 89-96

Strugnell J, Norman M, Jackson J, Drummond AJ, and Cooper A (2005) Molecular phylogeny of coleoid cephalopods (Mollusca: Cephalopoda) using a multigene approach; the effect of data partitioning on resolving phylogenies in a Bayesian framework. Mol Phy Evo 37: 426-441

Swofford DL (2003) PAUP. Phylogenetic Analysis Using Parsimony (and Other Methods). Version 4. Sinauer Associates, Sunderland, Massachusetts

Takezaki N, Figueroa F, Zaleska-Rutczynska Z, Klein J (2003) Molecular Phylogeny of Early Vertebrates: Monophyly of the Agnathans as Revealed by Sequences of 35 Genes. Mol Biol Evo 20(2): 287-292

Takumiya M, Kobayashi M, Tsuneki K, and Furuya H (2005) Phylogenetic relationships among major species of Japanese coleoid cephalopods (Mollusca, Cephalopoda) using three mitochondrial DNA sequences. Zool Sci 22: 147-155

Thompson JD, Gibson TJ, Plewniak F, Jeanmougin F, Higgins DG (1997) The ClustalX windows interface: flexible strategies for multiple sequence alignment aided by quality analysis tools. Nuc Acid Res 24: 4876-4882

Yamamoto M (1988) Normal embryonic stages of the pygmy cuttlefish, *Idiosepius* pygmaeus paradoxus Ortmann. Zoological Science 5(5): 989-998

Yamamoto M, Shimazaki Y, Shigeno S (2003) Atlas of the embryonic brain in the pygmy squid, *Idiosepius* paradoxus. Zool Sci 20: 163-179

Yokobori S, Fukuda N, Nakamura M, Aoyama T, and Oshima T (2004) Long-term conservation of six duplicated structural genes in cephalopod mitochondrial genomes. Mol Bio Evo 21(11): 2034-2046

Young RE, and Vecchione M (1996) Analysis of morphology to determine primary sister taxon relationships within coleoid cephalopods. Am Malacol Bull 12: 91-112

Young RE, Vecchione M, and Donovan DT (1998) The evolution of coleoid cephalopods and their present biodiversity and ecology. In: Payne AIL, Lipinski MR, Clarke MR, and Roeleveld AC (eds.) Cephalopod Biodiversity, Ecology and Evolution. S Afr J mar Sci 20: 393-420

Yoshida M, Tsuneki K, and Furuya H (2006) Phylogeny of Selected Sepiidae (Mollusca, Cephalopoda) based on 12S, 16S, and COI sequences, with comments on the taxonomic reliability of several morphological characters. Zool Sci 23: 341-351

Voss (1977) Present status and new trends in cephalopod systemtics. Symp Zool Soc Lond 38: 49-60

Whiting MF, Carpentar JM, Wheeler QD, Wheeler WC (1997) The Strepsiptera problem: phylogeny of the holometabolous insect orders inferred from 18S and 28S ribosomal DNA sequences and morphology. Syst Biol 38: 168-190

**Figure legend**

**Fig. 1** Phylogenetic relationships among decapodiformes according to various authers. **a**, According to Fioroni (1981); **b**, According to Bertheld and Engeser (1987); **c** , According to Clarke (1988); **d**, According to the molecular phylogeny using COIII genes (Bonnaud *et al.*, 1997); **e**, According to (Takumiya *et al.*, 2005); f, According to (Strugnell *et al.*, 2005). AA, amino acid sequences; I, idiosepiids; M, myopsids; NS, nucleotide sequecnces; O, oegopsids; Sd, sepiadariids; Se, sepiids; So, Sepiolids.

**Fig. 2** Phylogenetic trees derived from the analyses of rRNA genes. **a,** Maximum likelihood tree derived from the analysis of nuclear rRNAs (18S+28S) data set. The parameters in the model were defined as: rate matrix, R(a) [A-C] = 3.5860, R(b) [A-G] = 6.0172, R(c) [A-T] = 2.7949, R(d) [C-G] = 1.2249, R(e) [C-T] = 9.2851, R(f) [G-T] = 1.0000, gamma distribution shape parameter (Gammashape)=0.8638, and proportion of invariable sites (Pinvar)=0.4598. **b,** Maximum likelihood tree derived from the analysis of all rRNAs (18S+28S+16S+12S) data set. Best-fit model for all rRNA (18S+28S+16S+12S rRNA) data set under AIC framework was estimated for GTR+I+G model: Rmat=(0.4476, 4.1526, 3.3908, 0.2876, 3.3515), Gammashape=0.8062, Pinvar=0.6058. Numbers at node indicate the support values: bootstrap values of the maximum likelihood analysis/bootstrap values of the maximum parsimony analysis/posterior probabilities of the Bayesian analysis. Bootstrap values were estimated with 1,000 replications. Support values under 50% or 0.50 are not shown. Bars represent number of substitution per site. Bars in right

column indicate their taxonomic grouping.

**Fig. 3** Phylogenetic trees derived from the analyses of nuclear protein genes. **a,** Maximum likelihood tree derived from the analysis of first and second codon position of nuclear protein data set (Pax-6+Rhodopsin). The best-fit model for nuclear protein data set (first+second codon) was defined as SYM+I+G model under AIC framework: Rmat=(2.7733, 3.7198, 1.4509, 1.0686, 2.0712), Gammashape=0.5374, Pinvar=0.5737. **b,** Maximum likelihood tree derived from the analysis of all codon position of nuclear protein data set (Pax-6+Rhodopsin). The best-fit model for the nuclear protein data set (all codon) under AIC framework was defined as SYM+I+G model: Rmat=(3.5860, 6.0172, 2.7949, 1.2249, 9.2851), Gammashape=0.9268, Pinvar=0.4344. Numbers at node indicate the support values: bootstrap values of the maximum likelihood analysis/bootstrap values of the maximum parsimony analysis/posterior probabilities of the Bayesian analysis. Bootstrap values were estimated with 1,000 replications. Support values under 50% or 0.50 are not shown. Bars represent number of substitution per site. Bars in right column indicate their taxonomic grouping.

**Fig. 4** Phylogenetic trees derived from the analyses of mitochondrial protein genes. a, Maximum likelihood tree derived from the analysis of the first and second codon position of the mitochondrial protein gene data set (COI+Cytb+ND5). Best-fit model for mitochondrial protein gene (1st+2nd codon) data set under AIC framework was defined as SYM+I+G model: Rmat=(3.5860, 6.0172, 2.7949, 1.2249, 9.2851), Gammashape=0.9268, Pinvar=0.4344. b, Maximum likelihood tree

derived from the analysis of all codon position of mitochondrial protein gene data set (COI+Cytb+ND5). The best-fit model for the mitochondrial protein gene (all codon) data set under AIC framework was defined as TVM+I+G model: Rmat=(0.0965, 16.1831, 1.2986, 3.6813, 16.1831), Gammshape=0.2346, Pinvar=0.2358. Numbers at node indicate the support values: bootstrap values of the maximum likelihood analysis/bootstrap values of the maximum parsimony analysis/posterior probabilities of the Bayesian analysis. Bootstrap values were estimated with 1,000 replications. Support values under 50% or 0.50 are not shown. Bars represent number of substitution per site. Bars in right column indicate their taxonomic grouping.

**Fig. 5** Maximum likelihood tree derived from the analyses of amino acid sequences of mitochondrial protein genes (COI+Cytb+ND5). Numbers at node indicate the support values: bootstrap values of the maximum likelihood analysis/bootstrap values of the maximum parsimony analysis/posterior probabilities of the Bayesian analysis. Bootstrap values were estimated with 1,000 replications. Support values under 50% or 0.50 are not shown. Bars represent number of changes per site. Bars in right column indicate their taxonomic grouping.

**Fig. 6** Maximum likelihood trees derived from the restricted taxa. **a,** Maximum likelihood tree derived from the analysis by nucleotide sequences of the nuclear rRNA data set. This topology was supported with the highest likelihood concatenated. **b,** Maximum likelihood tree derived from the analysis by amino acid sequences of the mitochondrial protein data set. This topology was supported with

the second highest likelihood. Numbers on each node indicate RELL bootstrap values (10,000 replications). Bars represent number of changes per site.

**Table 1** List of cephalopods used in this study

| | Species | Mantle length (cm) | Sex | Locality | Colletion date |
|---|---|---|---|---|---|
| Idiosepiids | *Idiosepius paradoxus* | 1 | - | Ushimado, Okayama | 12.May.03 |
| Sepiids | *Sepia esculenta* | 6.4 | male | Minabe, Wakayama | 30.Jan.02 |
| | *Sepia officinalis* | 25.7 | male | * | 9.Sep.04 |
| Sepiolids | *Sepiadarium kochii* | 2.2 | female | Tosa, Kochi | 10.Mar.03 |
| | *Euprymna morsei* | 4.5 | male | Izumisano, Osaka | 8.Feb.03 |
| | *Rossia pacifica* | 7.1 | female | Uozu, Toyama | 6.Mar.03 |
| Myopsids | *Loligo bleekeri* | 14.5 | female | Uozu, Toyama | 5.Mar.03 |
| | *Sepioteuthis lessoniana* | 17.5 | female | Minabe, Wakayama | 29.Jun.03 |
| Oegopsids | *Berryteuthis magister* | 17 | male | Irino, Kochi | 6.Mar.03 |
| | *Ommastrephes bartramii* | 31 | female | Irino, Kochi | 14.Feb.03 |
| | *Todarodes pacificus* | 20 | female | Aomori, Aomori | 26.Sep.03 |
| | *Watasenia scintiluns* | 4.3 | male | Uozu, Toyama | 5.Mar.03 |

*, This specimen was imported from Morroco and collected at a fishery market in Osaka.

**Table 2.** Genes analyzed in this study

| | Length (bp) | Length (AA) | Base frequencies A | C | G | T | Primers | References |
|---|---|---|---|---|---|---|---|---|
| 18S rRNA | 1912 | - | 0.21 | 0.2773 | 0.3122 | 0.2005 | 18S1F, TACCTGGTTGATCCTGCCAGTAG<br>18S4R, GAATTACCGCGGATGATGG<br>18S3bf, GGGTCCGCCCTATCAACTG<br>18Sbi, GAGTCTCGTTCGTTATCGGA<br>18Sa2.0, ATGGTTGCAAAGCTGAAAC<br>18S9R, GATCCTTCCGCAGGTTCACCTAC | Giribet *et al.* 1996<br>Lindgren *et al.*2004<br>Whiting *et al.*1997 |
| 28S rRNA | 227 | - | 0.2463 | 0.2684 | 0.354 | 0.1313 | 28Sa, GACCCGTCTTGAAACACGGA<br>28Sb, TCGGAAGGAACCAGCTAC | Whiting *et al.* 1997 |
| Pax-6 | 273 | 90 | 0.248 | 0.2569 | 0.2886 | 0.2064 | Pax-6F1, AWKGKCAYAGWGTAAATCAGC | in this study |
| (Ex 3rd codon) | 182 | | 0.2575 | 0.2308 | 0.2967 | 0.2151 | Pax-6R1, ARGVTACACTTGGTATATTATCC | |
| Rhodopsin | 653 | 217 | 0.2416 | 0.2574 | 0.224 | 0.2771 | RhodF1, CAWSACCATGDCWATGGTCTCC<br>RhodR1N, GGTGCTCCTTGGGGWGGTG | in this study |
| (Ex 3rd codon) | 434 | | 0.277 | 0.205 | 0.2276 | 0.2904 | RhodF2, TACAAYGTMATYGGDAGACC<br>RhodR3, CATCATDGCCATCATYTC | |
| 16S rRNA | 414 | - | 0.3225 | 0.1121 | 0.2085 | 0.3569 | 16Sar, CGCCTGTTTRHCAAAAACAT<br>16Sbr, CCGGTYTGAACTCAGATCAYGT | Bonnaud *et al.* 1994 |
| 12S rRNA | 318 | - | 0.333 | 0.0904 | 0.1647 | 0.4118 | 12Sd, YAAACYRGGATTAGATACC<br>12Se, GAGRGYGACGGGCGRTGTGT | Bonnaud *et al.* 1994 |

| | | | | | | | | |
|---|---|---|---|---|---|---|---|---|
| COI | 591 | 196 | 0.2742 | 0.2016 | 0.1705 | 0.3537 | HCO1490, GGTCAACTCATAAAGATATTGG | Folmer *et al.* 1994 |
| (Ex 3rd codon) | 394 | | 0.2091 | 0.231 | 0.2214 | 0.3385 | LCO2198, TAAACTTCAGGGTGACCAAAACA | |
| Cyt*b* | 975 | 324 | 0.2436 | 0.1109 | 0.1898 | 0.4556 | CytbF1, GTTCATTRCGWAAAAVWCATCCTG | in this study |
| (Ex 3rd codon) | 650 | | 0.2243 | 0.1414 | 0.2205 | 0.4138 | CytbR1, GGRCTDCYHCCAATYCAWGTTA | |
| ND5 | 568 | 189 | 0.2744 | 0.1163 | 0.172 | 0.4373 | ND5F1, TTRGGDTGRGAYGGDTTAGG | in this study |
| (Ex 3rd codon) | 378 | | 0.2503 | 0.1539 | 0.1882 | 0.4076 | ND5R1, SWRTGRTAATATTWCCHCCACA | |

**Table 3.** The numbers of sequences in the aligned data sets

| Data sets | Total numbers of characters | Numbers of constant characters | Variable characters | Parsimony informative characters |
|---|---|---|---|---|
| Nuclear rRNA | 2,117 | 1,764 | 375 | 214 |
| All rRNA | 2,871 | 2,309 | 569 | 370 |
| Nuclaer protein (all codons) | 925 | 560 | 365 | 258 |
| $1^{st}+2^{nd}$ codon | 616 | 487 | 129 | 70 |
| Mitochondrial protein (all codons) | 2,134 | 1,128 | 1,006 | 732 |
| $1^{st}+2^{nd}$ codon | 1,422 | 1,065 | 357 | 209 |

**Table 4** The sister taxon of idiosepiids by the analyses in each data set

| | ML | MP | Bayes |
|---|---|---|---|
| nuclear RNA | teuthoids | teuthoids | teuthoids |
| all rRNA | teuthoids | teuthoids | sepiids |
| nuclear protein (1+2 codon) | the other decapodidormes | the other decapodidormes | - |
| nuclear protein (all codon) | myopsids+sepiids | the other decapodidormes | myopsids+sepiids |
| mitochondrial protein (1+2) | oegopsids | oegopsids | - |
| mitochondrial protein (all codon) | oegopsids | oegopsids | multifurcating |

**Table 5** Comparisons of log-likelihood with constraint trees and likelihood ratio tests using PAUP*

| 18S+28S | | | | |
|---|---|---|---|---|
| | -ln L | Δln L | *P*-value KH | *P*-value SH |
| No constraint | <5554.70> | | | |
| ((I.par,I.pyg,S.koc)) | 5572.35 | 17.65 | 0.06 | 0.034* |
| (((I.par,I.pyg,S.koc),H.haw,S.leu,S.aff)) | 5576.15 | 21.45 | 0.017* | 0.013* |
| Pax+Rhod (1st+2nd codon) | | | | |
| | -ln L | Δln L | KH | SH |
| No constraint | <2200.60> | | | |
| ((I.par,I.not,S.koc)) | 2222.17 | 21.58 | 0.016* | 0.011* |
| (((I.par,I.not,S.koc),R.pac,E.mor)) | 2228.56 | 27.97 | 0.008** | 0.004** |
| COI+Cytb+ND5 (1st+2nd codon) | | | | |
| | -ln L | Δln L | KH | SH |
| No constraint | <5756.50> | | | |
| ((I.para,S.koch)) | 5785.24 | 28.74 | 0.052 | 0.024* |
| (((I.para,S.koch),R.pacifica,E.morsei)) | 5787.61 | 31.11 | 0.043* | 0.021* |

The log-likelihoods, ln L, of the ML trees are given in angle brackets and the differences, Δln L, of the constraint trees from that of the ML tree are shown. The constraint trees were analyzed under constraints making Idiosepius form a clade with Sepiadarium, or with sepiolids. The likelihood differences evaluated by KH test and SH test using PAUP*. The P-values are listed and the values under 0.05 are shown with astalisk (*>0.05, **>0.01).

**Table 6** Comparisons of log-likelihood of tree topologies

| | 18S+28S | | Pax+RhodA | | COI+Cytb+ND5A | | Total | |
|---|---|---|---|---|---|---|---|---|
| | -Δln L±SE | RELL BP | -Δln L±SE | BP | -Δln L±SE | BP | -Δln L±SE | BP |
| COI+Cytb+ND5A NJ | 16.2±16.0 | 0.0164 | 27.3±15.2 | 0.0035 | 10.5±10.0 | 0.1171 | 27.5±24.3 | 0.0276 |
| COI+Cytb+ND5A ML | 16.1±16.0 | 0.1287 | 27.0±15.0 | 0.0018 | <4287.3> | 0.7573 | 16.7±22.0 | 0.258 |
| Pax+RhodA NJ | 18.9±12.1 | 0.0317 | 1.2±7.2 | 0.3344 | 57.8±23.4 | 0 | 51.3±27.4 | 0.0035 |
| Pax+RhodA ML | 18.9±12.1 | 0.0048 | <1757.0> | 0.3267 | 53.1±24.6 | 0.0009 | 45.5±27.4 | 0.0145 |
| 18S+28S NJ | 5.0±4.8 | 0.1215 | 7.1±13.6 | 0.0972 | 34.3±19.6 | 0.0044 | 19.9±24.4 | 0.0142 |
| 18S+28S ML | <4731.1> | 0.692 | 3.9±12.4 | 0.2362 | 22.6±20.1 | 0.1067 | <10802.0> | 0.6821 |
| 16S+12S NJ | 42.7±19.9 | 0.0031 | 37.1±12.7 | 0 | 60.8±28.6 | 0.0096 | 114.1±37.1 | 0 |
| 16S+12S ML | 44.7±19.2 | 0.0018 | 45.1±16.9 | 0.0002 | 58.0±26.9 | 0.004 | 121.3±37.2 | 0.0001 |

The log-likelihood, ln L, of ML trees are given in angle brackets, and the differences, Δln L, of alternative trees from that of ML trees are shown with their SEs (following ±). The log-likelihood, ln L, of ML trees are given in angle brackets, and the differences, Dln L, of alternative trees from that of ML trees are shown with their SEs (following ±). RELL Bootstrap values (BP) are estimated by Resumpling of the Estimated Log-Likelihood Bootstrap values (BP) are estimated by the RELL method (Kishino *et al.*, 1990) using molphy 2.3b3.

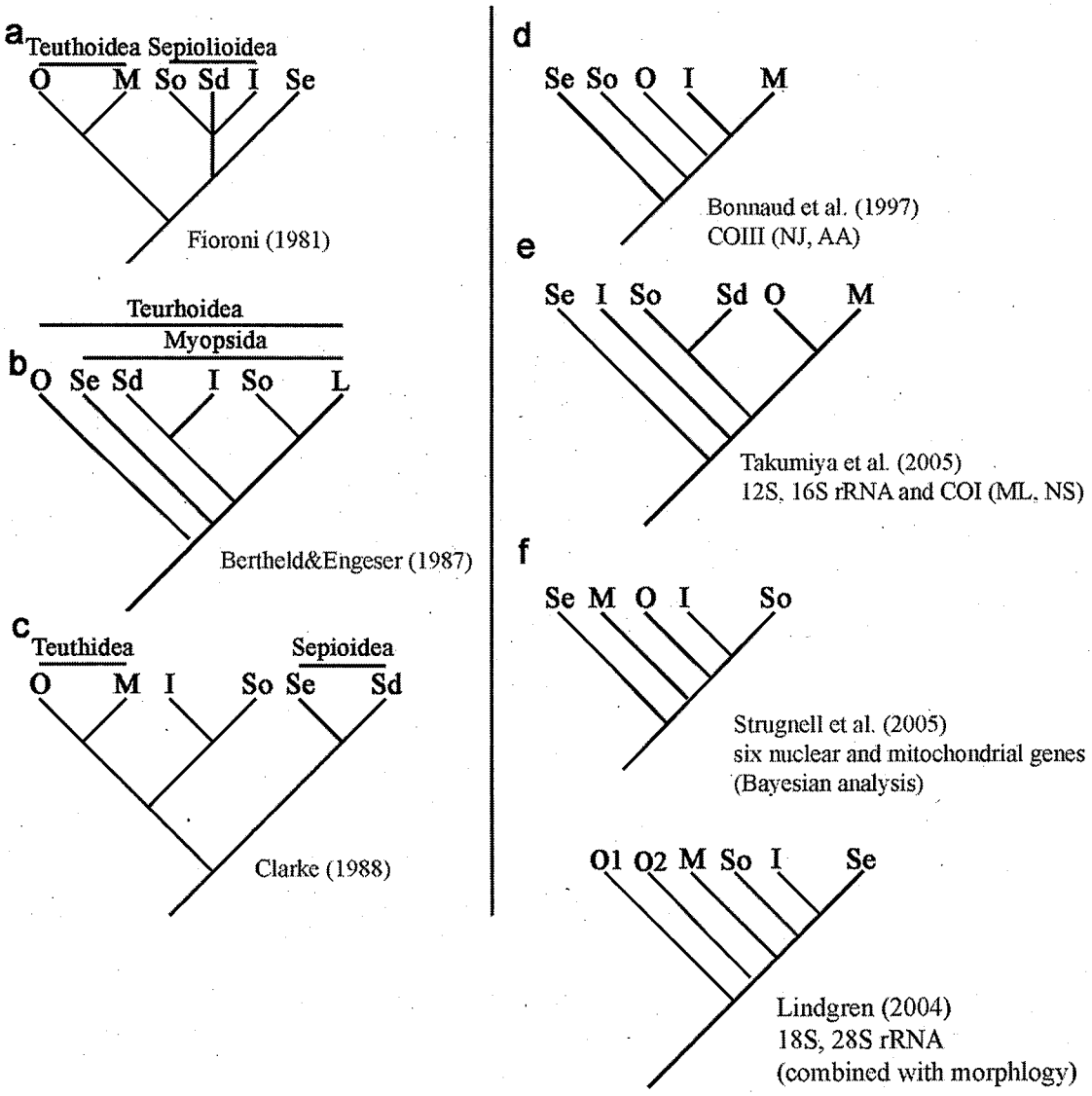
a
Teuthoidea Sepiolioidea
O M So Sd I Se
Fioroni (1981)
Teurhoidea
Myopsida
b
O Se Sd I So L
Bertheld&Engeser (1987)
c
Teuthidea
Sepioidea
O M I So Se Sd
Clarke (1988)
d
Se So O I M
Bonnaud et al. (1997)
COIII (NJ, AA)
e
Se I So Sd O M
Takumiya et al. (2005)
12S, 16S rRNA and COI (ML, NS)
f
Se M O I So
Strugnell et al. (2005)
six nuclear and mitochondrial genes
(Bayesian analysis)
O1 O2 M So I Se
Lindgren (2004)
18S, 28S rRNA
(combined with morphlogy)

**Fig. 1**

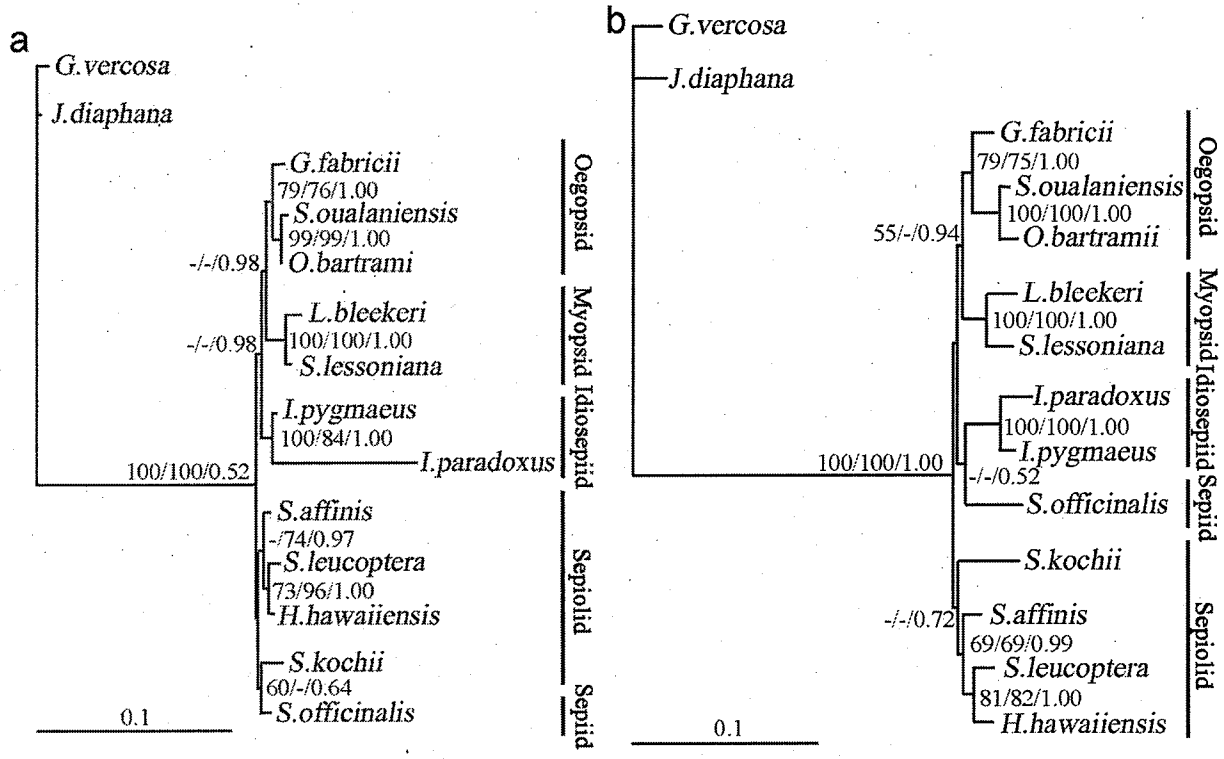
a
G.vercosa
J.diaphana
G.fabricii
79/76/1.00
S.oualaniensis
99/99/1.00
O.bartrami
-/-/0.98
L.bleekeri
100/100/1.00
S.lessoniana
-/-/0.98
I.pygmaeus
100/84/1.00
I.paradoxus
100/100/0.52
S.affinis
-/74/0.97
S.leucoptera
73/96/1.00
H.hawaiiensis
S.kochii
60/-/0.64
S.officinalis
0.1
Oegopsid
Myopsid
Idiosepiid
Sepiolid
Sepiid
b
G.vercosa
J.diaphana
G.fabricii
79/75/1.00
S.oualaniensis
100/100/1.00
O.bartramii
55/-/0.94
L.bleekeri
100/100/1.00
S.lessoniana
I.paradoxus
100/100/1.00
I.pygmaeus
-/-/0.52
S.officinalis
100/100/1.00
S.kochii
S.affinis
69/69/0.99
-/-/0.72
S.leucoptera
81/82/1.00
H.hawaiiensis
0.1
Oegopsid
Myopsid
Idiosepiid
Sepiid
Sepiolid

**Fig. 2**

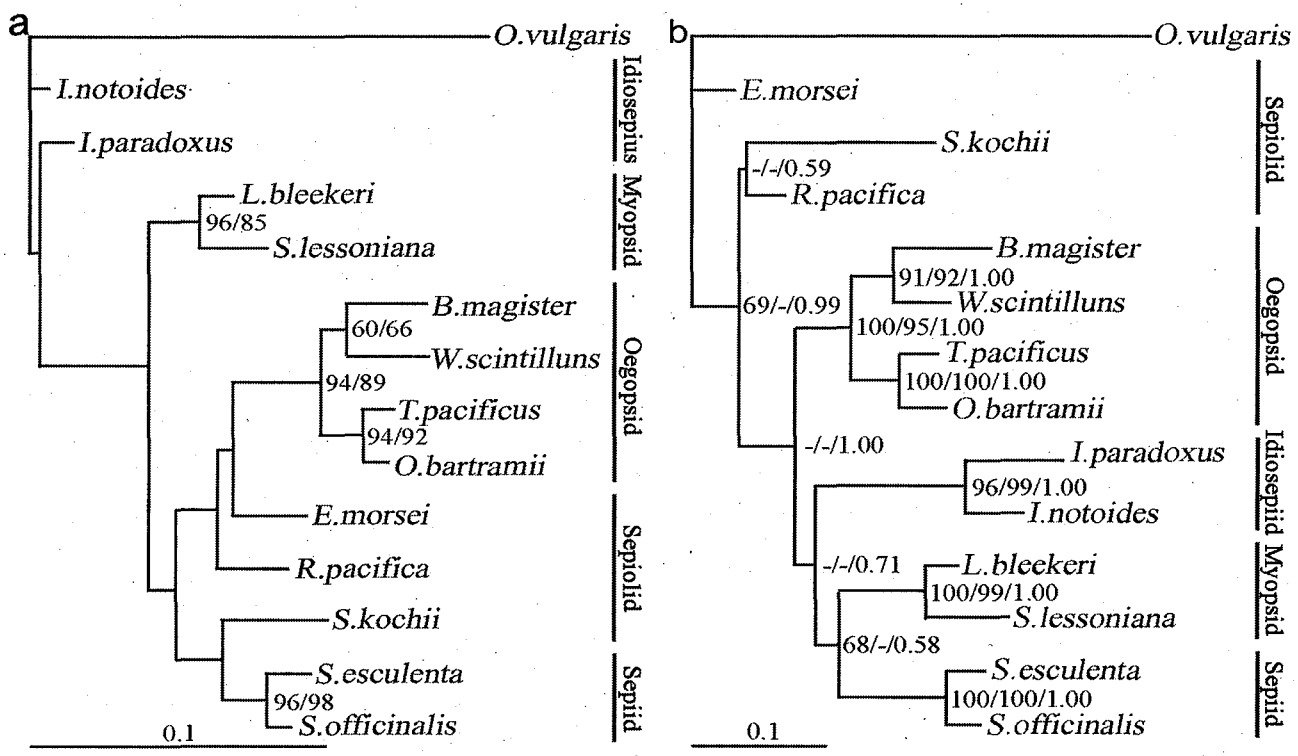
a
O.vulgaris
I.notoides
I.paradoxus
L.bleekeri
96/85
S.lessoniana
B.magister
60/66
W.scintilluns
94/89
T.pacificus
94/92
O.bartramii
E.morsei
R.pacifica
S.kochii
S.esculenta
96/98
S.officinalis
0.1
Idiosepius
Myopsid
Oegopsid
Sepiolid
Sepiid
b
O.vulgaris
E.morsei
S.kochii
-/-/0.59
R.pacifica
B.magister
91/92/1.00
W.scintilluns
69/-/0.99
100/95/1.00
T.pacificus
100/100/1.00
O.bartramii
-/-/1.00
I.paradoxus
96/99/1.00
I.notoides
-/-/0.71
L.bleekeri
100/99/1.00
S.lessoniana
68/-/0.58
S.esculenta
100/100/1.00
S.officinalis
0.1
Sepiolid
Oegopsid
Idiosepiid
Myopsid
Sepiid

**Fig. 3**

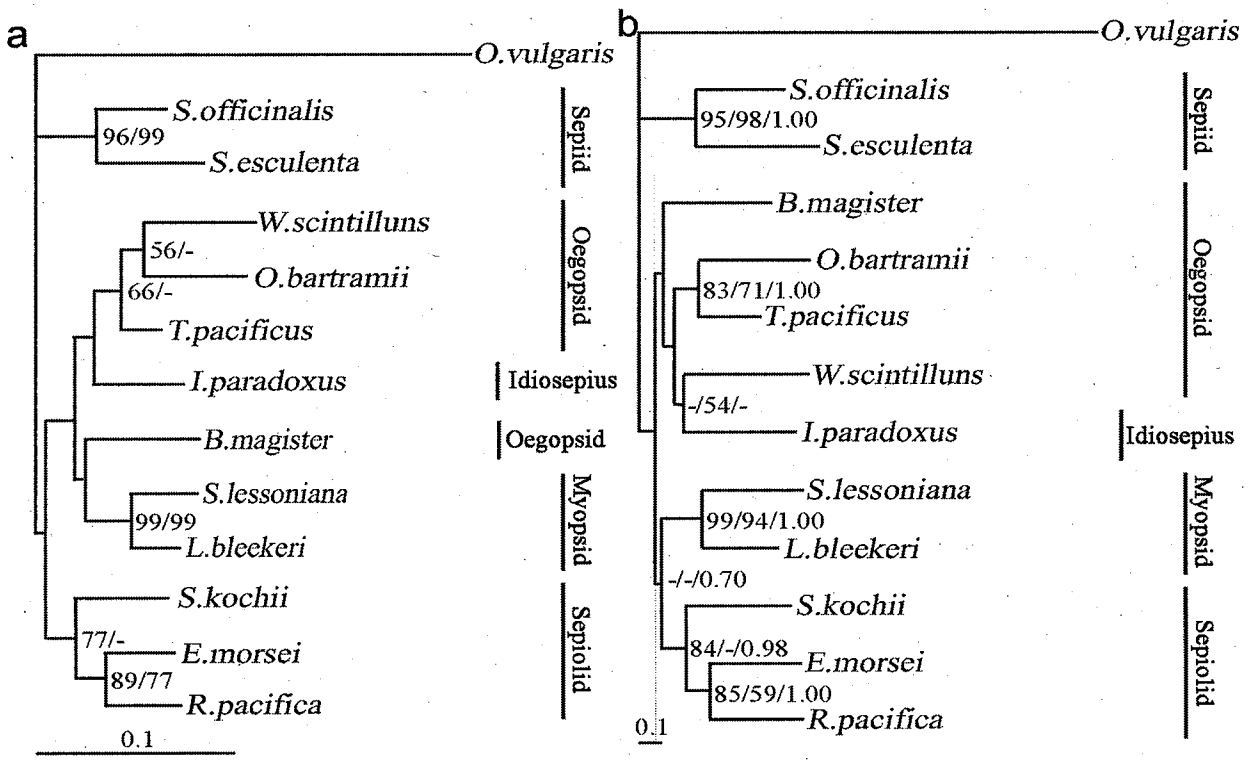
a
O.vulgaris
S.officinalis
96/99
S.esculenta
W.scintilluns
56/-
O.bartramii
66/-
T.pacificus
I.paradoxus
B.magister
S.lessoniana
99/99
L.bleekeri
S.kochii
77/-
E.morsei
89/77
R.pacifica
0.1
Sepiid
Oegopsid
Idiosepius
Oegopsid
Myopsid
Sepiolid
b
O.vulgaris
S.officinalis
95/98/1.00
S.esculenta
B.magister
O.bartramii
83/71/1.00
T.pacificus
W.scintilluns
-/54/-
I.paradoxus
S.lessoniana
99/94/1.00
L.bleekeri
-/-/0.70
S.kochii
84/-/0.98
E.morsei
85/59/1.00
R.pacifica
0.1
Sepiid
Oegopsid
Idiosepius
Myopsid
Sepiolid

**Fig. 4**

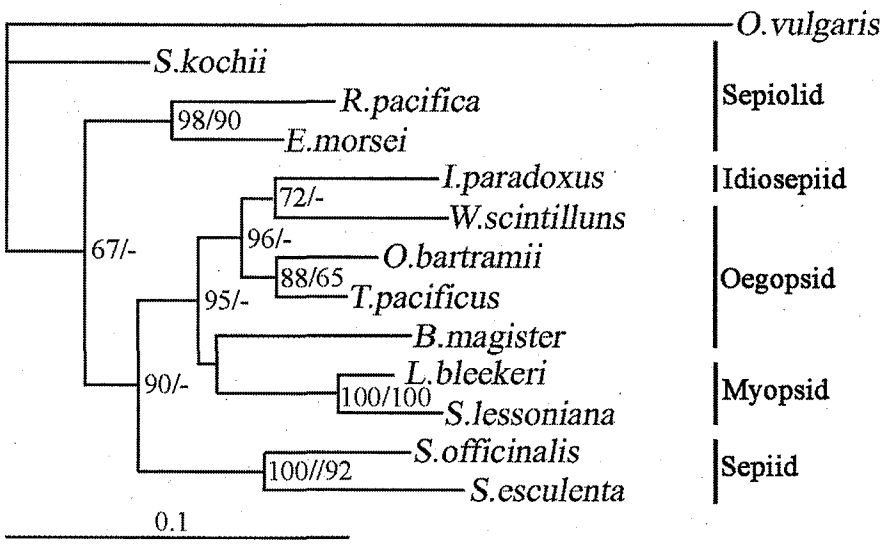
O.vulgaris
S.kochii
R.pacifica
98/90
E.morsei
I.paradoxus
72/-
W.scintilluns
96/-
O.bartramii
88/65
T.pacificus
67/-
95/-
B.magister
L.bleekeri
90/-
100/100
S.lessoniana
S.officinalis
100//92
S.esculenta
0.1
Sepiolid
Idiosepiid
Oegopsid
Myopsid
Sepiid

**Fig. 5**

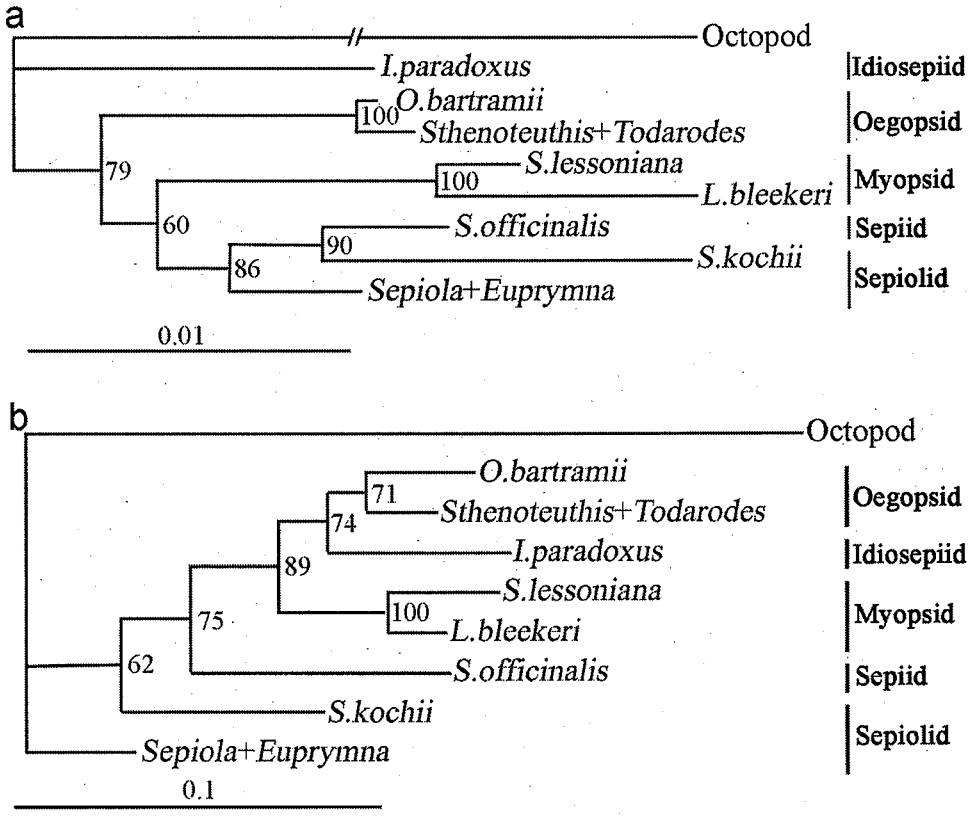
a
Octopod
I.paradoxus
O.bartramii
Sthenoteuthis+Todarodes
S.lessoniana
L.bleekeri
S.officinalis
S.kochii
Sepiola+Euprymna
100
79
100
60
90
86
0.01
Idiosepiid
Oegopsid
Myopsid
Sepiid
Sepiolid
b
Octopod
O.bartramii
Sthenoteuthis+Todarodes
I.paradoxus
S.lessoniana
L.bleekeri
S.officinalis
S.kochii
Sepiola+Euprymna
71
74
89
100
75
62
0.1
Oegopsid
Idiosepiid
Myopsid
Sepiid
Sepiolid

**Fig. 6**

## Chapter 3

Structure and expression of vascular endothelial growth factor receptor of the cephalopod, *Idiosepius paradoxus*

**Abstract**

The cephalopod molluscs have a closed blood-vascular system. Their vascular wall is quite different from the other molluscs in the presence of endothelial cells and is rather similar to the vertebrate vascular wall. However, the cephalopod circulatory system appears to derive from an open blood-vascular system of their ancestor.

Vascular endothelial growth factors (VEGFs) are the major inducers of vascular development and regulator of permeability of blood vessels in vertebrates. Their effects are mediated by tyrosine kinase receptors of the VEGF receptor (VEGFR) family. We cloned a VEGFR-like tyrosine kinase receptor from the pygmy-squid *Idiosepius paradoxus*, using a RACE method. Vertebrate VEGFRs have seven immunoglobulin (Ig) domains in the extracellular region and a split-type tyrosine kinase domain in the intracellular region. The protein blast suggests the intracellular tyrosine kinase domain of the *Idiosepius* VEGFR has a homology to *Branchiostoma* VEGFR (E=1e-62) and *Gallus* VEGFR3/FLT4 (E=5e-59). Phylogenetic analyses using amino acid sequence of the kinase region showed sister relationships between the *Idiosepius* and *Drosophila* VEGFR genes, but in *Idiosepius* six Ig domains existed in their extracellular region. The VEGFR gene was expressed in lateral regions of the vena cava in *Idiosepius* embryos. Subsequently, VEGFR was expressed in retina and peripheral blood vessels in the arms and brain. This suggests that vertebrates and cephalopods share similar developmental pattern of vascular systems. The VEGF pathway might be involved in the secondary innovation of a closed circulatory system lined with endothelium.

## Introduction

Extant cephalopods (nautiluses, octopuses, squids, and cuttlefishes) exhibit numerous morphological peculiarities among molluscs, not only in their nervous system, but also their closed circulatory system. The presence of highly derived circulatory system is essential to maintain organs with high metabolic rate, such as a brain and muscles. Their peculiarities appear to derive from a molluscan ancestor, which had the simple nervous system and the open vascular system. Because of the large differences between the cephalopod and the other molluscs, comparative studies in their development could contribute to understand the molluscan evolution and how the complex body plan as in the cephalopods was formed.

Vascular systems of invertebrates are different from those of vertebrates in the absence of a true endothelium, an adluminal continuous layer of epithelial cells interconnected by special junctional complexes. Large vessels of invertebrates are constituted of spaces located between the basement membranes of endodermal and coelomic epithelia, or between two coelomic epithelia. Cells adhered to the luminal surface of these basement membranes are occasionally present and, in some cases, abundant (reviewed in Casley-Smith 1980; Ruppert and Carle 1983). However, single vessels in the cephalopod are built in a vertebrate fashion, with an endothelial lining on the luminal side of a basal lamina (Budelmann et al. 1997). The basal lamina was surrounded by pericytes, which contain smooth muscle fibers. In the large aorta the muscle fiber cells are arranged in 5 to 7 layers of circular and longitudinal smooth muscle. The wall of blood vessels in the cephalopods is quite similar to the vertebrates,

but have no typical cellular junction among the endothelial cells. The peculiar blood vessels in the cephalopod are in all probably secondarily developed as in holothuroid among echinoderms and in vertebrates among chordates (Ruppert and Carle 1983). The occurrence of endothelia is assumed to be correlated functionally with blood vascular systems acting at high mechanical pressures as are described both for cephalopod and vertebrate systems (Wells 1978; Prosser 1973).

Vascular endothelial growth factors (VEGFs) are the major inducers of vascular development and regulator of permeability of blood vessels in vertebrates (Carmeliet et al., 1996; Ferrara et al., 1996; Ferrara and Davis-Smyth, 1997). The VEGF is related to a platelet derived growth factor (PDGF) family, which has important functions during development of the kidney, lung, blood vessels, and central nervous system (Heldin and Westermark, 1999). The effects of VEGF are mediated by tyrosine kinase receptors of the VEGF receptor (VEGFR) family (Neufeld et al., 1999). The VEGFRs are located on endothelial cells differentiating from mesodermal precursors in the vertebrate. In the embryo of *Drosophila*, an invertebrate organism without endothelial cells or blood vessels, a single VEGFR gene (Pvr) is expressed in developing and matured hemocytes (Cho et al., 2002; Heino et al., 2001). The three ligands, Pvf1-3, are expressed ubiquitously in a whole embryo and are concerned simultaneously with the blood cell development (Cho et al., 2002). The Pvf pathway also mediates border cell guidance during oogenesis (Ducheck et al., 2001). VEGFR-like tyrosine kinase is also known in a cnidarian, *Podocoryne carnea* (Seipel et al., 2004). The VEGFR-like receptor and the ligand are expressed in their gastrovascular system. Thus, the VEGF signalling pathway

probably has originated in the common ancestor of the Cnidaria and Bilateria. Recent studies have revealed that the VEGF signaling pathways are also present in various metazoan animals such as annelids, ascidians, and echinoderms (Duloquin et al., 2007; Eguileor et al. 2001; Gasparini et al., 2007). Tettamanti et al. (2003) reported that the botrytis tissue of the leech, *Hirudo medicinalis,* is responsible to human VEGF protein and then reorganize itself in hollow channels lined by endothelial-like cells in order to allow defensive hemocytes to reach the place of an eventual infection. Thus, VEGF signaling might play a role in epithelial-mesenchymal transition and become involved in inducing endothelium-like tissue in some metazoan lineages (Muñoz-Chápuli et al. 2005).

In the present study, a VEGFR-like tyrosine kinase receptor was cloned from a pygmy-squid, *Idiosepius paradoxus* Ortmann, 1888. The receptor of vascular endothelial growth factor was shown to be expressed in developing blood vessels of *Idiosepius* embryos.

## Materials and Methods

### *Animals*

Adult individuals of *Idiosepius paradoxus* were collected in *Zostrea* beds around the Ushimado Marine Laboratory, Okayama University. The squids were kept in a compact fish tank according to Yamamoto (1988). Spawned eggs were transferred to a petri dish and kept at 18°C. Embryonic stages were determined by using the normal table (see Yamamoto, 1988). A chorion was removed with forceps from embryos from Stage-22

to Stage-27. Prior to stage-21 the chorion was softened and removed according to Yamamoto et al. (2003), because the embryo has a narrow perivitelline space. The embryo of Stage-27 and the subsequent stages were anesthetized in seawater containing 1% ethanol and they were fixed overnight at 4°C in the phosphate buffered saline (PBS) containing 4% paraformaldehyde and 0.1% Tween 20. Embryos for in situ hybridization were progressively dehydrated with gradual series of methanol/PBS+1% Tween20 (25/75, 50/50, 75/25, 100/0). The dehydrated embryos were stored at -20°C until further use.

*Molecular cloning of cDNAs*

A short fragment with homology to the class V receptor tyrosine kinase domains was isolated from *Idiosepius* cDNA using nested degenerate PCR. Primers for the degenerate PCR were designed according to Seipel *et al.* (2004): VEGFR-FI (5'-vgigayytigcngcnmgiaa-3'), VEGFR-FII (5'-aarathksigayttyggnytigc-3'), VEGFR-RI (5'-ccanariaviayiccrtangacca-3'). A 115bp fragment was used to design homologous primers for 5' and 3' RACE.

5'- and 3'-regions of the VEGFR was obtained using a BD SMART RACE cDNA amplification kit (Clontech). Ready-to-use first strand cDNA was synthesized by a manufacture protocol. The cDNA was synthesized from total RNA extracted from a number of hatchling specimens of *I. paradoxus* using an RNeasy mini RNA extraction kit (QIAGEN). The primers used to amplify the VEGFR cDNA extremities were VEGFR-GSP1 (5'-cgcttttcgttgtgtagattctgtgtg-3') and VEGFR-GSP2

(5'-ctgttacaagtctgcggaatatcat-3').

The product of the 5'-RACE reaction was approximately 4kbp and gel-purified using a Freeze extraction column (BIO-RAD Laboratories) and was cloned into a vector using a TOPO cloning kit (Invitrogen). The 1,294bp product of the 3'-RACE reaction was also purified using Freeze extraction column and cloned into a plasmid using a pGEM T-vector system (Promega). Plasmid DNA from transformant colonies was purified with a GenElute™ Plasmid Miniprep kit (Sigma-Aldrich). Both strands of the plasmid DNA were fully sequenced downstream of an insert site by the dideoxy chain-termination method using Applied Biosystems BigDye® Terminators v. 3.1 (Sanger *et al.*, 1997). Primers for the determination of the plasmids were as follows; M13 Forward primer (5'-gtaaaacgacggccagt-3'), 5'-VEGFR SeqPr1 (5'-caatgcacagtgactgatcc-3'), 5'-VEGFR SeqPr2 (5'-tccattgtgtcgacaaagtt-3'), 5'-VEGFR SeqPr3 (5'-tgctgtacatcttgcagaaa-3'), 5'-VEGFR SeqPr4 (5'-ccggctattgaacttccaac-3'), 5'-VEGFR SeqPr5 (5'-ttgtaacgtgacatgcaacc-3'), 5'-VEGFR SeqPr6 (5'-ggggacttatcgttgtcttg-3'), 5'-VEGFR SeqPr7 (caaagcagggagagagcgag), M13 Reverse primer (5'-caggaaacagctatgac-3'), 3'-VEGFR SeqPr1 (5'-atctccaggaatacatgaac-3'), 3'-VEGFR SeqPr2 (5'-cagaatcctgagtcatgtaa-3', 3'-VEGFR SeqPr3 (5'-ggacaaaatacccttaggaa-3'), and 3'-VEGFR SeqPr4 (5'-tgtcactgtcctcttgatgg-3').

Another short fragment was isolated using nested degenerate PCR with the primers VEGFR-FI, VEGFR-FII, and VEGFR-RI. The fragment showed a homology to FGFR

and was used to design homologous primers for RACE. The primers used to amplify the FGFR cDNA extremities were FGFR-GSP1 (5'-cacatcacttttagttgttgtatattttt-3') and FGFR-GSP2 (5'-atattgattactataagaagacaacag-3'). The product of the 5' and 3'-RACE reactions were gel-purified using Freeze extraction columns and was cloned into vectors using pGEM T-vector. Both strands of the plasmid DNA were fully sequenced using following primers; 5'-FGFR SeqPr1 (actgaccgtttcagtcatgg), 5'-FGFR SeqPr2 (taacattttcacaccacgg), 5'-FGFR SeqPr3 (aatcaggagagccatttgttc), and 5'-FGFR SeqPr4 (ggtacaacatcttttatggtt).

To obtain a homolog of Stem Cell Leukemia (SCL)/Tal-1 gene, a short fragment with the homology to a basic helix loop helix domain was isolated from *Idiosepius* cDNA using nested degenerate PCR. Primers for the degenerate PCR were SCL-F1 (acnaaywsnmgtgarmgttgg), SCL-R1 (yttyttrtcnggiggrtg), and SCL-R3 (tttswnryttyttrtc). The primers used to amplify the SCL cDNA extremities were as follows: SCL-GSP1 (ttggtacctaaccgcctcaattccgc), SCL-GSP2 (ggcgtcagcaaaacgtgaacggggc). The product of the 5' and 3'-RACE reactions were gel-purified using Freeze extraction columns and cloned into vectors using pGEM T-vector. Both strands of the plasmid DNA were fully sequenced.

A short fragment with the homology to cytoplasmic Actin gene was isolated from *Idiosepius* cDNA using nested degenerate PCR. Primers for the degenerate PCR were Actin-FIII (5'-ytigayttygarcargaratg-3') and Actin-RII (5'-mgigtdatytcyttytgcat-3'). A

255bp fragment showed a homology to molluscan Actin II and was used to design homologous primers for RACE; Actin II-GSP1 (5'-ttccattccaaggaaagagggttgga-3') and Actin II-GSP2 (5'-ctgccgcttcttcaagctctttgga-3'). The 917bp product of the 5'-RACE and 759bp product of the 3'-RACE reactions were gel-purified using Freeze extraction columns and was cloned into vectors using pGEM T-vector. Both strands of the plasmid DNA were fully sequenced.

*Molecular cloning from database*

VEGF-like growth factor was obtained from the database using tblastn web-search. When *Drosophila* Pvf gene was used as a query, DB912248 was obtained from the tblastn search. The DB912248 gene transcript is similar to the AGAP009549-PA of *Anopheles gambiae* (E=6e-10) and Pvf3, CG34378-PD of *Drosophila melanogaster* (E=4e-06). The primers used to amplify the VEGF cDNA extremities were VEGF-GSP1 (atacctccgtcggctcttgctgaaa) and VEGF-GSP2 (caggatgcaagaaagaatgcccaagtc).

Ets-like transcriptional factor was obtained from the database using tblastn web-search. When *Drosophila* Ets-1 gene was used as a query, DB913089 was obtained from the tblastn search. The DB913089 gene transcript is similar to the v-ets erythroblastosis virus E26 oncogene (blastx, E=8e-67). The EST deposit was used to design homologous primers for RACE. The primers used to amplify the Ets-1 cDNA extremities were Ets1-GSP1 (ttggatagatgtttccgttcggcg) and Ets1-GSP2 (aagttgtatcacctgggagggccg).

*Phylogenetic analysis*

Multiple sequence alignments and phylogenetic analyses based on the neighbor-joining (NJ) method were performed using Clustal X (Thompson et al., 1997). Sequences were aligned with default parameters. Positions with gaps were excluded from the phylogenetic analyses. Accession numbers for protein sequences used in the analyses are as follows: FGFR1-Hs, P11362; FGFR2-Hs, P21802; FGFR3-Hs, P22607; FGFR4-Hs, P22455; FGFRL-Hv, AY193769; Flt3-Hs, P36888; Fms-Hs, P07333; Kit-Hs, P10721; PDGFR -Hs, P16234; PDGFR -Hs, P09619; PTK7-Hs, Q13308; Pvr-Dm, AY079187; U24116-Hv, U24116; VEGFR1- Hs, P17948; VEGFR2- Hs, P35968; VEGFR3-Hs, and P35916.

*In situ hybridization*

A 677bp fragment at 3' end of VEGFR was amplified with primers VEGFR-GSP2 and 3'-VEGFR SeqPr4. A 534bp fragment of 5' fragment of VEGFR was also amplified with primers 5'-VEGFR SeqPr5 and SeqPr7. The PCR products were subcloned into the pGEM T-vector and used as a template to generate digoxigenin (DIG)–labeled antisense probe by *in vitro* transcription with a DIG-RNA labeling kit (Roche) using SP6 RNA polymerase (Roche). The sense control probe was reversely transcribed using T7 RNA polymerase (Roche).

The 5' fragment of Actin II was used to amplify RNA probe. A fragment at 3' end of 412bp was amplified with primers FGFR-GSP2 and 3-FGFR-IntPr

(ctttgagacatggaggaatactggc). A 510bp fragment at 5' end of the FGFR gene was amplified with primers FGFR-GSP1 and 5-FGFR-IntPr (ctgtgaaaatgttaaaagaggatgc).

For probe syntheses a 401bp fragment at 3' end of SCL was amplified with primers SCL-GSP2 and 3-SCL-IntPr (tatgcctgggttaaccggc). A fragment at 5' end of the VEGF gene was amplified with primers VEGF-GSP1 and VEGF 5-VEGF-IntPr (cccatcatgcaccgtgttac). A fragment of the Ets gene was amplified with primers with Ets-GSP1 and GSP2.

In situ hybridization was carried out using following procedures. Embryos were progressively rehydrated in methanol/PBS+1% Tween20. Then they were incubated in PBS containing 6% hydrogen peroxide and 1% Tween20 for 1hr at room temperature (RT). After two washes for 5min in PBST, they were incubated in a detergent mix solution (1% NP-40, 1% SDS, 0.05g/ml deoxycholate, 1mM EDTA, and 0.15M NaCl in 50mM Tris, pH8.0). This step was skipped in the stage-27 and the subsequent stage embryos. The embryos were treated with 10μg/ml proteinase K in PBST, post-fixed at RT for 20 min in PBST containing 4 % paraformaldehyde, and transferred into a hybridization buffer (50 % formamide, 5 x SSC, 1 % SDS, 50 μg/ml yeast tRNA and 50 μg/ml Heparin), followed by two washes in PBST. The embryos in the hybridization buffer were stored at -20 °C.

Embryos were pre-heated at 70-72 °C. After a total of 1 μg RNA probe was added, hybridizations were performed overnight at 70-72 °C. The probes were washed out twice at 70-72 °C in SolutionX (50 % formamide, 2 x SSC and 1 % SDS) for 30min. A

half volume of the SolutionX was removed and replaced to TBST (137 mM NaCl, 50 mM TrisHCl, pH 7.4, and 1% Tween20). Embryos were blocked in TBST containing 10% lamb serum for 2hr at RT. Antibody incubation was performed overnight at 4 °C in TBST containing 1 % lamb serum and 1:5000 dilution of anti-digoxigenin antibody. Detection was performed by immunochemical staining with anti-DIG Fab-AP (Roche) using nitroblue tetrazolium/5-bromo-4-chloro-3-indolyl phosphate (NBT/BCIP, Roche) as a substrate. Before the color detection, embryos were washed three times in TBST containing 2mM levamisol for 10 min, five times in TBST for 1hr and let stand overnight at RT in TBST. Then the embryos were washed three times with freshly prepared NTMT buffer (100 mM NaCl, 100 mM Tris, pH 9.5; 50 mM MgCl2, and 0.1% Tween20). The color reaction was performed in NTMT containing 20μl/ml NBT/BCIP solution for 1-2hr. The stained embryos were let stand overnight in TBST to clear.

For photography, embryos were progressively dehydrated in glycerol/TBST series (30/70, 50/50, 70/30). Specimens were obserbed with an Olympus BX61 microscope.

*Microinjection*

To visualize vasculatures of embryos, rhodamine-conjugated Retrobeads (Lumafluor) was diluted half with PBS and injected into their optic sinus. The injected embryos were let stand for 1hr and then were fixed in 4% paraformaldehyde in PBS. After progressive dehydration in glycerol/TBST series, the embryos were observed with an Olympus BX61 microscope.

**Results**

*Identification of* Idiosepius *VEGFR gene*

The VEGFR cDNA is 5,093 bp with a start codon at position 660 followed by an open reading frame of 3,892 bp, ending at position 4,552. The gene product has 1,299 amino acids (Fig. 1a). The signal sequence is followed by six immunoglobulin (Ig)-like domains, a transmembrane region, and a split type tyrosine kinase domain. The catalytic domain contains tyrosine protein kinase specific active-site and ATP-binding signatures with aspartic and lysine residues that are important for the catalytic activity and ATP binding. The signature sequence GxHxivNLLGACT, typical for split-type kinase domain of receptor tyrosine kinase classes III to V (Grassot et al., 2003), was slightly modified to GqHlnivNLLGAVT in the *Idiosepius* VEGFR, as well as in the *Drosophila* Pvr gene. The protein blast suggests the intracellular tyrosine kinase domain of the *Idiosepius* VEGFR has a homology to *Branchiostoma* VEGFR (E=1e-62) and *Gallus* VEGFR3/FLT4 (E=5e-59).

The *Idiosepius* VEGFR was most closely related to the *Drosophila* Pvr (Fig. 1b), however, the extra-cellular region of the *Idiosepius* VEGFR contains only six Ig-domains. The class V receptors of tyrosine kinase, such as the vertebrate VEGFR and *Drosophila* Pvr genes, are characterized by seven immunoglobulin (Ig)-like domains. Class IV receptors, such as the vertebrate PDGFR, includes five Ig domains. FGFRs are class III receptors characterized by three Ig domains. *Drosophila* has no class IV receptor, so that the Pvr gene is regarded as a homolog of both VEGFR and PDGFR

genes. The phylogenetic tree suggests the *Idiosepius* VEGFR is also a homolog of the VEGFR/PDGFR of vertebrates.

*Expression of the VEGFR gene and vascular formation in* Idiosepius *embryo*

*In situ* hybridizations were performed with the VEGFR cDNA (antisense) probe, ActinII probe (cytoplasmic Actin, for positive controls), and VEGFR sense probe (for negative controls). Transcripts of ActinII were detected in a whole embryo. Non-specific signals were often seen in a shell sac using a VEGFR sense probe.

The embryonic development of the cephalopods is quit different from the other molluscs and characterized by a large amount of yolk, meroblastic blastoderm, possible epibolic gastrulation, and direct development without typical molluscan larval stages. At the beginning of the embryonic development, a blastodisc is formed on animal pole of an ellipsoidal egg (Fig. 2a, b). The blastodisc expands over the surface of yolks (Fig. 2c). When the 2/3 of the egg surface is cellulated, various organ primordials, such as the eyes, statocysts, shell gland, and mouth, appear in the form of ectodermal placode (Fig. 2c). No transcript of the *Idiosepius* VEGFR was detected at the epibolic stages (data not shown). Embryonic body begins to stand up from the egg surface at stage 21. Most stage-21 embryos start to rotate clock-wise in the chorion. The transcripts first appeared at stage-21 embryos (Fig. 3a). In this stage embryo, primary vena cava was observed in the visceral mass using fluorescent beads. The vena cava located in the ventral midline branches into future branchial hearts at the both sides (Fig. 4a). Before systemic and branchial hearts begin to beat, embryonic circulation is driven by peristaltic pulsation of

the outer yolk sac envelope. The VEGFR transcripts appeared in two spots beside the vena cava (Fig. 4a').

By the late organogenesis stage (from stage-24 to -25), a mantle completely covers the gill (Fig. 1e). The rotational movement gradually stops but the yolk sac pulsation becomes stronger. Significant VEGFR-specific signal was observed in developing structures in the arms and the brain in the embryos at stage-25 (Fig. 3b). The expressions were also found in retinas of the embryos. Microangiography showed vena cava, brachial sinus, ophthalmic sinus, and a pair of branchial hearts at the stage-25 embryos. However, no blood vessel was observed in their brain and the arms (Fig. 4b). At stage-27 embryos, blood vessel network appears to surround the arm and flow into the branchial sinus (Fig. 4c). An arm vein is located aboral to arm artery. The VEGFR was still expressed throughout the retina at the stage-27 embryos. However, no transcript was detected in the other organs (Fig. 3c).

Ets-1 transcript was detected in a part of anterior sub-esophageal mass (ASM) of the brain (Fig. 5a). The region probably corresponds in position to an inferior buccal lobe (ibL). The ibL appears as a pair of small masses on the ventro-lateral surface of the buccal mass at stage 22. The Ets-1 transcripts were seen in a surface of optic lobe and a funnel organ, and also observed continuously in the ibL at the later stages (data not shown). FGFR transcript was detected in the arm base regions between arm I and arm II, the buccal mass, and the suckers. (Fig. 5b). No SCL specific signal was detected in the embryos (Fig. 5c).

**Discussions**

The *Idiosepius* VEGFR contains overall characteristics of the class V receptor tyrosine kinase. The class V receptors were characterized by the presence of seven Ig-domains in the extracellular region; however, the *Idiosepius* VEGFR transcripts have only six Ig-domains. Vertebrate VEGFs are closely related to PDGFs and compose a PDGF/VEGF family (Franchini et al., 2006). Invertebrate VEGF genes are also related to the PDGF/VEGF protein family (Tarsitano et al. 2006; Duloquin et al. 2007; Harris et al. 2007). The *Drosophila* Pvr gene, a homolog of the VEGFR/PDGFR gene, contains seven Ig-like domains (Cho et al., 2002). The amino acid numbers of the *Idiosepius* VEGFR (1,299aa) is similar to that of the human KDR/VEGFR-2 (1,356aa). Compared to the human VEGFR gene, the *Idiosepius* VEGFR lacks the 4th Ig-domain. The 2nd and 3rd Ig-domains of the human VEGFRs act as a binding domain to the ligand (Yamazaki and Morita, 2006). The lack of 4th Ig-domain might have no effect on ligand recognition. The molluscan or cephalopod linage has possibly lost one of the seven Ig domains.

*Function of VEGF pathway in cephalopod vascular formation*

The VEGF signaling pathways in the vertebrate vascular endothelial cells are know to be involved in vasculogenesis and angiogenesis. Angiogenesis is a process of blood vessel formation from pre-existing tissues (Risau 1997). Expressions of the *Idiosepius* VEGFR were observed apparently in the blood vessels of the brain and the arms in the stage-25 embryos. This result suggests the VEGFR was associated with the angiogenic

processes of the peripheral blood vessels, such as the arm vessels and the brain arteries. However, the microangiography showed no signal in the corresponding regions in the stage-25 embryos. Subsequently, blood vessel network was observed around their arms of stage-27 embryos. Microangiography probably labeled only the lumens of fully formed and functional vessels, so that this method may not be useful for visualizing active behaviors of vascular cells or their progenitors, such as sprouting and migration of endothelial cells (Cha and Weinstein, 2007). This temporal discrepancy suggests that the VEGF signaling is correlated with early tubular formation in the *Idiosepius* embryo. In vertebrates sprouts possess a tip region where the endothelial cells are organized as a compact string without a lumen (Patan, 2000). Subsequently, the sprouts mature into new vessels with lumen, and a continuous basement membrane is formed (Davis and Senger, 2005). Vascular lumenization of intersegmental arteries in zebrafish is derived from intracellular and intercellular fusion of vacuoles within an endothelial cord (Kamei et al., 2006). Nemerteans have a closed endothelium-lined vascular system; their presumed vessels are formed from solid cords of mesodermal cells through a process identical to the schizocoelic formation of the coelom in protostomes (Turbeville 1991). The expression patterns of the VEGFR indicate that the peripheral blood vessels in *Idiosepius* first appear as an endothelial cord, then penetrate into the tissue, and finally lumenize. The cephalopod VEGFR may contribute to their angiogenic processes before lumenization.

In the vertebrates vasculogenesis gives rise to the heart and the primitive single

large artery and vein, which are generated by the differentiation from the lateral mesoderm (Risau and Flamme, 1995; Patan, 2000). In cephalopods the circulatory system appears as a narrow hemal space between the yolk syncytium and the envelope (Boletzky, 1975). The embryonic sinuses smoothly shift from narrow spaces to tubules, the first of which are the primitive paired venae cavae. Microangiography showed that blood flows through the primitive vena cava to a visceral mass in the *Idiosepius* embryo. The embryonic circulation is driven by the peristaltic pulsation of the outer yolk sac. Ultrastructural studies showed that the octopus vascular system appears initially as lacunar (schizocoelic) spaces, and subsequently is surrounded by a basal lamina and endothelium (Boletzky, 1975; Boletzky, 1987). The *Idiosepius* VEGFR was expressed in both sides of the primitive vena cava of stage-21 embryos. Fioroni (1978) reported that "coelom-mesoblast complex" is located beside primitive vena cava in *Octopus* embryos. The progenitor of endothelial cells might originate out of ventral side of the body and move into the primary tube of the vein. In several invertebrate groups, such as annelids, molluscs, echinoderms, and cephalochordates, a type of hemocyte, called as amoebocyte, has been shown to adhere to the basement membrane (Fernández et al. 1992; Smiley 1994; Ruppert 1997). In cephalopods as well as in holothurians the adhered amoebocytes are so abundant that they show the appearance of endothelium (Smiley, 1994; Budelmann et al., 1997). Ruppert and Carle (1983) have claimed that these animal groups actually bear an endothelium-lined vascular system. On the other hand, Muñoz-Chápuli et al. (2005) assumed that a true endothelium must be characterized by the presence of intercellular junctions, and the adherent amoebocytes

are free cells that migrate throughout the inner surface of the vessels. The expression of the VEGFR in the cephalopod indicates that the cephalopod endothelium is derived from a hemocyte progenitor, although the peripheral blood vessels are formed as solid cords, and later lumenized in their angiogenic process.

A pair of branchial heart is a specific organ of cephalopods, it pumps blood into gills (Budelmann et al., 1997). These organs are developed ontogenetically and phylogenetically from veins (Fiedler and Schipp, 1987). In mid-stage (stage XII) of *Octopus* embryonic development, branchial hearts appear as lumens on both sides within the mesodermic masses underlying the gill buds (Boletzky 1987). The rudimentary branchial hearts begin to pulsate soon after formed a lumen and before a systemic heart actively beats. The expressions of the VEGFR support the assertion that the branchial hearts have the same origin as the blood vessels.

Most invertebrates have no endothelium in vascular walls, so the cephalopod represents an exceptional instance of invertebrates having a vertebrate type blood vessel. The blood vessels of the cephalopods, regardless of the caliber and the type, have fundamentally three layers, the pericyte, basal lamina, and endothelium (Budelmann et al., 1997). The wall structure is similar to that in the vertebrates, although the endothelium is often incomplete and has no typical cellular junctions (Schipp, 1987). Tubular sprouting is the most important angiogenic mechanism in the vertebrates, and involves to the development and growth of new vessels starting from evagination of the

endothelial wall. In the cephalopod aortic formation occurs after the embryonic body stands up on the yolk. Aorta cephalica develops from a systemic heart at late embryonic stage and runs down dorsal side of the body. Brain and arm arteries branch from the aorta cephalica by the angiogenesis-like process. The VEGF is a critical inducer of proliferation, migration, sprouting, and tube formation in tissues during the angiogenesis (Tammela et al., 2005). In metazoans, the branching of tubular structures occurs in various organs of different embryonic origin, such as, the ectodermally derived *Drosophila* tracheas (Ghabrial et al. 2003), endodermally derived tubules of jellyfish (Seipel et al. 2004), ectodermally derived vessels of colonial ascidian *B. schlosseri* (Gasparini et al. 2007), and mesodermally derived vertebrate vessels (Risau 1997). Although the *Drosophila* tracheas are formed using a FGF pathway, the VEGF signal accompanies these sprouting structure. On the other hand, the VEGF signal pathway takes part in the formation of solid nerves (Weinstein 2005) and in development of non-branching tubular structures, such as of vertebrate myocardium and *Drosophila* salivary glands (Tomanek et al. 2006; Harris et al. 2007). Thus, an identical germ layer origin is not required for formation of the tubular or solid structures using the VEGF pathway. Seipel et al. (2004) hypothesized that the tube formation in cnidarians probably reflects the ancestral function of the VEGF-signaling pathway. The VEGF pathway might have co-opted during metazoan evolution in several morphogenetic/differentiative processes. The presence of VEGFR in the cephalopod vascular formation is likely associated with secondary derivation of cephalopod vasculature from a molluscan ancestor, although the VEGF expression is not reported in

the other molluscs. Some transcription factors are known to be upstream and enhancer of the vertebrate Flk-1 (Kappel, et al., 1999). Ets-1 or SCL are critical for the endothelium-specific expression of Flk-1 (Kappel et al., 2000). Their homologs were not expressed in the *Idiosepius* embryos, but the SoxE expressions were observed in the blood vessels of *Octopus* embryo (Shigeno, personal communication). This result suggests that the cephalopod VEGF pathway is regulated by some regulatory genes, which are different from those of vertebrates. Secondary derivations of the cephalopod endothelium are possibly supported by the presence upstream regulatory genes of VEGF pathway.

*Possible function of the cephalopod VEGF pathway in retinal development*

The retina is one of the organs abundant with blood vessels. The VEGF is related to the neovascular diseases including diabetic retinopathy (Adamis *et al.,* 1994; Aiello *et al.,* 1995; Amin *et al.,* 1997). In these diseases Flk-1/VEGFR-2 is expressed in microvascular endothelial cells and Flt-1/VEGFR-1 is expressed in both endothelial cells and pericyte (Nomura *et al.,* 1995; Takagi *et al.,* 1996). The cephalopod eye is highly developed and similar to the vertebrate eye, as well as the circulatory system. However, the retina appears as an ectodermic placode in the cephalopod embryos, not as in the vertebrate embryos. Many blood vessels were observed within the *Idiosepius* retinae, as Budelmann et al. (1997) reported in the other cephalopod retina. However, the VEGFR expression was observed in the whole retina of the *Idiosepius* embryos, not only in the endothelium. The expression may be correlated to retinal development in the

cephalopod. The Pax-6 has some conserved roles in development of brains and eyes of metazoan animals, and also in development of retina of a squid, *Euprymna scolopes* (Hartmann et al., 2003). The Pax-6 in *Euprymna* expressed in the eye primordia prior to closure of eye vesicles. The *Idiosepius* VEGFR begins to express in the retina after closure of eye vesicles. Thus, the VEGFR may not contribute to early development of neural retina.

In the vertebrates VEGF-positive endothelial cells and PDGF-positive glial cells coordinately regulate retinal development. PDGF-A is expressed by ganglion cells in developing retina (Fruttiger et al., 1996, 2000) and has a role in the recruitment of PDGFRα-positive astrocytes to the retina. The astrocytes populate the retinal surface during late embryonic stage in the vertebrates (Huxlin et al., 1992). They form a network across the retinal surface that subsequently works as a scaffold for angiogenic sprouting. The PDGFRβ is involved in the developmental processes in the pigmented and neural retina, the lens, corneal epithelium, and the mesenchyme (Božanić et al., 2006; Li et al. 2007; Nagineni et al. 2005). Additionally, its appearance in the human eye microvasculature might indicate its role in the development of the eye blood vessels (Mudhar et al. 1993). The class III tyrosine kinase receptor, such as PDGFR, have never been reported in the invertebrates. The cephalopod VEGFR may contribute to glial development in the similar fashion to the vertebrate PDGFRs.

**Acknowledgement**

We thank Prof. T. Sakamoto and Mr. W. Godo of Ushimado Marine laboratory,

Okayama University for their kind help in collecting specimens. We also would like to express our gratitude to Prof. H. Nishida and his colleagues of Department of Biology, Osaka University, and Dr. S. Shigeno of the University of Chicago for their valuable suggestions.

This study was supported by the grants from the Research Institute of Marine Invertebrate Foundation and from the Japan Society for the Promotion of Science (Research grant 18570087).

**References**

Adamis, A. P., Miller, J. W., Bernal, M. T., D'Amico, D. J., Folkman, J., Yeo, T. K., and Yeo, K. T. (1994) Increased vascular endothelial growth factor levels in the vitreous of eyes with proliferative diabetic retinopathy. American Journal of Ophthalmolology, 118: 445– 450.

Aiello, L. P., Pierce, E. A., Foley, E. D., Takagi, H., Chen, H., Riddle, L., Ferrara, N., King, G. L., and Smith, L. E. (1995) Suppression of retinal neovascularization in vivo by inhibition of vascular endothelial growth factor (VEGF) using soluble VEGF-receptor chimeric proteins. Proceedings of the National Academy of Sciences of the USA., 92: 10457–10461.

Amin, R. H., Frank, R. N., Kennedy, A., Eliott, D., Puklin, J. E., and Abrams, G. W. (1997) Vascular endothelial growth factor is present in glial cells of the retina and optic nerve of human subjects with nonproliferative diabetic retinopathy. Investigative Ophthalmology and Visual Science, 38: 36–47.

Boletzky, S. v. (1975) A contribution of the study of yolk absorption in the Cephalopoda. Zeitschrift fur Morphologie der Tiere, 80: 229-246.

Boletzky, S. v. (1987) Ontogenetic and phylogenetic aspects of the cephalopod circulatory system. Experientia, 43: 478-483.

Božanić, D., Bočina, I., Saraga-Babić, M. (2006) Involvement of cytoskelatal proteins and growth factor receptors during development of the human eye. Anatomical Embryology, 211: 367–377.

Budelmann, B. U., Schipp, R., and Boletzky, S. v. (1997) Cephalopoda. In F. W.

Harrison and E. E. Ruppert (eds.). Microscopic Anatomy of Invertebrates. Vol. 6A: Mollusca II. Wiley-Liss, New York, pp. 119–414.

Carmeliet, P., Ferrata, V., Breier, G., Pollefeyt, S., Kiecken, L., Gertsenstein, M., Fahrig, M., Vandenhoeck, A., Harpal, K., Eberhardt, C., Declercq, C., Pawling, J., Moons, L., Collon, D., Risau, W., and Nagy, A. (1996) Abnormal blood vessel development and lethality in embryo lacking a single VEGF allele. Nature. 380: 435-439.

Casley-Smith, J. R. (1980) Comparative fine structure of the microvasculature and endothelium. In: Altura, B. M., Davis, E., Harder, H. (eds.). Vascular endothelium and basement membranes. Basel, Karger, pp. 1–44.

Cha Y. R. and Weinstein B. M. (2007) Visualization and experimental analysis of blood vessel formation using transgenic zebrafish. Birth Defects Research (Part C), 81: 286–296.

Cho, N. K., Keyes, L., Johnson, E., Heller, J., Ryner, L., Karim, F., Krasnow, M. A. (2002) Developmental control of blood cell migration by the Drosophila VEGF pathway. Cell, 108(6): 865-876.

Davis and Senger (2005)

Ducheck, P., Somogyi, K., Jekely, G., Beccari, S., and Rorth, P. (2001) Guidance of cell migration by the *Dorosophila* PDGF/VEGF receptor. Cell, 107: 17-26.

Duloquin, L. Lhomond, G., and Gache, C. (2007) Localized VEGF signaling from ectoderm to mesenchyme cells controls morphogenesis of the sea urchin embryo skeleton. Development, 134: 2293-2302.

Eguileor, M., Grimaldi, A., Tettamanti, G., Ferrarese, R., Congiu, T., Protasoni, M.,

Perletti, G., Valvassori, R., and Lanzavecchia, G. (2001) *Hirudo medicinalis*: A new model for testing activators and inhibitors of angiogenesis. Angiogenesis, 4: 299–312.

Evans, C. J., Hartenstein, V., and Banerjee, U. (2003) Thicker than blood: conserved mechanisms in *Drosophila* and vertebrate hematopoiesis. Developmental Cell, 5: 673–690.

Fernández, J., Téllez, V., and Olea, N. (1992) Hirudinea. In F. W. Harrison and F. S. Chia (eds.). Microscopic Anatomy of Invertebrates. Vol. 7: Annelida. Wiley-Liss, New York, pp. 323–393.

Ferrara, N., and Davis-Smyth, T. (1997) The biology of vascular endothelial growth factor. Endocrine Reviews, 18: 4–12.

Ferrara, N., Carver-Moore, K., Chen, H., Dowd, M., Lu, L. O'Shea, K. S., Powell-Braxton, L., Hillan, K. J. and Moore, M. W. (1996) Heterozygous embryonic lethality induced by targeted inactivation of the VEGF gene. Nature, 380: 439-442.

Fiedler, A., and Schipp, R. (1987) The role of the branchial heart complex in circulation of coleoid cephalopods. Experientia, 43: 544-553.

Fioroni, P. (1978) Cephalopoda, Tintenfische. In F. Seidel, (eds.). Morphogenese der Tiere, Erste Reihe, Deskriptive Morphologenese, Lieferung 2:G5-I. Gustav Fisher Verlag, New York.

Franchini, A., Malagoli, D., and Ottaviani, E. (2006) Cytokines and invertebrates: TGF-beta and PDGF. Current Pharmaceutical Design, 12: 3025–3031.

Fruttiger, M., Calver, A. R., Kruger, W. H., Mudhar, H. S., Michalovich, D., Takakura, N., Nishikawa, S. I., and Richardson, W.D. (1996) PDGF mediates a neuron-astrocyte interaction in the developing retina. Neuron, 17: 1117–1131.

Fruttiger, M., Calver, A. R., Richardson, W. D. (2000) Platelet-derived growth factor is constitutively secreted from neuronal cell bodies but not from axons. Current Biology, 10: 1283–1286.

Gasparini, F., Longo, F., Manni, L., Burighel, P. and Zaniolo, G. (2007) Tubular sprouting as a mode of vascular formation in a colonial ascidian (Tunicata). Developmental Dynamics, 236: 719 –731.

Gerhardt, H., Golding, M., Fruttiger, M., Ruhrberg, C., Lundkvist, A., Abramsson, A., Jeltsch, M., Mitchell, C., Alitalo, K., Shima D., and Betsholtz, C. (2003) VEGF guides angiogenic sprouting utilizing endothelial tip-cell filopodia. Journal of Cell Biology, 161:1163–1177.

Ghabrial (2003)

Grassot, J., Mouchiroud, G., and Perrière, G. (2003) RTKdb: database of receptor tyrosine kinase. Nucleic Acids Research, 31:353-358.

Hartmann, B., Lee, P.N., Kang, Y.Y., Tomarevc, S., de Couetb, H.G., and Callaertsa, P. (2003) Pax6 in the sepiolid squid Euprymna scolopes: evidence for a role in eye, sensory organ and brain development. Mechanisms of Development, 120: 170-183.

Harris, K. E., Schnittke, N., and Beckendorf, S. K. (2007) Two ligands signal through the *Drosophila* PDGF/VEGF receptor to ensure proper salivary gland positioning. Mechanisms of Development, 124: 441–448.

Heino, T. I., Kärpänen, T., Wahlström, G., Pulkkinen, M., Eriksson, U., Aitalo, K., and Roos, C. (2001) The *Dorosophila* VEGF receptor homolog is expressed in hemocytes. Mechanisms of Development, 109: 69-77.

Heldin, C. H. and Westermark, B. (1999) Mechanism of action and in vivo role of platelet-derived growth factor. Physiological Reviews, 79: 1283–1316.

Huxlin, K. R., Sefton, A. J., and Furby, J. H. (1992) The origin and development of retinal astrocytes in the mouse. Journal of Neurocytology, 21(7): 530-44.

Isogai, S., Horiguchi, M., and Weinstein, B. M. (2001) The vascular anatomy of the developing zebrafish: An atlas of embryonic and early larval development. Developmental Biology, 230: 278-301.

Kamei, M., Saunders, W. B., Bayless, K. J., Dye, L., Davis, G. E. and Weinstein, B. M. (2006) Endothelial tubes assemble from intracellular vacuoles in vivo. Nature 442: 453–456.

Kappel, A., Rönicke, V., Damert, A., Flamme, I., Risau, W. and Breier, G. (1999) Identification of vascular endothelial growth factor (VEGF) receptor-2 (Flk-1) promoter/enhancer sequences sufficient for angioblast and endothelial cell-specific transcription in transgenic mice. Blood, 93: 4284-4292.

Kappel, A., Schlaeger, T. M., Flamme, I., Orkin, S. H., Risau, W. and Breier, G. (2000) Role of SCL/Tal-1, GATA, and Ets transcription factor binding sites for the regulation of *Flk-1* expression during murine vascular development. Blood, 96: 3078-3085.

Kendel, R. L., and Thomas, K. A. (1995) Inhibition of vascular endothelial cell growth

factor activity endogenously encoded soluble receptor. Proceedings of National Academy of Sciences of the USA., 90: 10705-10709.

Kendel, R. L., Wang, G., and Thomas, K. A. (1996) Identification of a natural soluble form of the vascular endothelial growth factor receptor, FLT-1, and its heterodimerization with KDR. Biochemical and Biophysical Research Communications, 226: 324-328.

Lee, P. N., Callaerts, P., de Couet, H. G. and Martindale, M. Q. (2003) Cephalopod Hox genes and the origin of morphological novelties. Nature. 424: 1061-1066.

Li, R., Maminishkis, A., Wang, F. E. and Miller, S. S. (2007) PDGF-C and -D Induced proliferation/migration of human RPE is abolished by inflammatory cytokines. Investigative Ophthalmology and Visual Science, 48(12): 5722-5732.

Mudhar, H. S., Pollock, R. A., Wang, C., Stiles, C. D., and Richardson, W. D. (1993) PDGF and its receptors in the developing rodent retina and optic nerve. Development, 118:539–552.

Muñoz-Chápuli, R., Carmona, R., Guadix, J. A., Macías, D. and Pérez-Pomares, J. M. (2005) The origin of the endothelial cells: an evo-devo approach for the invertebrate/vertebrate transition of the circulatory system. Evolution and Development, 7: 351-358.

Nagineni, C. N., Kutty, V., Detrick, B., Hooks, J. J. (2005) Expression of PDGF and their receptors in human retinal pigment epithelial cells and fibroblasts: regulation by TGF-beta. Journal of Cell Physiology. 203: 35–43.

Neufeld, G., Cohen, T., Gengrinovitch, S., and Poltorak, Z. (1999) Vascular endothelial

growth factor (VEGF) and its receptors. FASEB Jornal, 13: 9–22.

Nomura, M., Yamagishi, S., Harada, S., Hayashi, Y., Yamashima, T., Yamashita, J., and Yamamoto, H. (1995) Possible participation of autocrine and paracrine vascular endothelial growth factor in hypoxia-induced proliferation of endothelial cells and pericytes. Journal of Biochemistry, 270: 28316 –28324.

Patan, S. (2000) Vasculogenesis and angiogenesis as mechanisms of vascular network formation, growth and remodeling. Journal of Neurooncology 50: 1–15.

Prosser, C. L. (1973) Comparative Animal Physiology. 3rd ed. WB Saunders, Philadelphia.

Risau, W. (1997) Mechanisms of angiogenesis. Nature 386: 671–674.

Risau W, and Flamme I. (1995) Vasculogenesis. Annual Review of Cell and Developmental Biology, 11:73–91.

Ruppert, E. E. (1997) Cephalochordata (Acrania). In F. W. Harrison and E. E. Ruppert (eds.). Microscopic Anatomy of Invertebrates. Vol. 15: Hemichordata, Chaetognatha and the Invertebrate Chordates. Wiley-Liss, New York, pp. 349–504.

Ruppert, E. E. and Carle, K. J. (1983) Morphology of the metazoan circulatory systems. Zoomorphology, 103: 193-208.

Sanger, F., Nicklen, S., Coulson, A. R. (1977) DNA sequencing with chain-terminating inhibitors. Proceedings of the National Academy of Sciences of the USA., 74: 5436-5467.

Schipp, R. (1987) The blood vessel of cephalopods. A comparative morphological and functional survey. Experientia, 43: 525-537.

Seipel, K., Eberhatdt, M., Müller, P., Pescia, E., Yanze, N., and Schmid,V. (2004) Homologs of vascular endothelial growth factor and receptor, VEGF and VEGFR, in jellyfish *Podocoryne carnea.* Developmental Dynamics, 231: 303-312.

Shigei, T., Tsuru, H., Ishikawa, N., and Yoshipka, K. (2001) Absence of endothelium in invertebrate blood vessels: significance of endothelium and sympathetic nerve/medial smooth muscle in the vertebrate vascular system. Japanese Journal of Pharmacology, 87: 253-260.

Smiley, S. (1994) Holothurioidea. In F. W. Harrison and F. S. Chia (eds.). Microscopic Anatomy of Invertebrates. Vol. 14: Echinodermata. Wiley-Liss, New York, pp. 401–471.

Takagi, H., King, G. L., and Aiello, L. P. (1996) Identification and characterization of vascular endothelial growth factor receptor (Flt) in bovine retinal pericytes. Diabetes, 45: 1016 –1023.

Tammela, T., Enholm, B., Alitalo, K., Paavonen, K. (2005) The biology of vascular endothelial growth factors. Cardiovascular Research, 65: 550 –563.

Tarsitano, M., De Falco, S., Colonna, V., McGhee, J. D., and Persico, M. G. (2006) The *C. elegans* pvf-1 gene encodes a PDGF/VEGF-like factor able to bind mammalian VEGF receptors and to induce angiogenesis. FASEB Journal, 20: 227–233.

Tettamanti, G., Grimaldi, A., Valvassori, R., Rinaldi, L. and de Eguileor, M. (2003) Vascular endothelial growth factor is involved in neoangiogenesis in *Hirudo medicinalis* (Annelida, Hirudinea). Cytokine, 22: 168-179.

Thompson, J. D., Gibson, T. J., Plewniak, F., Jeanmougin, F., and Higgins, D. G.

(1997) The ClustalX windows interface: flexible strategies for multiple sequence alignment aided by quality analysis tools. Nucleic Acids Research, 24: 4876-4882.

Tiozzo, S., Voskoboynik, A., Brown, F. D., and De Tomaso A. W. (2008) A conserved role of the VEGF pathway in angiogenesis of an ectodermally-derived vasculature. Developmental Biology, 315: 243-255.

Tomanek, R. J., Ishii, Y., Holifield, J. S., Sjogren, C. L., Hansen, H. K., and Mikawa, T. (2006) VEGF family members regulate myocardial tubulogenesis and coronary artery formation in the embryo. Circulation Research, 98: 947–953.

Turbeville, J. M. (1991) Nemertinea. In F. W. Harrison and B. J. Bogitsh (eds.) Microscopic Anatomy of Invertebrates. Vol. 3: Platyhelminthes and Nemertinea. Wiley-Liss, New York, pp. 3859–4328

Weinstein, B. M. (2005) Vessels and nerves: marching to the same tune. Cell, 120(3): 299-302.

Wells, M. J. (1978) Octopus. Physiology and Behaviour of an Advanced Invertebrate. London: Chapman and Hall. 417 pp.

Yamazaki, Y. and Morita, T (2006) Molecular and functional diversity of vascular endothelial growth factors. Molecular Diversity, 10: 515–527.

Yamamoto, M. (1988) Normal embryonic stages of the pygmy cuttlefish, *Idiosepius pygmaeus paradoxus* Ortmann. Zoological Science, 5(5): 989-998.

Yamamoto, M., Shimazaki, Y and Shigeno, S. (2003) Atlas of embryonic brain in the pygmy squid, *Idiosepius paradoxus*. Zoological Science, 20: 163-179.

**Figure legends**

**Fig. 1 a,** Amino acid sequence of the *Idiosepius* VEGFR. **b,** The phylogenetic relationship of receptor tyrosine kinase domains. The split kinase domain receptors have three (class III), five (class IV), and seven (class V) Ig-like domains. PTK7 is a regular tyrosine kinase receptor with seven Ig-like domains and used as an outgroup. The *Idiosepius* VEGFR is most closely related to *Drosophila* Pvr gene, although the gene has only six immunoglobulin domains. Numbers at the nodes indicate the bootstrap support values (calculated by 1,000 repetition). Bar length indicates the number of substitution per site.

**Fig. 2** Normal embryonic development of *Idiosepeius paradoxus.* **a,** First cleavage plane (arrow) corresponds to the median plane of the Stage-2 embryo. **b,** Mesoendoderm formed by invagination of marginal cells of blastodisc (bd) at Stage-10. **c,** About half of the egg surface is cellulated at Stage-16. Subsequently, primordia of mantle, eyes, shell gland, mouth, and arms begin to be formed on the blastodisc (bd) as placodes. **d,** Embryobic body begins to stand up from the yolk sac (yo) at Stage-16. **e,** The yolk sac (yo) is completely separated from the embryonic body at Stage-24. **f,** Hatchling (Stage-30). Young squid hatches after their yolk mass is lost. Embryonic stages were determined using the normal table of Yamamoto (1988).

**Fig. 3** Expression of VEGFR gene in *Idiosepius* embryos. **a-c,** *In situ* hybridization with probes for vascular endothelial growth factor receptor (VEGFR). **d,** Control experiment with sense probes for VEGFR. Non-specific signal is detected at the

shell sac (sh). **e,** Positive control with probes for ActinII. **a,** Stage-21. **b,** Stage-24. **c,** Stage-27. **d,** Stage-24. **e,** Stage-24. **b'**, Enlarged view of an arm vein in Stage-24. **b''** Expression in a pair of branchial hearts of mantle-removed specimen in Stage-24. (a) Expression of the VEGFR emerged in the visceral mass of the embryo. The VEGFR positive cells are located lateral side of primary vena cava (vc) and grow down into the mantle and head. (b) The VEGFR gene is strongly expressed by developing vessels (arrowheads) in their all arms and part of brain, and optic lobe (ol). The expression was also observed in the retina (r) and the pair of branchial hearts (bh). (c) The VEGFR remains to be expressed in the retinal cells. Yolk sacs (yo) are removed in b, c, e. All embryos are viewed from ventral with posterior to the upper side, except (b), which is seen from dorsal. Scale bars = 100μm.

**Fig. 4** Embryonic circulatory system of *Idiosepius* embryos visualized by microinjection of rhodamine-conjugated beads. **a,** Stage-21. **b,** Stage-24. **c,** Stage-27. **a',** Expression of the VEGFR in the Stage-21 embryo. **a'',** merged image of a and a'. **b',** Cells of the body are stained with DAPI. (a) The VEGR positive cells are located laterally to primary vena cava (vc). (b) Optic sinuses surrounding the optic lobe (ol), brachial sinus (bs), pair of branchial hearts (bh), and vena cava (vc) are visualized by fluorescent beads injection, but no vessel appeared in the arms and brain at Stage-24. (c) Peripheral blood vessels are observed within the arms (arrowhead) and mantle (arrows). Yolk sac (yo) was removed in (b). All embryos are viewed from ventral side with posterior to the upper side. Bars = 100μm.

**Fig. 5** Expression of Ets-like, FGFR, and SCL genes by *in situ* hybridization of the *Idiosepius* genes. **a-c,** Stage-24. (a) Expression of Ets-like gene was observed in a part of the opitic lobes (ol) and in their anterior subesophageal mass (asm). (b) The FGFR was expressed in the arm bases (arrowheads) between arm I (aI) and arm II (aII), the buccal mass (bm), and the suckers. Non-specific signal is detected at the shell sac (sh). (c) No SCL expression was observed. Ventral view in all pictures. Yolk sac (yo) is removed in (b). Bars = 100μm.

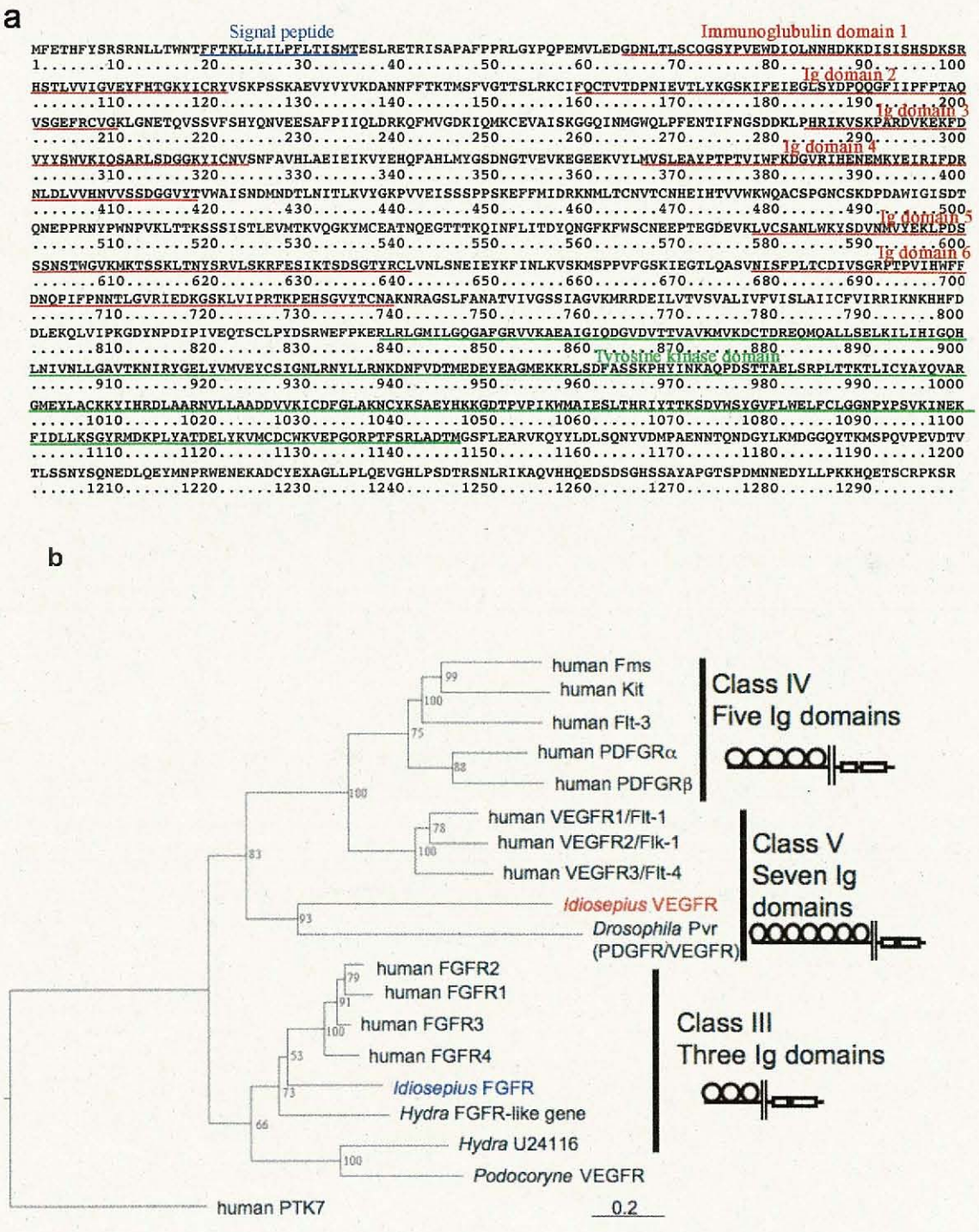
a
Signal peptide
Immunoglubulin domain 1
Ig domain 2
Ig domain 3
Ig domain 4
Ig domain 5
Ig domain 6
Tyrosine kinase domain
b
human Fms
human Kit
human Flt-3
human PDFGRα
human PDFGRβ
Class IV
Five Ig domains
human VEGFR1/Flt-1
human VEGFR2/Flk-1
human VEGFR3/Flt-4
Idiosepius VEGFR
Drosophila Pvr
(PDGFR/VEGFR)
Class V
Seven Ig
domains
human FGFR2
human FGFR1
human FGFR3
human FGFR4
Idiosepius FGFR
Hydra FGFR-like gene
Hydra U24116
Podocoryne VEGFR
Class III
Three Ig domains
human PTK7
0.2

Fig. 1

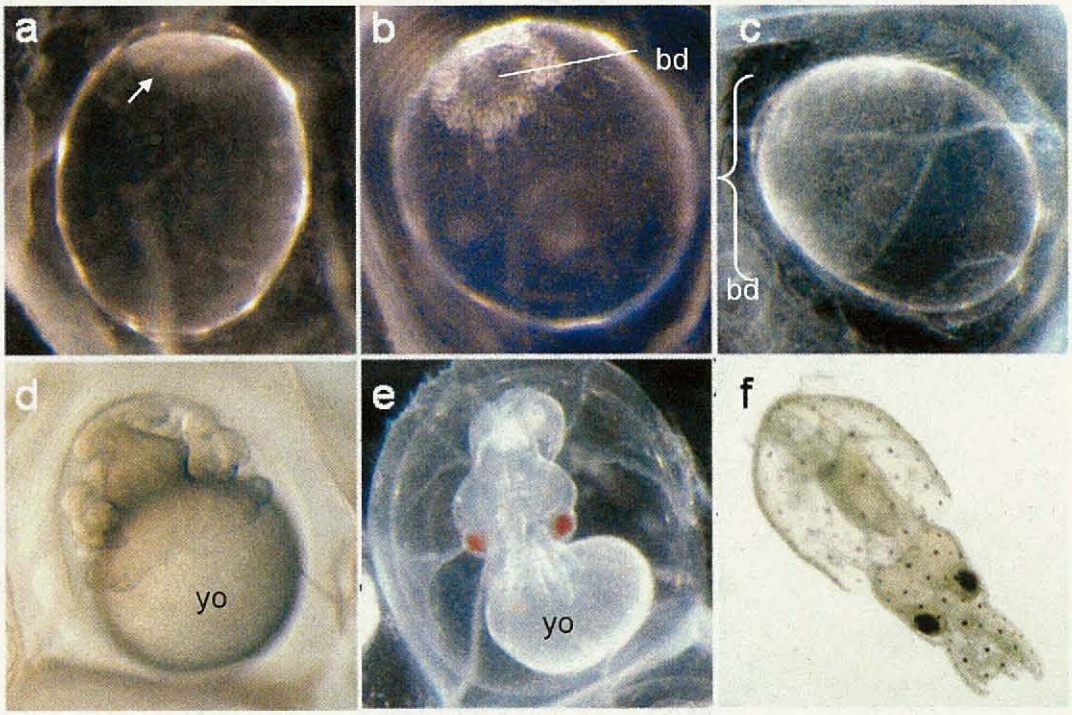


Fig. 2

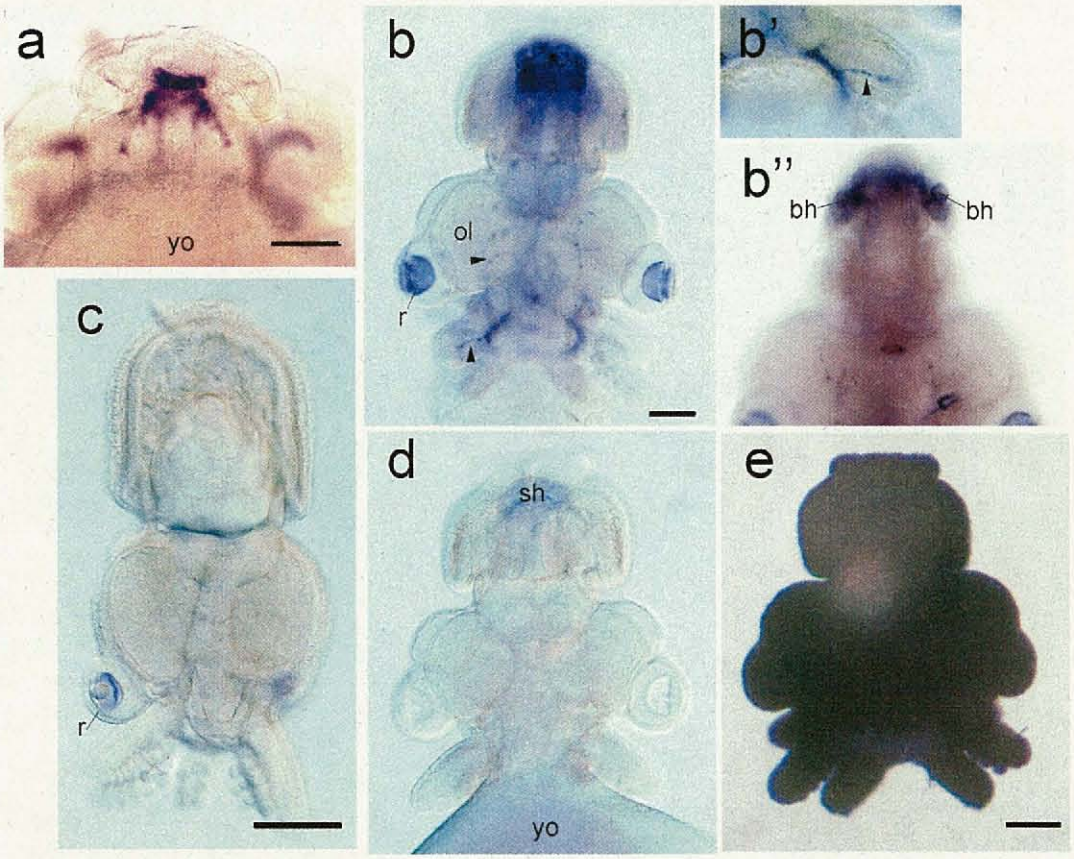


Fig. 3

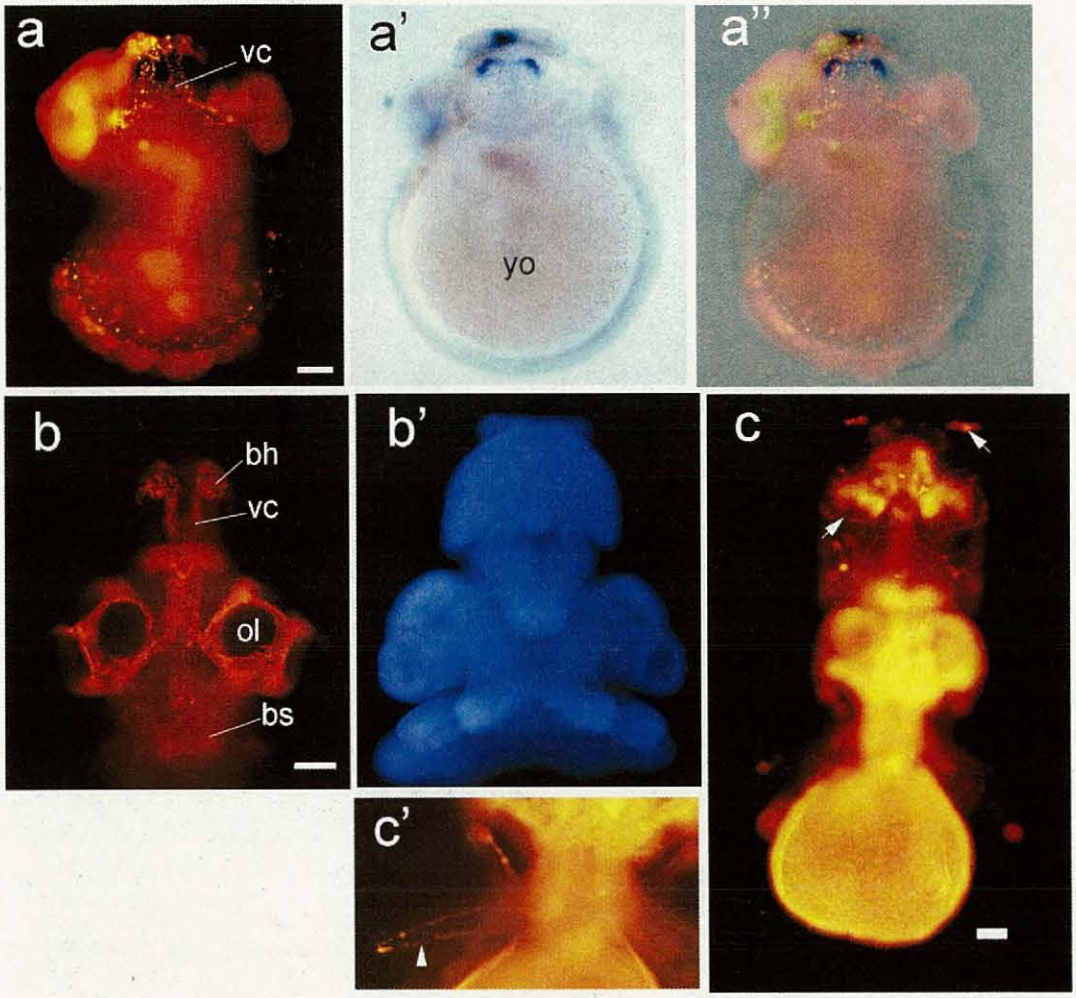


Fig. 4

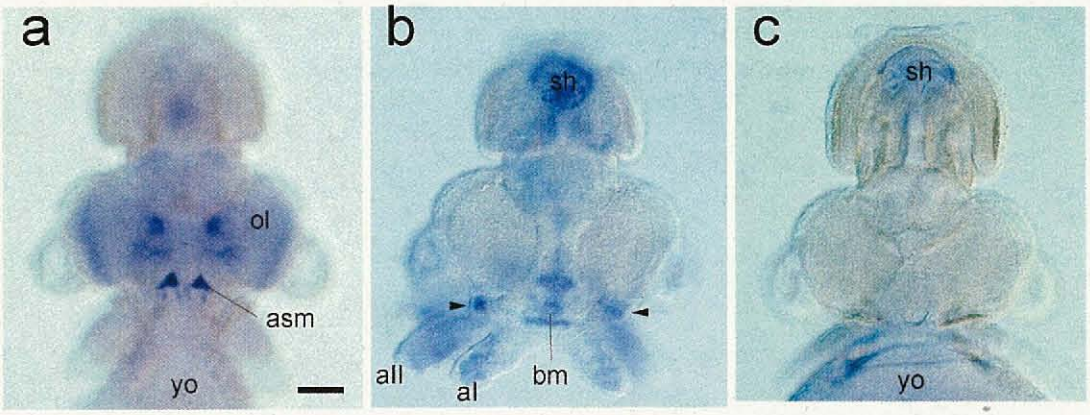


Fig. 5

## Conclusion

Molecular phylogenetic analysis of cuttlefishes using three mitochondrial genes revealed that they are divided into four well-supported clades. This analysis did not support phylogenetic reliability of prior classifications based on the cuttlebone shapes and the suckers on tentacular clubs. The molecular and morphological analyses still remain to be reconciled, but the "*Doratosepion*" clade, among the Sepiidae, forms a monophyletic group both in molecular and morphological analyses. I found a new taxonomic character of *Doratosepion*, that is a loss of membranous structure in their cuttlebones. Membranous structure is commonly observed in the other sepiids. Thus the loss of membranous structure is considered as a synapomorphy for the *Doratosepion* clade. Therefore, I propose the *Doratosepion* clade, excluding *S. madokai*, as a distinct and valid genus, *Doratosepion* Rochebrune, 1884.

Molecular phylogenetic analysis of decapodiformes including *Idiosepius paradoxus* suggested that idiosepiids are related to oegopsids or myopsids, but not to sepiolids. *Idiosepius* and *Sepiadarium* share common features, such as regression of gladius and the presence of mediolateral-rounded fins. These similarities are apparently due to morphological convergence.

The cephalopods have a closed blood-vascular system lined by endothelial cells. However, the circulatory system appears to derive from an open blood-vascular system of their ancestors. I showed the receptor of vascular endothelial growth factor (VEGFR) is expressed in developing blood vessels of *Idiosepius* embryos. This result suggests the cephalopod VEGFR is associated with the angiogenic processes similar to the

vertebrates. In this innovation of the vascular system, recruitment of pre-existing regulatory genes or even regulatory networks could contribute to generate new structures, that is, the endothelium. Because of large differences between the cephalopod and the other molluscs, comparative studies in their development would reveal the molluscan evolution and how the complex body plan as in the cephalopods was formed.

Why did the endothelium occur in the cephalopod? The buoyancy device is probably a crucial factor for this question. The *Nautilus* circulatory system seems to be relatively open with an extended peripheral sinus (Schipp, 1987). The buoyancy is regulated by hydrostatic adaptations accomplished by the caramel liquid, which is added or removed from the shell chambers. This alteration is performed by osmotic pressure of blood in their siphuncle. Transport of the caramel liquid in sepiid shell can be explained by a change of the liquid's osmotic pressure (Denton and Gilpin-Brown, 1959). This is insufficient to explain chamber emptying in the chambered *Nautilus*. At 240 m depth, the hydrostatic pressure forcing shell chambers exceeds the maximum osmotic emptying pressure. *Nautilus* is frequently found below 240 m depth, where simple osmotic emptying cannot function. The counter-current system enhances siphuncular blood concentration, which could 'draw' water from chambers below 240 m, and account for transport against both osmotic and hydrostatic gradients (Greenwald et al., 1980). Ancestral cephalopods might first have blood vessels with counter-current systems. After a loss of solid buoyancy device, extant coleoid cephalopods possibly improved secondary athletic performance using the developed vascular systems with

endothelium.

**References**

Denton, E. J. and Gilpin-Brown, J. B. (1959) Buoyancy of the Cuttlefish. Nature, 184: 1330-1331.

Greenwald, L., Ward P. D., and Greenwald, O. E. (1980) Caramel liquid transport and buoyancy control in chambered nautilus (*Nautilus macromphalus*). Nature, 286: 55-56.

Schipp, R. (1987) The blood vessel of cephalopods. A comparative morphological and functional survey. Experientia, 43: 525-537.